EVALUATION OF XMX/2L-MIL VIRTUAL IMPACTOR PERFORMANCE AND CAPTURE AND RETENTION OF AEROSOL PARTICLES IN TWO DIFFERENT COLLECTION MEDIA

THESIS

Jon E. Black, Major, USAF, BSC

AFIT/GIH/ENV/11-M01

DEPARTMENT OF THE AIR FORCE
AIR UNIVERSITY

AIR FORCE INSTITUTE OF TECHNOLOGY

Wright-Patterson Air Force Base, Ohio

AFIT/GIH/ENV/11-M01

EVALUATION OF XMX/2L-MIL VIRTUAL IMPACTOR PERFORMANCE AND CAPTURE AND RETENTION OF AEROSOL PARTICLES IN TWO DIFFERENT COLLECTION MEDIA

THESIS

Presented to the Faculty

Department of Systems and Engineering Management

Graduate School of Engineering and Management

Air Force Institute of Technology

Air University

Air Education and Training Command

In Partial Fulfillment of the Requirements for the

Degree of Master of Science in Industrial Hygiene

Jon E. Black, MS

Major, USAF, BSC

March 2011

AFIT/GIH/ENV/11-M01

EVALUATION OF XMX/2L-MIL VIRTUAL IMPACTOR PERFORMANCE AND CAPTURE AND RETENTION OF AEROSOL PARTICLES IN TWO DIFFERENT COLLECTION MEDIA

Jon E. Black, MS
Major, USAF, BSC

Approved:

_____//Signed//_____	__07 Mar 2011__
Lt Col Dirk P. Yamamoto, PhD (Chairman)	Date
_____//Signed//_____	__04 Mar 2011__
Lt Col Jeremy M. Slagley, PhD (Member) USAF School of Aerospace Medicine Technical Services Branch	Date
_____//Signed//_____	__07 Mar 2011__
Charles A. Bleckmann, PhD (Member)	Date
_____//Signed//_____	__04 Mar 2011__
Capt Casey W. Cooper, MS, MBA (Member) USAF School of Aerospace Medicine Risk Analysis Division	Date

Abstract

The United States Air Force uses the XMX/2L-MIL (XMX) high volume air sampler to collect samples for biological analysis. The XMX uses a virtual impactor to concentrate particles 1.0 to 10 µm in size into a secondary flow prior to sample collection using a liquid impinger in a collection tube. There are no known published studies regarding virtual impactor inter-instrument variability, effect of reducing the secondary flow on particle concentration, or capture and retention efficiency (CRE) of particles in the collection media performance characteristics when using the XMX. These performance characteristics were evaluated by lofting test aerosols of Arizona Road Dust or fluorescent polystyrene latex (FPSL) spheres into a 14 m^3 test chamber, measuring the chamber and post-virtual impactor particle concentrations using aerodynamic particle sizers, and measuring the concentration of FPSL spheres captured and retained in the collection media using a fluorometer. Notable findings include detection of significant inter-instrument virtual impactor variability, significant difference in particle concentration at reduced secondary flow, and significant differences in CRE due to particle size and secondary flow. This research demonstrates that when using an XMX limit of detection precision is suspect and the importance of collecting and analyzing multiple samples for improved risk assessment.

Acknowledgements

I would like to thank my advisors, Lt Col Jeremy Slagley and Lt Col Dirk Yamamoto, for their guidance and support throughout the course of this thesis effort. I would, also, like to thank my research sponsor, Lt Col Darrin Ott, from the School of Aerospace Medicine for the support provided to me in completing this research.

I am also indebted to Dr. Jacky Rosati and the many professionals working with her at the Environmental Protection Agency whose knowledge and expertise were essential to completing the experimental work associated with this project. Special thanks go to Dr. Daniel Felker, Dr. Edward White, and TSgt Carrissa Acosta for their assistance in performing microscopy, conducting statistical analysis, and in developing fluorometric calibration curves, respectively. I am particularly indebted to Capt Casey Cooper and grateful for his outstanding dedication, expertise, and assistance in this endeavor from its beginning to its end.

Lastly, I am ever so blessed, thankful, and grateful for the unending support, willful sacrifice, and unconditional love of my wife and son throughout this odyssey, without which this work could not have been completed.

Jon E. Black

Table of Contents

Page

Page

List of Figures

Figure Page

List of Tables

Table Page

EVALUATION OF XMX/2L-MIL VIRTUAL IMPACTOR PERFORMANCE AND CAPTURE AND RETENTION OF AEROSOL PARTICLES IN TWO DIFFERENT COLLECTION MEDIA

I. Introduction

Motivating Factors for Biological Agent Sampling

The United States (US) faces many national security threats, both in the homeland and abroad. The US Air Force (AF) is a vital asset of the federal government in protecting and defending the nation from all threats, foreign and domestic. Since the US possesses the most dominant, experienced, and best equipped military force, most potential nation state adversaries are loath to directly challenge and confront the US in a conventional war (National Research Council, 2007). Additionally, there are many terrorist organizations that wish to harm US citizens and damage national assets in a manner that engenders fear or panic. The intention of antagonists is to intimidate the US, using terroristic tactics and threats, such that the federal government will alter national policies or goals the antagonists find objectionable. As conventional military weapons are fairly well understood by members of the general public in terms of the basic nature of most armaments, direct causes and types of injuries, and typical methods of avoidance and protective measures, unconventional weapons are considered to be the modern terrorists' most desired weapon of choice when the intent of the attack is to generate fear, panic, hysteria, or alter the policy of the federal government (Hodge, 2002).

Additionally, unconventional weapons offer both nation state and terrorist organizations the capability to engage the US in asymmetric, rather than direct battlefield, conflict. There are nominally four types of unconventional weapons: chemical, biological, radiological, and nuclear. This thesis is focused solely on biological agents, whether used maliciously or simply appearing via natural occurrence.

There are notable characteristics of biological agents that make them attractive to adversaries to use as weapons against the US. Biological agents can be cultured or produced in significant quantities using dual-use equipment and facilities, which can make a biological agent production facility difficult to identify or prove it is engaged in a biological weapons program (Alibek, 1999). Many biological agents are endemic disease-causing agents, which may make it very difficult to distinguish between naturally-occurring and maliciously introduced epidemics. Biological agents are ideally suited for covert attacks, with the potential for a significant time period in between the initial use of a biological agent and recognition of the ensuing epidemic it caused (Alibek, 1999). The use of biological weapons would most likely lead to widespread panic, disruption, and extraordinary costs in medical resources and decontamination efforts (Bush, 2010).

Due to the aforementioned likely characteristics of potential adversaries of the US, the appealing aspects of biological agents as weapons, and the potential disturbance resulting from civilian fear, panic, and use of medical resources, the federal government is highly motivated to protect and defend the US from the malicious use of biological agents. In addition, there also exists the risk of an event, outbreak, or pandemic of a naturally-occurring biological agent not associated with any malicious activity. In recent

history, the federal government has acted in response to events such as the Hanta virus outbreak (Simonsen, et al., 1995), Avian Influenza pandemic (Schofield, et al., 2005), Sever Acute Respiratory Syndrome (SARS) epidemic (Ksiazek, et al., 2003), recurring Adenovirus outbreaks (Echavarria, et al., 2000), H1N1 Swine influenza pandemic (Smith, et al., 2009), and the Post 9/11 Anthrax letter attacks (Canter, 2005). Critical to protecting and defending against biological threats is the ability to detect and identify biological agents. Collecting and analyzing biological samples is the most fundamental requirement to detect and identify biological agents.

Basic Model of Airborne Biological Agent Exposure and Impact

The fundamental etiology of biological infection is perhaps best exemplified by the triad model of Host-Agent-Environment (HAE). Simply stated, the HAE model conveys that a biological agent infects and lives in a host and can be subsequently transmitted to another host by direct contact or indirectly through the environment (Vaccari, et al., 2006). There are two general disease conditions for an agent embedded in the HAE model: prepathogenesis and pathogenesis. Prepathogenesis is the period when an agent is either in the environment prior to exposure of a host or, subsequently, in a host as a result of exposure and adapting to the environment presented by the host. Pathogenesis is the period after which a host has become infected due to adaption and establishment of the agent in the host. If the immune response of the host prevents the agent from adapting and establishing itself in the host, pathogenesis is averted and the host does not become infected by the agent (Vaccari, et al., 2006).

There are many potential pathways of exposure by which a host can become infected by an agent, with the most common being ingestion, absorption through the skin, contact with wounds on the skin or mucous membranes, and inhalation. While airborne biological agents can lead to host infection by all the aforementioned pathways, the most relevant pathway of concern for airborne agents is inhalation. Inhalational exposure provides nearly ideal conditions for a biological agent to infect a host as one must breathe air to survive, the presence of aerosolized biological agent is not readily recognized absent air sampling and analysis, and depending upon the size of the carrier aerosol particle, the biological agent can penetrate deeply into the respiratory system of the host. Once inhaled into the host, the biological agent can deposit into the incubator-like environment of the respiratory system or potentially cross the air-blood barrier in the alveolar region and enter the circulatory system of the host. Once having deposited in the respiratory system or invaded the circulatory system, barring sufficient immunological response, a biological agent can easily advance from the prepathogenesis to the pathogenesis stage and give rise to full infection and symptomatic manifestation of disease.

Collection of Airborne Biological Agents

There are two successive processes involved in detecting a biological agent: collecting a sample and analyzing the sample. A sample is normally collected from a single source media. The basic source media from which a sample is collected are air, water, soil, bulk material, plant, animal, or human. This work is focused on air as the

source media for biological agents and, particularly, on the process of collecting a sample from ambient air.

The ambient air is an aerosol, which is to say that ambient air is a gas with fine solid particles or liquid droplets suspended and carried in it. For purposes of simplicity, the term aerosol particle is used in this document to refer to both solid particles and liquid droplets in ambient air unless explicitly stated otherwise. Sampling ambient air typically involves drawing air into and through a device, with the aerosol particles being either analyzed immediately and exhausted or retained. If retained, aerosols are captured on a nominally dry collection surface or within a liquid collection media, and analyzed at a later time. Instruments that immediately analyze and exhaust aerosol particles are typically only used to measure the size distribution or concentration of aerosol particles and are not capable of biological analysis of the aerosol particles. When collecting air samples for biological agents it is necessary to retain a sample of the aerosol particles so that they may subsequently subjected to biological analyses.

Two common methods of retaining a sample on a collection surface are filter collection and solid impaction. In filter collection, the air is drawn through a filter made of a particular material and pore size, and aerosol particles are largely collected due to three predominate collection mechanisms: impaction, interception, and diffusion (Hinds, 1999). In solid impaction, the air is drawn through an individual or series of nozzles or orifices or along a centrifugal path, and due to flight characteristics that are a function of aerosol particle size, aerosol particles are separated and deposited on a surface based upon their size (Marple, et al., 1991). Examples of samplers that exploit solid impaction

surface collection are slit, Anderson, and cyclones samplers, which are illustrated in Figure 1.

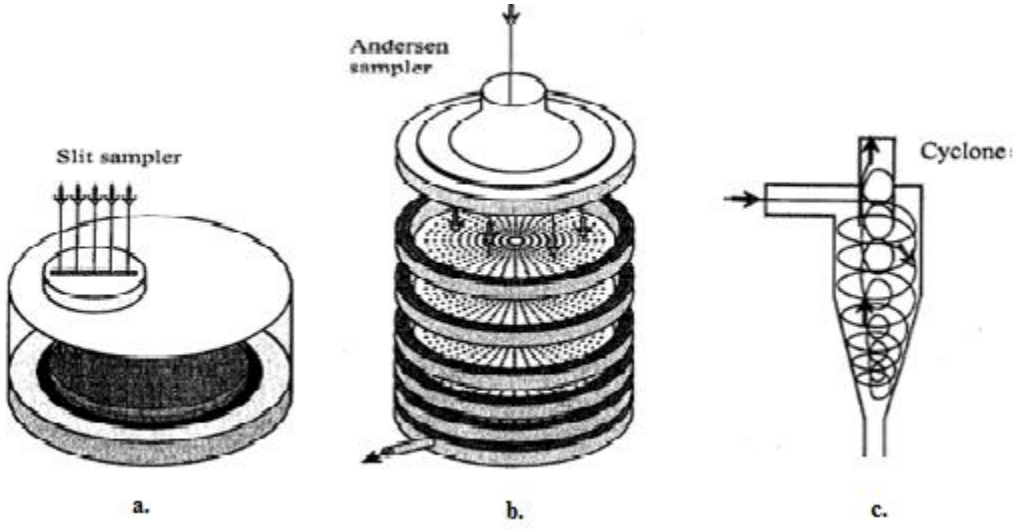

Figure 1: Slit, Anderson, and cyclone impaction-based aerosol samplers (Verreault, et al., 2008. Reproduced with Permission from American Society of Microbiology)

The general method for retaining a sample within a liquid collection media is liquid impaction. In liquid impaction, the sampled air is drawn through an impinger tube which is either a certain distance from and directed towards or inserted into a liquid collection media surface. Aerosol particles either impact and are captured by the surface of the liquid collection media or are injected into and retained in the bulk of the liquid collection media (Willeke, et al., 1998). Examples of impinger samplers that exploit liquid impaction are the more recently developed swirling aerosol collector, commercially known as the Biosampler®, and the classic All Glass Impinger® (AGI), which are illustrated in Figure 2. AGI samplers are further classified and named based upon the set distance, in millimeters (mm), that the airflow exit is set vertically above the bottom of the liquid vessel. The airflow exits of the AGI-30 and AGI-4 are 30 mm and

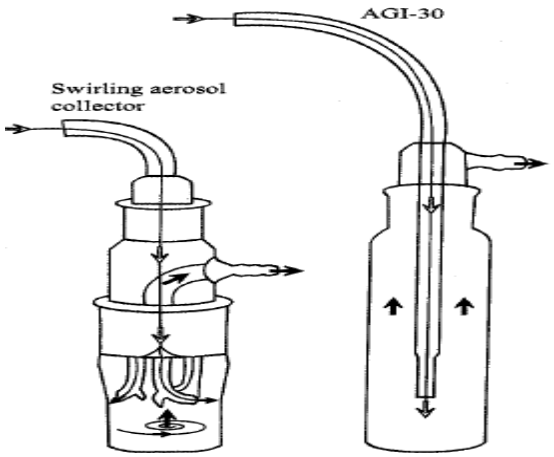

Figure 2: Swirling aerosol collector and All Glass Impinger (AGI) liquid impactors (Verreault, et al., 2008. Reproduced with Permission from American Society of Microbiology)

4 mm, respectively, above the bottom of the liquid vessel (Lin, et al., 1997).

There are competing advantages and disadvantages to consider in selecting the type of sampler technology and collection method to use, such as filter collection, solid impaction, or liquid impaction, when collecting a sample from ambient air for biological analysis. The two most important considerations is volume of the air to be sampled, which is normally determined by the sampler flow rate and chosen sampling period, and the biological agent of interest, if known (Brasel, et al., 2005). The majority of scenarios directing the AF to conduct air sampling for biological agents are focused on terrorist or combatant attacks at large facilities or in outdoor environments where concentrations of biological agents would likely be relatively low. Additionally, commanders want presumptive analytical test results as quickly as possible to support operational decision making in emergency response or wartime situations. Therefore, due to nature of suspected biological agent attack scenarios and commanders' decision making needs, the implied preference is to use a sampler that will enable analyzing the largest volume of air

in the shortest period of time, which directs the selection of high volume samplers. However, other crucial factors to consider are the biological viability requirements of the analytical method that will be used to analyze the collected sample. For simplicity, in this work the term 'viable' shall refer to the biological agent in question existing in such a state or condition as to permit detection by a particular method. For example, polymerase chain reaction (PCR) methods do not require the biological agent of interest to be active, in the case of viruses, or alive, in the case of bacteria; therefore, viruses, when inactive, and bacteria, when dead, are viable to PCR-based detection methods (Bermingham & Luettich, 2003). However, if the ribonucleic acid (RNA) of an inactive virus or the deoxyribonucleic acid (DNA) of a dead bacteria has been compromised in some way such that PCR-based methods are no longer effective in detecting the virus or bacteria, then inactive virus and dead bacteria are no longer viable. Therefore, when collecting a biological agent sample for analysis, it is critical that the sampling method maintain the viability of the collected sample for the analytical detection methods to be employed. With the desired sampling characteristics then being to analyze a large volume of air, in as short a sampling time as possible, and offer superior maintenance of biological agent viability, a strong argument can be made that, the optimum sampler would be a high volume, liquid impaction-based sampler.

Primary Air Force Airborne Biological Agent Sampling Equipment

The federal government responded to the 9/11 attack, post 9/11 anthrax letter attacks, and increased terrorist threats to use biological agents against US interests by designing, developing, and deploying the Portal Shield monitoring system (Institute of

Medicine, 2010). The Portal Shield monitoring system, developed by the DoD, is a modular collection of individual units that can collect and analyze ambient air for a variety of biological agents. The Portal Shield units are deployed throughout the world to high value, high risk fixed sites that are likely targets to terrorist attacks to monitor ambient air. Although Portal Shield units provided biological agent detection capability at fixed AF assets, the units offered no practical capability to address the need for mobile biological agent detection capability for rapidly responding to immediate threats, emergency response incidents, or battlefield actions. To address the need for rapid, mobile biological agent detection, the AF purchased the DFU-1000 and the XMX/2L-MIL, which are manufactured by Lockheed Martin Integrated Technologies and Dycor Technologies, Inc. (Dycor), respectively.

The DFU-1000 was purchased for use by AF Civil Engineering (CE) Emergency Management (EM) personnel. The DFU-1000 is a high volume air sample that employs the filter collection method to obtain an aerosol sample. The DFU-1000 sampling flow rate is approximately 800 liters per minute (lpm) and is rated for continuous duty, with a 40,000 hour life. The DFU-1000 uses a standard 47 millimeter (mm) diameter polyester felt filter, with a pore size of 1.0 micrometer (μm). This filter was evaluated for particle sizes as small as 100 nanometers (nm) and found to have a collection efficiency of 75 percent for 100 nm particles (Lawrence, 2003). The DFU-1000 was intended for indoor use only; however, an updated version, the DFU-2000, was subsequently produced for outdoor use in harsh environments that features an exterior shelter, an inlet mast extendable up to nine feet, and a pre-separator to eliminate large particles or debris (JPEO-CBDX, 2008).

The XMX/2L-MIL, which shall hereafter be referred to as the XMX, was purchased for use by AF Bioenvironmental Engineering (BE) personnel. The XMX is a high volume air sampler that combines virtual impaction particle flow separation and the liquid impaction collection method to collect an aerosol sample. Virtual impaction differs from aerosol inertial impaction as the main sampling flow drawn into the instrument is physically separated into two flows, a primary flow containing the particles below a particular cut-point size and a secondary flow containing the particles above the cut-point size (Loo & Cork, 1988). The XMX draws in a sampling flow of approximately 700 lpm, with particles larger than 10 µm removed at the device inlet, which is then separated at the first stage of the virtual impactor into a primary flow containing the particles smaller than 1.0 µm and a secondary flow containing the particles larger than 1.0 µm. The secondary flow is approximately 12 lpm, and, therefore, is highly concentrated with particles between 1.0 and 10 µm as all the particles in this size range that were drawn in with the main sampling flow should be contained in the secondary flow. The secondary flow then passes through the second stage of the virtual impactor, which serves to reject aerosol particles smaller than 1.0 µm that undesirably passed through the first stage of the virtual impactor to the primary flow. Lastly, the vacuum pump, which creates the secondary flow, draws the secondary flow through the third stage of the virtual impactor into a liquid impinger. The liquid impinger contains collection media that captures and retains the particles in the secondary flow. The collection media is typically either sterile water or a phosphate buffered saline (PBS) solution; however, other collection media, such as Remel MicroTest M5 Multi-Microbe Media® (Remel M5), are available to address specific user requirements.

Thesis Objectives and Limitations

This study seeks to resolve three hypotheses regarding the flow rates of the XMX, two hypotheses regarding the performance of the virtual impactor of the XMX, and two hypotheses regarding the performance of two different collection media used with liquid impactor of the XMX. Other objectives include producing two experimentally determined graphs showing the concentration ratio (CR) as a function of particle size for virtual impactor secondary flow rates of 5 and 10 lpm. The following questions will be used to evaluate XMX and collection media performance, with an overview of specific hypotheses that will be tested presented in Table 1:

1. Do the flow rates of AF-fielded XMXs match those reported by the manufacturer?
2. Does the virtual impactor performance vary with the secondary flow rate?
3. Is the virtual impactor performance consistent across XMXs?
4. Do different collection media capture and retain particles equally?
5. Does collection media capture and retain particles equally at different secondary flow rates?

The XMX is a high volume liquid impinger air sampler, reportedly having a total flow rate of 800 lpm, standard secondary flow rate of 12 lpm, and a reduced secondary flow rate between 4 and 5 lpm. As these flow rates are important in designing an effective sampling plan, determining the limit of detection (LOD) for sampling methods,

Table 1: Overview of the hypotheses to be tested

Test performed	Null hypothesis	Alternate hypothesis	Analysis method
Total flow rate	The total flow rate of the XMX equals the manufacturer's specification	The total flow rate of the XMX does not equal the manufacturer's specification	Measure total flow rate for several XMXs and compare sample mean to manufacturer's specification
Standard secondary flow rate	The standard secondary flow rate of the XMX equals the manufacturer's specification	The standard secondary flow rate of the XMX does not equal the manufacturer's specification	Measure standard secondary flow rate for several XMXs and compare sample mean to manufacturer's specification
Reduced secondary flow rate	The reduced secondary flow rate of the XMX equals the manufacturer's specification	The reduced secondary flow rate of the XMX does not equal the manufacturer's specification	Measure reduced secondary flow rate for several XMXs and compare sample mean to manufacturer's specification
Virtual impactor performance	The secondary flow rate does not affect virtual impactor performance	The secondary flow rate does affect virtual impactor performance	Determine the concentration ratio at two secondary flow rates and evaluate variability via ANOVA
Inter-instrument variability	Virtual impactor performance consistent across XMXs	Virtual impactor performance not consistent across XMXs	Evaluate virtual impactor performance variability via ANOVA
Collection media performance at same secondary flow rate	PBS solution and Remel M5 equally capture and retain particles at the same secondary flow rate	PBS solution and Remel M5 do not equally capture and retain particles at the same secondary flow rate	Determine fraction of particles captured and retained in collection media and evaluate variability via ANOVA
Collection media performance at different secondary flow rates	PBS solution equally captures and retains particles at two secondary flow rates	PBS solution does not equally capture and retain particles at two secondary flow rates	Determine fraction of particles captured and retained in collection media and evaluate variability via ANOVA

and evaluating and comparing XMX performance, it is essential to verify if these flow rates correctly reflect those of fielded XMXs. There are three hypotheses regarding these flow rates, with the null hypotheses being that the manufacturer's reported flow rate is equal to the experimentally measured flow rate of fielded XMXs, and the alternative hypotheses being that the manufacturer's reported flow rate is not equal to the experimentally measured flow rate of fielded XMXs.

Virtual impactor performance is characterized by the CR, which is defined as the ratio of the particle concentration in the secondary flow of the XMX to the particle concentration in the ambient air. Any evaluation to determine the air concentration limit of detection (LOD) for a biological agent when using the XMX requires knowing the CR applicable to the aerosol and sampling conditions. Dycor has provided a graph showing how the CR varies with particle size when operating the virtual impactor of the XMX at a secondary flow rate of 1 lpm. However, Dycor reports that the standard secondary flow is 12 lpm, and a previous study found that it was necessary to reduce the secondary flow rate to 5 lpm to prevent excessive foaming of collection media Remel M5 (Cooper, 2010).

The first hypothesis regarding virtual impactor performance concerns variability due to the secondary flow rate. The null hypothesis is that secondary flow rate, when it is either 5 or 10 lpm, does not have a significant effect on the experimentally determined CR, and the alternative hypothesis is that the secondary flow rate, when it is either 5 or 10 lpm, does have a significant effect on the experimentally determined CR. The second hypothesis regarding virtual impactor performance concerns inter-instrument variability. The null hypothesis is that the virtual impactor used does not have a significant effect on

the experimentally determined CR, and the alternate hypothesis is that the virtual impactor used does have a significant effect on the experimentally determined CR. The status quo represented by AF operating procedures for the XMX in these cases is expressed in both of these null hypotheses.

The first hypothesis regarding collection media performance concerns inter-media variability. The null hypothesis is that the collection media, when it is either PBS solution or Remel M5, does not have a significant effect on the experimentally determined capture and retention of particles in the collection media at a secondary flow rate of 5 lpm, and the alternative hypothesis is that the collection media, when it is either PBS solution or Remel M5, does have a significant effect on the experimentally determined capture and retention of particles in the collection media at a secondary flow rate of 5 lpm. The second hypothesis regarding collection media performance concerns intra-media variability. The null hypothesis is that secondary flow rate, when it is at 5 lpm or 10 lpm, does not have a significant effect on the capture and retention of particles in PBS solution collection media, and the alternative hypothesis is that the secondary flow rate, when it is at 5 lpm or 10 lpm, does have a significant effect on the capture and retention of particles in PBS solution collection media.

II. Literature Review

Overview

This section seeks to review scientific literature relevant to using the XMX to collect air samples for subsequent biological agent analysis. Several areas of applicable interest are presented including selected cases of air sampling for biological agents, aerosol characteristics and sampling methods, virtual impaction, AF fielded high volume air samplers, collection media, and fluorometry. Field and laboratory-based studies will be reviewed. The AF uses high volume air sampling equipment that employ dry filtration, virtual impaction, and liquid impinger methods to collect biological agent samples. This review will focus on virtual impaction and liquid impinger collection methods, two collection media, and using fluorometry to evaluate capture and retention of fluorescing spheres in collection media.

Selected Cases of Air Sampling for Biological Agents

Air Sampling for SARS.

SARS spread rapidly around the world in 2003. An initial epidemiology study performed by Olsen sought to evaluate the risk, if any, to fellow passengers of in-flight SARS-associated coronavirus (SARS-CoV) infection due to the infected passengers when traveling on commercial flights (Olsen, et al., 2003). The study included three specific commercial flights in which between one and four passengers were either SARS symptomatic or infected. Olsen found that the relative risk of infection was 3.1 for those passengers who were seated in the three rows in front of the infected passenger as

compared to passengers sitting elsewhere in the aircraft. Additionally, only one of the 561 passengers on board the two flights that were 90 minutes in duration became infected, whereas 22 of the 120 passengers on board the flight that was 180 minutes in duration became infected. Taken together, the relative risk and infection during flight time findings suggest an airborne proximity exposure risk and a minimal infective dose associated with SARS, which suggests the importance of obtaining air sampling results in settings with similar exposure conditions.

To better characterize the risk of airborne transmission of SARS, Booth employed novel air sampling to investigate environmental contamination in SARS units (Booth, et al., 2005). Air samples were collected using both wet air and dry air filtering techniques from 19 rooms in the SARS unit of four healthcare facilities in Toronto, Canada, where SARS patients were staying. The collected specimens were tested for the presence of SARS-CoV using PCR and cell culture analyses. Wet air sampling was performed using a high-resolution slit sampler developed by Defence Research and Development Canada (DRDC). Dry air filter sampling was performed using a closed-face, 3-piece disposable plastic cassette with a polytetrafluoroethylene (PTFE) membrane filter with a 0.3 µm pore size. Viral RNA was extracted from the wet air samples and analyzed using a one-step reverse-transcriptase (RT)-PCR technique for two different targets on the SARS-CoV genome. Viral RNA from PTFE membrane filters was similarly analyzed after having been extracted by immersion in a suitable buffer fluid and rotated for 20 minutes on an orbital shaker. Two of the ten wet air samples were positive for SARS-CoV and all 28 of the dry air filter samples were negative for SARS-CoV. Booth provided the first

experimental confirmation of viral aerosol generation by a SARS patient, which indicated the possibility of airborne transmission of SARS.

Air Sampling for Adenoviruses.

Adenoviruses have impacted basic military trainees for many years. Artenstein was possibly the first to evaluate air sampling for acute respiratory disease agents affecting military recruits (Artenstein & Miller, 1966). Artenstein used the Large Volume Sampler (LVS) produced by Litton Industries, Inc., in support of an epidemiological study of an acute respiratory disease caused mainly by adenoviruses. The LVS, which had an electrostatic precipitator and used liquid collection media, was employed to maximize sensitivity to detection. Ill recruits were monitored individually in hospital rooms with volumes of 40.8 cubic meters (m^3). The LVS was run for five minutes at a flow rate of 10.1 cubic meters per minute (m^3/min), for a total sample volume of 50.5 m^3. Artenstein recovered 1 adenovirus unit per 7.84 m^3 of air sampled and concluded that it was clear that an AGI operating at 12.5 lpm was inadequate for collecting adenoviruses at such low concentrations, thereby stressing the need for a high volume sampling approach for detecting adenoviruses.

Following the loss of adenovirus vaccines in 1999, adenoviruses re-emerged as a source of acute respiratory disease in military recruit settings. Russell sought to better understand the transmission dynamics of adenovirus in the living quarters of military recruits (Russell, et al., 2006). Active surveillance for acute respiratory diseases were performed on 341 recruits and support personnel and environmental samples were simultaneously collected. Environmental sampling methods performed included swipe

sampling pillows, lockers, and rifles and air sampling using the DFU-1000. The DFUs were run for 12 hours per day, during the evening, night, and early morning hours when the recruits were typically there after completing their daily routine. The two DFU filters were subsequently analyzed for adenovirus, one by molecular testing and the other by growth in cell cultures. A total of 19 air samples were analyzed, with 42% found positive for adenovirus. Russell found that the greatest quantity of adenovirus DNA detected in the environment was significantly associated with adenovirus infections.

Implications of Select Studies to use of XMX for Biological Agent Sampling.

There are two primary implications of the reviewed selected cases concerning air sampling for SARS and adenoviruses that are informative when considering the utility of the XMX: sample volume and collection method. Artenstein stressed the importance of having a large sample volume, which is particularly relevant for probable biological agent attack scenarios in large facilities or outdoor environments where biological agent concentrations would likely be quite low due to dilution effects. The XMX would have a sample volume of 3,500 liters during the desired five minute sampling period, which is in relative proximity to the 7,840 liters in which Artenstein demonstrated the ability to detect 1 adenovirus unit. In comparison, the highly regarded swirling aerosol collector developed by Willeke would collect a sample volume of 62.5 liters in the same sampling period (Willeke, et al., 1998). The preference for a large sample volume was further emphasized by Olsen concerning SARS-CoV. The disparity in the SARS attack rate for passengers in the flight of 180 minutes in duration compared to passengers in the flights of 90 minutes in duration, 18.3% and 0.2%, respectively, indicate the potential for

particularly low biological agent concentrations in ambient air due to infectious subjects in a relatively confined space, highlighting the importance of sample volume.

The collection method used can have a notable impact on maintaining viability of biological agents to support detection during analysis. In analyzing air samples for SARS-CoV, Booth had two of ten wet air samples test positive using RT-PCR, as opposed to zero of 28 dry air filter samples, which suggests superior performance for wet sampling over dry sampling in maintaining the viability of SARS-CoV samples for detection by RT-PCR analysis. However, Russell showed that dry air filter sampling can be effective in maintaining sufficient viability for detection of adenoviruses. Russell collected 19 dry air filter samples using the DFU-1000 and was able to detect adenovirus on 42% of the samples. These findings illustrate that viability maintenance sufficient for detection varies amongst biological agents, and follows the finding by Verreault (Verreault, et al., 2008) that wet air sample methods are generally superior to dry air sample methods at maintaining viability of viral agents.

Aerosol Characteristics and Sampling Methods

Particle Size and Settling Characteristics.

Particle size is probably the most important characteristic of an aerosol. Aerosols are particles that remain suspended in the air. The settling velocity of a particle describes the average speed at which the particle travels downward, and when combined with the height of a particle, provides an estimate of how long the particle will remain suspended in the air. Particles of sizes 1 and 100 μm require 24 hours and 10 seconds, respectively, to settle to the ground from a height of 3 meters. The tendency for particles to remain

airborne increases dramatically for those less than a micrometer in size, with the smallest particles remaining aloft for as long as several months or more (Utrup & Frey, 2004). Therefore, when developing sampling strategies for biological agent detection, the period over which air sampling is conducted should be sufficiently long so as to account for the settling of the smallest relevant particle size and the altitude at which the suspected biological agent was released.

Relevance of Particle Size on Human Health Effects.

This research concerns collecting particles containing biological agents, which are assumed to be associated with deleterious health effects. Health risks associated with aerosols are principally due to particle composition and the region in which they deposit in the respiratory tract. The location of respiratory tract deposition is largely determined by particle size. Particles deposit in the respiratory tract due mainly to interception, impaction, diffusion, and settling collection mechanisms. Collectively, these collection mechanisms lead to the characteristic deposition probability as a function of particle diameter curve shown in Figure 3 (Maynard & Kuempel, 2005). Particles larger than 10 µm (10^4 nm) in diameter are normally prevented from entering the lower respiratory tract as they are deposited in the head region, either in the nose, mouth, or upper airways. For this reason, air samplers are commonly designed to have a 10 µm cut-point prior to the sample collection or particle analysis point. Particles 2.5 µm (2.5×10^3 nm) in diameter are the size least likely to deposit in the respiratory system. Particles most likely to deposit in the alveolar region are approximately 0.01 µm (10 nm) in diameter. Hogan

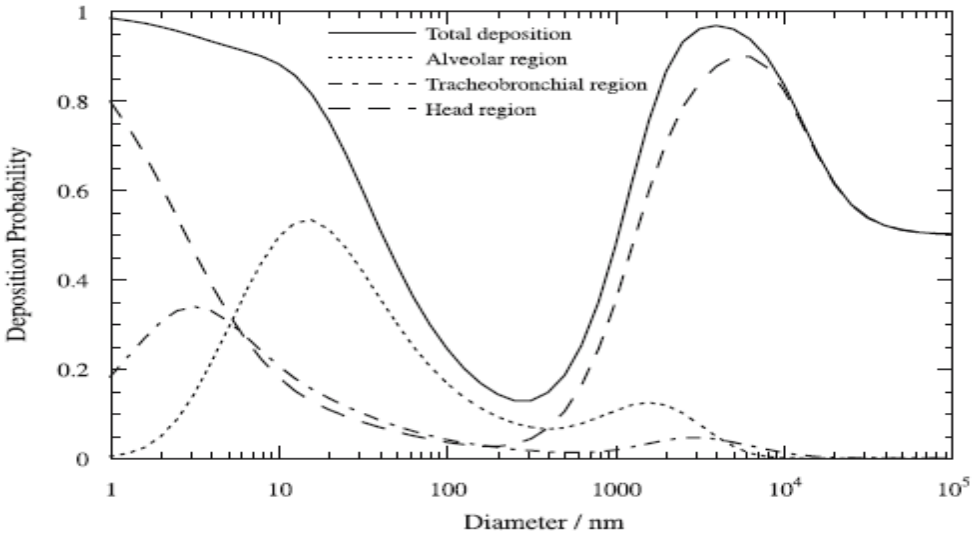

Figure 3: Respiratory deposition probability
(From Maynard & Kuempel, 2005. Reprinted with permission from Springer Science)

suggested that sub-micrometer particles likely pose a more significant role in morbidity as they offer the greatest potential to deposit and deliver virus-containing particles to the alveolar region (Hogan, et al., 2005), which then permits a virus to diffuse through the alveolar membrane and enter the blood stream (Madigan, et al., 1997). Ideally, the collection efficiency of an air sampler for sub-micrometer particles would be at least equal to the respective alveolar deposition probability for the particle size of interest.

Measurement of Particle Size Distribution.

The particle size distribution of an aerosol can be measured using a variety of different particle sizing devices. Aerosol sampling devices capable of measuring particle size distributions are generally of one of two classes: real time measurement or gravimetric analysis. Examples of real time measurement and gravimetric analysis aerosol sampling devices are the aerodynamic particle sizer (APS), manufactured by TSI,

Inc. (TSI), and cascade impactors, respectively. The APS uses the time-of-flight of individual particles that are accelerating through a flow field to determine particle size. The time-of-flight for the particle being analyzed is determined, matched to the time-of-flight for a unit density sphere, and is then reported to be the size of the unit density sphere having the same time-of-flight (Chen, et al., 1998). The APS is an example of an evaluated method for particle sizing as the size of the particle of interest is not expressly measured, but rather, some other characteristic of the size of the particle is used as a surrogate for size and compared to an accepted standard. Microorifice uniform deposit impactor (MOUDI), manufactured by MSP Corporation (MSP), or cascade impactors are direct methods for measuring the size of the particles. The pre- and post-sampling masses of the impactor stages are measured, and, when combined with the known cut-point size of each stage and density of the particle material, permit the direct calculation of the particle size distribution (Marple, et al., 1991).

The APS measures and reports the particle size distribution over the particle size range of 0.5 to 20 μm. Peters experimentally compared the performance of the TSI model 3321 APS to a cascade impactor and found that the APS counting efficiency for the particle size range 1 to 3 μm and 4 μm particles was 45% and 60%, respectively (Peters & Leith, 2003). Peters found that, despite having lower counting efficiencies for these particle size ranges, the APS produced a particle size distribution that was similar in shape to that of the cascade impactor, and proposed the use of an adjustment factor on the APS particle concentration data. Volckens further evaluated the deficient counting efficiency of the model 3321 APS (Volckens & Peters, 2005), building on the work of

Kinney (Kinney & Pui, 1995), who identified inertial impaction on the inlet nozzle for particles larger than 3 μm, and Armendariz (Armendariz & Leith, 20002), who identified that collecting data in the correlated mode led to errors in the reported size distribution and concentration. Volckens characterized the counting efficiency for the model 3321 APS for the particle size range of 0.8 to 10 μm using both liquid and solid particles. Volckens found that counting efficiencies ranged from 85% to 95% and 75% to 25% over the 0.8 to 10 μm size range for solid and liquid particles, respectively, with the drop in liquid particle counting efficiency attributable to larger liquid droplets impacting and adhering to the instrument's inner nozzle. Peters investigated possible alternative devices to the APS for particle size distribution measurements in the sub-micrometer range using three monodisperse polystyrene latex spheres (PSL) spheres and polydisperse Arizona Road Dust (ARD) (Peters, et al., 2006). Peters found that the Grimm 1.108 and 1.109 portable aerosol spectrometers, which employ optical properties to size particles, detect particles smaller than 0.7 μm with greater efficiency than the APS. Therefore, when evaluating the performance of air sampling equipment in experimental laboratory studies, consideration should be given to selecting a particle size distribution measuring device or system that is as accurate and appropriate as possible for all relevant particle sizes and the design of the experiment performed.

Air Sampling Methods.

Dry filtration, solid impaction, liquid impinger, and virtual impaction methods are commonly employed to collect airborne biological agent samples. Dry filtration is frequently used to collect airborne viral biological agents as most other sampling methods

exhibit comparatively lower collection efficiencies for aerodynamic particles sizes less than 0.5 μm (Hinds, 1999). Impaction and interception are dominant particle collection mechanisms in dry filtration for particles larger than 0.3 μm. Diffusion is the dominant particle collection mechanism in dry filtration for particles smaller than 0.3 μm. In the sub-micrometer range, impaction, interception, and diffusion are least efficient at collecting particles 0.3 μm in size; therefore, filter efficiency increases for particles larger or smaller than 0.3 μm, which is the rationale for using 0.3 μm as the size benchmark for filter efficiency (Verreault, et al., 2008). However, dry filters are not ideal for biological agent sampling as they can cause structural damage to microorganisms or interfere with culture analysis of biological agent samples due to desiccation. Structural damage to or desiccation of microorganisms could lead to a false negative sample analysis, an extremely undesirable result when responding to an event where a biological agent attack is suspected. Burton used a *Bacillus anthracis* simulant to evaluate which combinations of four filters and extraction methods demonstrated the best recovery performance (Burton, et al., 2007). Burton found that mixed cellulose ester (MCE) and 1 μm PTFE filters in combination with vortexing and shaker extraction demonstrated the best recovery performance.

Impactors and cyclones are air samplers that employ solid impaction. Solid impactors draw a sampling air stream through a slit and direct the accelerated flow toward a solid surface. The flow streamlines abruptly change directions as the flow approaches the impaction surface, and the inertia of particles larger than the impactor's cut-point size deviate from the streamlines and strike the impactor (Verreault, et al.,

2008). Single stage solid impactors do not permit particle size or mass concentration evaluation for more than a single size range; those particles larger than the impactor cut-point size and smaller than a maximum particle size cut-point due to the sampler inlet utilized. The MOUDI was developed to permit evaluation of multiple size ranges. The MOUDI is a vertical stack of solid impactors. The successive stages of the MOUDI have smaller orifice holes than the previous stage, thereby enabling the MOUDI to operate as a series of single stage impactors with specific, individual particle size cut-point (Marple, et al., 1991). The MOUDI was inspired by the initial use of a single stage micro-orifice impactor to classify sub-micrometer aerosol particles (Kuhlmey, et al., 1981). Cyclones differ from solid impactors in that circular streamlines and centrifugal forces lead to particle deposition on a solid surface, and cyclones do not have as sharp a particle size cut-point as impactors (Hinds, 1999). Both impactors and cyclones tend to compromise biological agent viability due to the effects of impaction and desiccation. However, cyclones have been developed that use a wetted collection surface to diminish the effects of desiccation and improve culturability of biological agents (Griffiths, et al., 1997). Macher evaluated the performance of dry, personal cyclones against dry filtration in field experiments and found they performed similarly in collecting airborne fungi; however, the cyclones exhibited greater uncertainty at lower fungi concentrations (Macher, et al., 2008).

Liquid impingers have been used to sample for airborne biological agents for more than 70 years (Miles & Mistra, 1938) and comparatively evaluated for over 50 years (May & Harper, 1957). The evaluation of liquid impingers saw renewed interest as

the need for bioaerosol sampling grew in the 1990s. Interest in using liquid impingers was further enhanced as the collection media was more suitable to maintaining viability of biological agents and for subsequent splitting into multiple aliquots for separate analyses (Grinshpun, et al., 1997). The two liquid impingers most commonly used at present are the AGI-30 and the Biosampler®, manufactured by SKC, Inc., both typically operated at 12.5 lpm and considered low volume samplers as the sampling rates are less than 40 lpm (Verreault, et al., 2008). The AGI-30 performs well in collecting particles 2.0 μm and larger, but experiences a notable drop in collection efficiency for sub-micrometer particles. Presented in Table 2 are collection efficiencies of the AGI-30 and Biosampler®, as experimentally measured by Willeke (Willeke, et al., 1998). Willeke concluded that the design of the Biosampler® reduced the evaporative loss of collection fluid compared to the AGI-30, thereby reducing the reaerosolization of sub-micrometer particles and exhibiting superior collection efficiency for such particles.

Samplers that collect air samples at rates greater than 40 lpm are generally considered high volume samplers. The multistage liquid impinger is the most notable classic liquid impinger that operates as a high volume sampler. The multistage liquid impinger has three stages and can be run as high as 55 lpm. Each stage of the multistage impinger consists of a vertically oriented impinger tube that the sampled air is drawn through and towards a wetted disc. Particles larger than the cut-point size will strike the wetted disc and be retained. Particles that are smaller than the stage cut-point size will

Table 2: Particle collection efficiency of AGI-30 and Biosampler®
(Adapted from Willeke, et al., 1998)

Particle Size (Microns)	AGI-30 Collection Efficiency (%)	Biosampler Collection Efficiency (%)
0.3	69	78
0.6	71	88
0.8	72	91
1.1	82	92
1.7	93	93
2.0	95	95

follow the air flow and proceed to the next stage, with each successive stage having a smaller particle cut-point size (May, 1966). The multistage liquid impinger has two primary advantages over the critical orifice impinger: minimal violence of impingement minimizes damage to delicate cells and superior sustainment of flow rate through the compact third stage due to greatly reduced splashing and frothing of collection liquid on the wetted discs (Cown, et al., 1957). One limitation of the multistage liquid impinger is that its performance is degraded for very dilute aerosols (May, 1966).

Virtual Impaction

Virtual impaction is similar to classic solid impaction in that the inertia of a particle is used to separate particles in different size ranges. However, the most notable difference between virtual and solid impaction is that in solid impaction particles larger than a cut-point size are collected on a surface, whereas in virtual impaction no particles are technically collected, but rather, are separated into two different flow streams, with

one containing particles smaller than the cut-point size and the other containing particles larger than the cut-point size. Due to this separation in flows, virtual impactors are commonly referred to as dichotomous samplers as a single flow is separated into two distinct flows containing particles in different size ranges based on a single cut-point size (Loo, et al., 1976). However, a virtual impactor sampler can have multiple stages, as was the case with the first virtual impactor sampler. Hounam introduced a virtual impactor sampler that operated at 30 lpm with three different stages having corresponding cut-points of 1.2, 4, and 14 μm (Hounam & Sherwood, 1965).

Schematic diagrams of the basic design elements of a virtual impactor and a low cut-point virtual impactor are shown in Figure 4. The total flow is drawn through the acceleration nozzle, which accelerates the air and aerosol particles. The minor flow, typically 10 to 20% of the total flow, is drawn through the collection probe. The major flow, typically 80 to 90% of the total flow, produces sharply curved streamlines and proceeds to flow through the major flow cavity. Particles larger than a certain size lose fidelity with the major flow, due to their greater inertia, and cross over streamlines and enter the collection probe to enter the minor flow. Designing a virtual impactor with a sub-micrometer cut-point is a significant challenge as the necessary high jet velocities require low pressures downstream of the jet nozzle (Sioutas, et al., 1994). Sioutas found that theoretical predictions matched experimental results for virtual impactor performance as a reduction in the minor flow from 20% to 10% of the total flow leads to a larger cut-point size, an increase in particle losses, and a steeper collection efficiency curve.

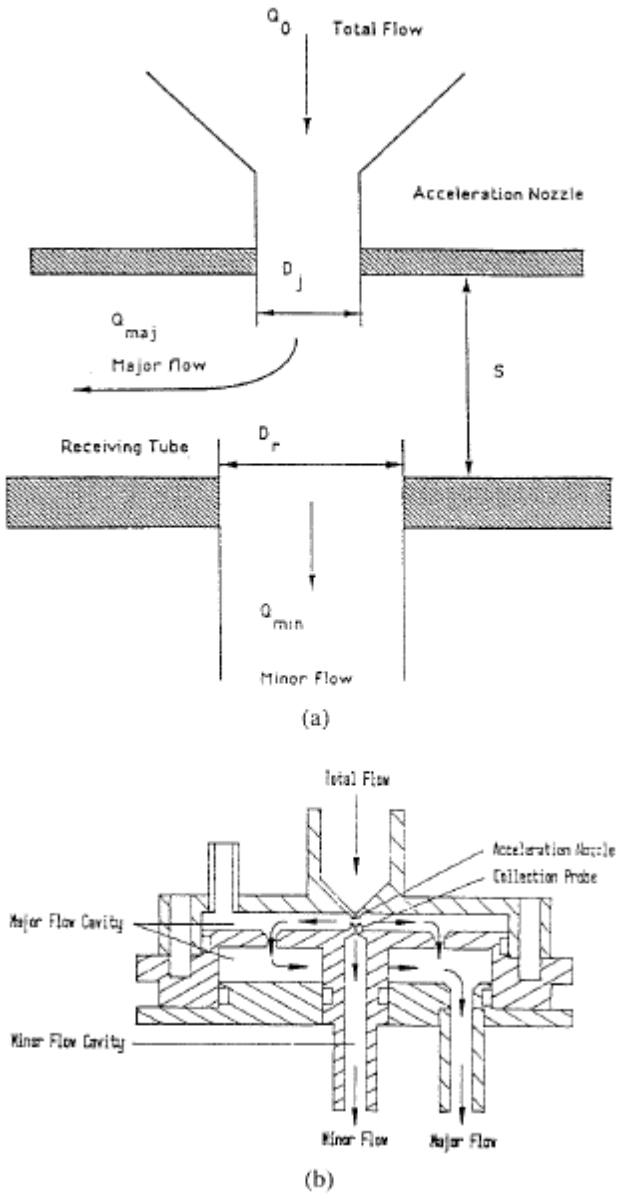

Figure 4: Schematics of a (a) virtual impactor and (b) low cut-point virtual impactor (From Sioutas, et al., 1994. Reprinted with permission from Taylor & Francis)

A key advantage offered by virtual impactors when sampling to detect low concentrations of biological agents in ambient air is that they concentrate particles in a minor flow, thereby substantially increasing the operative sample size while still

permitting the use of traditional biological agent analysis methods. Romay developed a three stage concentrating virtual impactor (CVI) that concentrated 50% to 90% of the particles in the 2.3 to 8.4 μm size range from a total flow of 300 lpm into a minor flow of 1 lpm (Romay, et al., 2002). The design of this CVI included features such as multiple nozzles to reduce the pressure drop for a given flow rate and cut-point and substantially reducing inadvertent deposition of large particles on internal surfaces by arranging nozzles to oppose each other (Marple, et al., 1990). However, virtual impactors have two distinct shortcomings in sampling for biological agents: (1) virtual impactors are not particle collectors, but only direct particles to separate flows to facilitate collection and (2) inherent to virtual impactor design is the practical mutual exclusion of simultaneously having a high total flow rate with substantial particle concentration and a sub-micrometer cut-point size. These are notable deficiencies when sampling ambient air containing a low concentration of sub-micrometer particles dispersing biological agents.

Air Force Fielded High Volume Samplers

The AF has elected to predominantly use high volume samplers, the DFU-1000 and XMX, when attempting to detect airborne biological agents. High volume sampling is particularly important when trying to detect biological agents in dilute outdoor ambient air (Cox & Wathes, 1995). The decision to use high volume samplers, rather than low volume samplers, helps minimize the risk of false negative detections due to low airborne biological agent concentrations and overall biological agent detection time period, so that informed command decisions can be made as quickly as possible. The DFU-1000 was used in a field study by Russell to evaluate environmental exposures of military training

recruits to adenovirus subtype 4 in their barracks (Russell, et al., 2006). Air samples were collected using two different methods: the DFU-1000 and an electrostatic precipitator. Positive PCR analyses for 42% and 50% of the samples collected by the DFU-1000 and electrostatic precipitator, respectively, demonstrated a credible sampling capability by the DFU-1000, as compared to the electrostatic precipitator. However, PCR analysis does not require active, culturable virus; therefore, Russell's study did not demonstrate that the DFU-1000 is effective in ensuring biological agent viability in cases when it is needed for detection or quantification.

There have been at least two field studies using the XMX, or a highly similar system, to collect biological agent samples. Brenner used a US Army prototype biological air sampler, the XM2, to determine the presence of animal viruses, coliphages, and bacteria in various locations at a wastewater management system irrigation site (Brenner, et al., 1988). The XM2 is a high volume, three stage, virtual impactor combined with a collection system using impingement and scrubbing to capture particles in a collection liquid. The total flow of the XM2 is 1,050 lpm, and the minor flow directed to the particle collection system is 15 lpm. The XM2 concentrates particles sized from 2 to 12 μm into the minor flow at a ratio of 8 to 1 compared to their respective concentrations in the total flow. The collection liquid was cultured in various media and observed for growth. No animal viruses were detected in cell cultures, but both coliphages and bacteria were recovered. Failing to detect animal viruses could have been due to use of inadequate cell culture media, inactivation of viruses, or the absence of viruses on particles in the size range collected (Brenner, et al., 1988). Schofield used the

XMX/2A and slit sampler arrays to collect air samples at a domestic poultry operation following an outbreak of Avian Influenza (AI) virus H7N3 (Schofield, et al., 2005). Other than having a secondary flow rate of 1 lpm instead of 12 lpm, the XMX/2A is nearly identical to the XMX, with both being manufactured by Dycor, except that the XMX/2A does not have a liquid impinger. Samples were collected in a variety of locations, inside and outside a barn, and conditions, upwind and downwind of a barn. A total of 240 samples were collected using slit sampler arrays and a total of 16 samples were collected using the XMX/2A. All samples were initially analyzed using PCR analysis. Any samples found positive for AI virus H7N3 by PCR were subsequently followed by virus cell culturing to demonstrate active virus. All samples collected by slit sampler arrays were negative by PCR. However, seven of the samples collected by the XMX/2A were positive by PCR, and two of these seven samples also yielded live virus by cell culture. Schofield had two conclusions important to outdoor environmental sampling for biological agents: (1) slit sampling technology, despite having been successfully used to collect SARS virus indoors (Booth, et al., 2005), was not effective in collecting AI virus outdoors and (2) live virus can be successfully collected using the XMX/2A outdoors. Schofield reasoned that the 30 lpm flow rate of the slit sampler arrays was probably too low to detect AI virus in outdoor conditions; therefore, use of low flow slit sampler arrays should not be a preferred selection to sample for AI virus in outdoor environments.

There has been at least one experimental laboratory study performed using both the DFU-1000 and XMX to collect biological agent samples. Cooper compared the

collection effectiveness of the DFU-1000 and XMX against low volume flow rate impingers using MS2 bacteriophage as a surrogate virus in an aerosol test chamber (Cooper, 2010). Cooper found that (1) the XMX could collect viral quantities within 25% of the quantities collected by low volume impingers when in moderate levels of airborne viral load, (2) the DFU-1000 performed marginally compared to the XMX for collection effectiveness in moderate levels and below of airborne viral load, (3) the DFU-1000 is unreliable for quantifying viral agent at moderate levels and below, and that (4) both the DFU-1000 and XMX could collect detectable levels of MS2 bacteriophage for PCR analysis for all concentrations tested. However, Cooper was unable to determine if Remel M5 was superior to PBS solution when used as the collection media for maintaining viability or capturing and retaining particles carrying MS2 bacteriophage when collecting samples using the XMX (Cooper, 2010).

Collection Media

Liquid impingers require collection media to capture and retain aerosol particles for analysis. PBS solution and sterile water are examples of commonly used collection media. It is important for the collection media to be at the very least benign and optimally supportive of the biological agent of interest when performing air sampling. PBS solution is probably the most commonly used collection media for liquid impingers when sampling for biological agents. PBS solution is a water-based salt solution that contains sodium chloride, sodium phosphate, and may also contain potassium chloride and potassium phosphate in certain formulations. The buffer, sodium chloride and sodium phosphate, helps to maintain a constant pH, and PBS solution is isotonic and non-

toxic to cells. Hermann compared the effects of various additives on PBS solution to optimize a sample collection process for porcine reproductive and respiratory virus (PRRSV) (Hermann, et al., 2006). Hermann compared additions of 1% activated carbon, 0.5% bovine serum albumin, 20% ethylene glycol, and a variety of combinations of all three additions to PBS solution. None of the additives or their combinations had a significant impact on the collection efficiency of PRRSV, with all results found to be within 10% of the standard PBS solution. However, the PBS solution with 20% ethylene glycol was found to be slightly more effective than standard PBS solution in collecting PRRSV. Additionally, Hermann confined virus quantification to PCR sample analysis; therefore, the effects of the additives on maintenance of active PRRSV were not evaluated.

Probably the most notable limitation of PBS solution and sterile water, when used as collection media for biological agent sampling, is that neither preserves viruses for an extended period of time (Cooper, 2010). For most AF operating environments, preservation of collected environmental virus samples is a necessary performance criterion when analysis for active virus is desired. Remel M5 media was found to be effective at preserving active virus for as long as 48 hours after specimen collection (Remel, 2005). Cooper used Remel M5 to collect MS2 bacteriophage in experimental studies and found that its use may have offered superior viral maintenance when compared to PBS solution (Cooper, 2010). However, Cooper found that Remel M5 performance was unacceptable when the XMX secondary flow rate was at the standard 12 lpm due to excessive foaming. Hermann evaluated the six anti-foaming agents to

determine their impact on viral infectivity and found that none had a significant effect on viral infectivity, although four did have a significant effect on host cells (Hermann, et al., 2006). Dycor subsequently developed a critical orifice flow reducer that reduced the XMX secondary flow rate to approximately 4.5 lpm and excessive foaming of Remel M5 was eliminated (Cooper, 2010). However, Hogan (Hogan, et al., 2005) and Riemenschneider both noted in their studies that reduced flow rate through the liquid impinger could have a significant effect on the sampler performance (Riemenschneider, et al., 2010). Additionally, Dycor has not provided any technical information concerning the impact on the performance of the XMX virtual impactor due to reducing the secondary flow rate. Therefore, if Remel M5 or any other collection media requiring a reduced liquid impinger flow rate is to be used as a collection media, then it is necessary to evaluate the performance of the virtual impactor at a reduced secondary flow rate, if determination of the limit of detection is desired.

Fluorometry

Fluorometry is a type of electromagnetic spectroscopy in which fluorescent light from a sample is analyzed (Sharma & Schulman, 1999). A beam of light excites the electrons of molecules of a certain compound, and the excited electrons emit light of a lower energy. Light emitted by an excited electron is fluorescent light. By measuring the intensity of the fluorescing light emitted, the quantity of the fluorescing compound can be determined. Fluorometry of liquid samples was pioneered by Eisinger (Eisinger & Flores, 1979). Eisinger developed several fluorometric techniques for evaluating blood samples (Eisinger & Flores, 1985). Fluorometry has been employed by many researchers

to evaluate the amount of fluorescent acid droplets or number of fluorescent PSL spheres in liquid media, including Marple, Sioutas, and Romay (Marple, et al., 1991; Sioutas, et al., 1994; and Romay, et al., 2002). In particular, Kesavan conducted fluorometric analysis to determine the number of fluorescent PSL spheres in 20 milliliters (mL) of filtered deionized water, after removing the PSL spheres from membrane filters by hand shaking and vortexing the mixture. Kesavan observed a linear response in the amount of fluorescent light emitted by the number of PSL spheres in the solution for PSL spheres ranging from 0.5 to 5 µm in size (Kesavan & Schepers, 2006).

Problem Statement and Summary

Previous literature provides a thorough background on laboratory and field studies on air sampling for biological agents. In previous studies using the XMX or a highly similar device, researchers were able to collect airborne biological agent samples and maintain agent viability for both PCR and virus cell culture analyses, demonstrating the capability of the XMX to support biological agent detection as a high volume air sampling platform. Also shown was the ability to successfully use multiple collection media, PBS solution and Remel M5, to collect biological agents for analysis. However, only one study evaluated the performance of the specific XMX model employed by the AF. Furthermore, for all other studies reviewed, the secondary flow rate of the XMX virtual impactor was 1 lpm, which is different from the standard secondary flow rate of 12 lpm and the reduced secondary flow rate of 4 to 5 lpm, used to prevent excessive foaming of Remel M5 collection media. The performance of the XMX is largely based upon two subcomponents: its virtual impactor and liquid impinger. The primary

performance metric for the virtual impactor is the CR and for the liquid impinger it is the percentage of particles that are captured and retained in the collection media. None of the previous studies evaluated either of these performance metrics for these two subcomponents, and values for both these performance metrics are needed to evaluate the limit of detection when using the XMX to collect biological agent samples.

The AF may wish to consider operational use of collection media other than PBS solution, particularly Remel M5, for improved maintenance of biological agent viability. To use Remel M5, and potentially other collection media, the secondary flow rate must be reduced substantially from the standard flow rate of 12 lpm to avoid excessive foaming; however, the AF has no information regarding how reducing the secondary flow rate impacts the CR of the virtual impactor. Further, the AF has no information regarding the variability of virtual impactor performance between XMX units. Additionally, the AF has no direct information regarding the performance of PBS solution or Remel M5 in capturing and retaining particles during sample collection. An experimental study should be conducted to evaluate the performance of the XMX virtual impactor. Specifically, the AF should evaluate how different secondary flow rates impact the CR of the virtual impactor; evaluate inter-instrument virtual impactor performance between XMX units; and produce plots of CR as a function of secondary flow rate for potential use in future limit of detection studies. Also, an experimental study should be conducted to evaluate the performance of PBS solution and Remel M5 collection media. Specifically, the AF should compare the performance of PBS solution and Remel M5 to capture and retain particles with the secondary flow rate at 5 lpm, and the AF should

compare the performance of PBS solution to capture and retain particles at two different flow rates to evaluate the impact of secondary flow rate on reaerosolization.

The focus of this research is to evaluate virtual impactor CR performance and variability at secondary flow rates of 5 lpm and 10 lpm, and determine the fraction of particles that are captured and retained in two different collection media, PBS solution and Remel M5, when operating the XMX at standard and reduced secondary flow rates.

III. Methodology

Objective

The section describes the methodology, procedures, and analyses used to evaluate the following performance characteristics when collecting an air sample for biological agent detection and analysis:

1. Measure the primary and secondary flow rates of the XMX.
2. Determine the CR of the XMX virtual impactor.
3. Evaluate the impact of changing the secondary flow rate on the observed CR.
4. Evaluate the inter-instrument variability of the CR for the three XMX samplers tested.
5. Produce plots of CR as a function of particle size for two different secondary flow rates for XMX samplers.
6. Determine the fraction of particles of particles passing through the liquid impinger that are captured and retained in collection media.
7. Compare the performance of two different collection media at the same secondary flow rate.
8. Compare the performance of a collection media at two different secondary flow rates.
9. Perform a microscopic analysis to determine the concentration of fluorescent PSL (FPSL) spheres in collection media.

Study Design Overview

The primary means for evaluating the XMX is to operate them individually in an aerosol test chamber (ATC) while selected test aerosol concentrations and conditions are measured and monitored. Due to the high primary flow rate, size, and heat generated by the XMX, the ATC must be sufficiently large and the XMX exhaust flow must be discharged outside the ATC, otherwise the test aerosol might not be suitably distributed in the ATC or the environmental conditions in the ATC could be adversely impact conducting the experimental data collection. Test aerosol selection, generation, fluorometry, and microscopy analysis methods must be established as well. The necessary methods, procedures, and selections for conducting this experimental study are described in this section. Experimental data were collected as detailed in the study schedule presented in Appendix A.

Aerosol Test Chamber Setup and Layout

Experimental studies were performed in an ATC operated by the US Environmental Protection Agency (EPA) in Research Triangle Park, North Carolina. The ATC has a volume 14 cubic meters (m^3), being 2.9 meters (m) long, 2.2 m wide, and 2.2 m high. The layout of the ATC is shown in Figure 5.

Particle size concentration measurements were made using either a TSI Aerodynamic Particle Sizer (APS), model number 3321, or a TSI Ultraviolet Aerodynamic Particle Sizer (UV-APS), model number 3314. Two or three APSs were in the ATC, one to monitor the ATC particle concentration and the others to monitor the particle concentration of the XMX secondary flow. The XMX was placed on a metal

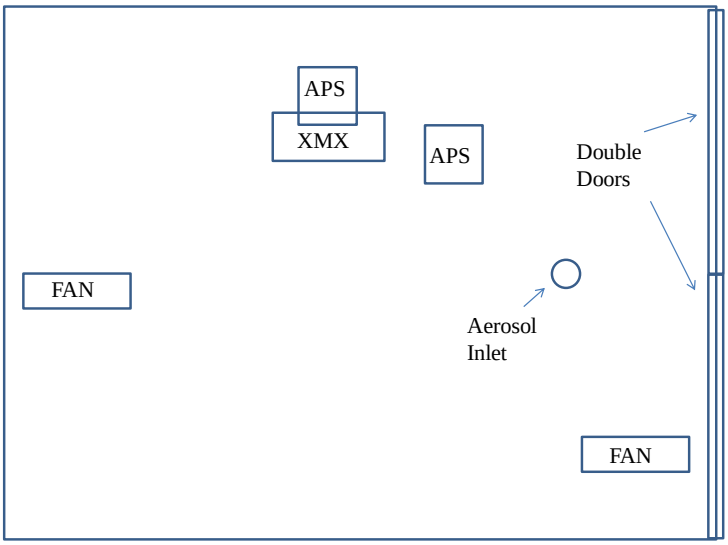

Figure 5: Aerosol test chamber layout

stand in the ATC. The test aerosol inlet was located approximately 0.9 m from the inlet of the APS monitoring the ATC particle concentration, 1.4 m from the inlet of the XMX, and 0.7 m from the double doors of the ATC. The inlets of the APS monitoring the ATC particle concentration and the XMX were both at a vertical height of approximately 1.7 m above the ATC floor. The ATC was equipped with two circulating fans for aerosol mixing.

Test Aerosol Generation

Two separate aerosol generation systems were used to generate the test aerosols used during this study. A polydisperse Arizona Road Dust (ARD) aerosol was used to evaluate the performance of the XMX virtual impactor, and two different PSL sphere

aerosols were used to evaluate the performance of collection media. The ARD test aerosol generating system is shown in Figure 6. The polydisperse ARD aerosol, named test aerosol 1 (TA1), manufactured by Powder Technology, Inc., was nominally categorized to generate aerosols with 95% of the total particle mass attributable to particles from 5 to 10 µm in size. The ARD was loaded into a model Wright Dust Feeder (WDF) Mark II, manufactured by BGI, Inc. The WDF was supplied by dried, compressed air at 40 pounds per square inch (psi) by a Compressed Air Dryer, manufactured by Wilkerson, Inc. The speed of the WDF was adjusted between 0.03 and

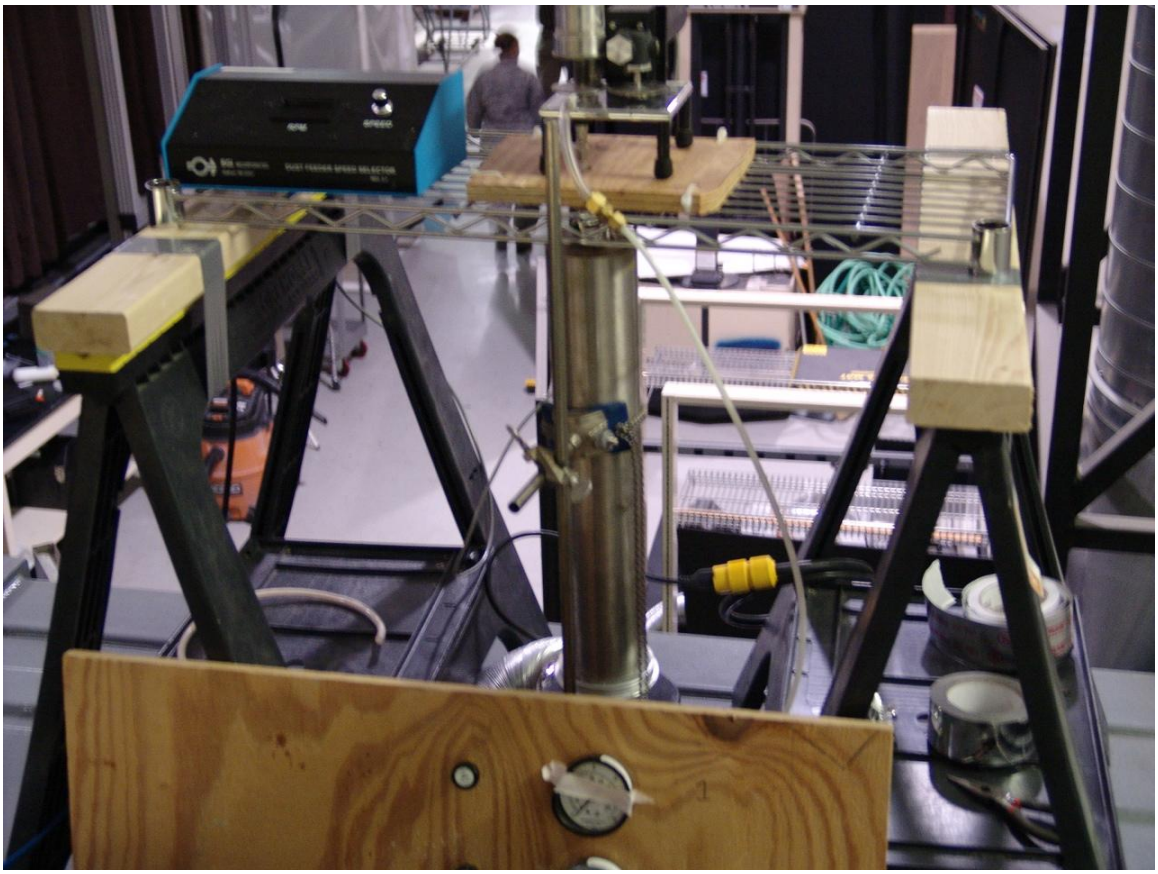

Figure 6: Arizona Road Dust aerosol generation system

0.04 revolutions per minute (rpm) throughout the experiment to simultaneously maintain a nominally consistent particle concentration distribution in the ATC and prevent saturation of either APS, which could lead to erroneous particle concentration measurements. The aerosol generated by the WDF was passed through a model 3054 Krypton-85 charge neutralizer, manufactured by TSI, Inc., to neutralize excess the charge of ARD particles. The ARD test aerosol was then injected into the ATC via the aerosol inlet in the ceiling of the ATC.

Two different fluorescent PSL (FPSL) sphere aerosols were used in this study, with one aerosol, named test aerosol 2 (TA2), containing 1.0 µm blue and 3.1 µm green FPSL spheres, and the other, named test aerosol 3 (TA3), containing 0.70 µm blue and 1.9 µm green FPSL spheres. All FPSL spheres were manufactured by Thermo Scientific, Inc., and product information for the FPSL spheres is presented in Table 3.

Table 3: Fluorescent PSL sphere test aerosols

Test aerosol	Diameter (µm)	Color	Part number	Lot number
2	1.0	Blue	B0100	35449
2	3.1	Green	G0300	34875
3	0.7	Blue	B700	37670
3	1.9	Green	G0200	37653

Both FPSL sphere test aerosols were generated using the same system. A model 9306 Six-Jet Atomizer (SJA), manufactured by TSI, Inc., was filled with a liquid mixture of 50% ethanol and 50% deionized water. The two different size and color FPSL spheres were added to the liquid mixture in the SJA using a pipette. The aerosol generated by the

SJA was passed through a model 3062 Diffusion Dryer, manufactured by TSI, Inc., filled with silica gel dessicant to dry the PSL particles. The FPSL test aerosols were then injected into the ATC via the aerosol inlet in the ceiling of the ATC.

Equipment Preparation

Preparation of XMX Units.

Five XMX units were made available for this study and three of these five XMX units were used to conduct the experimental work. The canister components of the XMX, shown in Figure 7 (LaRoche, 2009), were dipped in water, air dried, wiped by paper towels to remove any remaining liquid, and then reassembled per manufacturer's instructions. Three flow rates were measured for each of the five XMX units: total (exhaust) flow, standard secondary (sampling) flow, and reduced secondary flow. The total flow was measured using a HI-Q Flow Calibrator, model D-AFC-1100L-PRES,

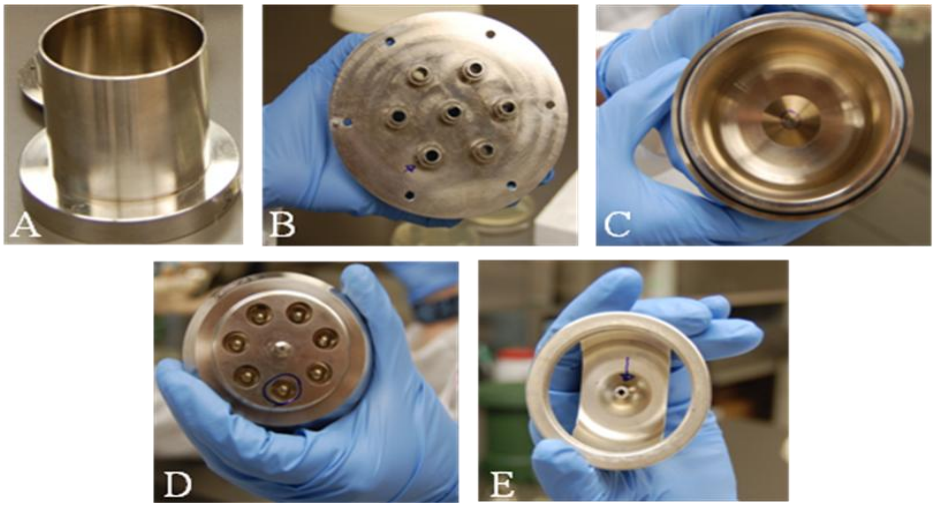

Figure 7: Components of XMX/2L-MIL virtual impaction module
A - Primary inlet, B - Primary nozzle plate, C - Upper canister, D - Lower canister
E - Final nozzle (LaRoche, 2009)

manufactured by HI-Q Environmental Products, Inc. The flow calibrator was attached in-line to the exhaust port on the XMX, the XMX was turned on, and exhaust flow rate and temperature readings were recorded every 30 seconds for five minutes, for a total of ten actual flow rate readings. The ten actual flow rate readings were converted to standard flow rate values by correcting for exhaust temperature, as the air is heated as it flows through the XMX blower immediately before being exhausted. The standard secondary flow was measured using a DryCal Flow Calibrator, model Defender 520-H, manufactured by BIOS International Corp. The DryCal Flow Calibrator was inserted in the vacuum pump line that draws the secondary flow through the XMX virtual impactor. A 50 mL sample collection tube was filled with 5 mL of water and inserted into the XMX liquid impinger module per manufacturer's instruction. The vacuum pump line and liquid impinger module of an XMX are shown in the left image of Figure 8 and a sample collection tube installed in the liquid impinger module of an XMX is shown in the right image of Figure 8. The XMX was turned on and flow rate measurements were recorded approximately every 30 seconds for approximately five minutes, for a total of ten flow rate readings. The reduced secondary flow was measured exactly as the standard secondary flow, except that each XMX had its flow reducer inserted in the vacuum pump line upstream of the DryCal Flow Calibrator. The flow reducer, provided by Dycor, is a critical orifice created by drilling a small hole length-wise through a brass cylinder that is approximately 5 mm in diameter and 25 mm long. The flow reducer is designed to be inserted in the vacuum pump line between the liquid impinger module and the fluid trap and reduce the secondary flow from approximately 12 lpm to between 4 and 5 lpm

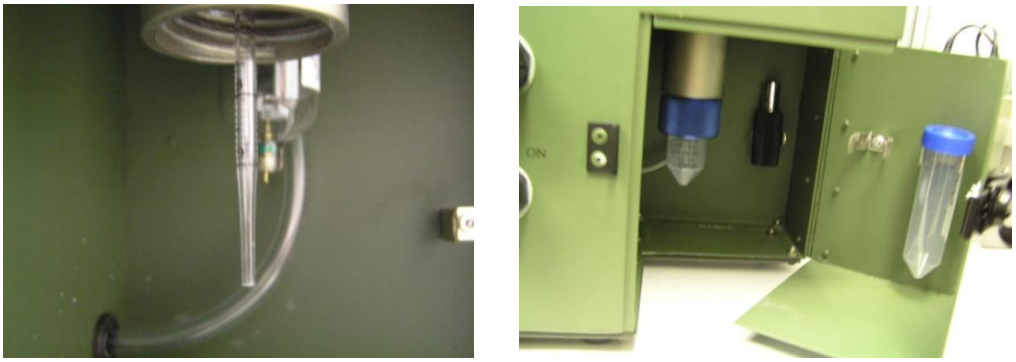

Figure 8: XMX impinger module with (right) and without (left) collection tube (Cooper, 2010)

(Cooper, 2010). The ambient temperature and pressure in the lab were 21.2 degrees Celsius and 100.5 kilo Pascals, respectively. The DryCal flow calibrator automatically corrects for pressure; therefore, secondary flow rate measurements were not corrected for temperature or pressure.

Preparation of Collection Media.

Two different collection media were used in this study: PBS solution and Remel M5. PBS solution was selected because it is recommended by Dycor and is a preferred collection media for biological agents (Hermann, et al., 2006). Remel M5 was selected as a potential alternative to PBS solution, which facilitates particle capture and retention performance comparison between PBS solution and Remel M5 at reduced secondary flow. Cooper noted superior collection effectiveness of MS2 bacteriophage when operating the XMX at reduced secondary flow using Remel M5 collection media as compared to that found when operating the XMX at standard secondary flow using PBS solution collection media (Cooper, 2010). Equivalent particle capture and retention performance of PBS solution and Remel M5 at reduced secondary flow would indicate

that the superior collection effectiveness noted by Cooper was due to superior maintenance of MS2 bacteriophage viability by Remel M5 as compared to that of PBS solution.

The PBS solution was produced at the EPA laboratories by adding sodium chloride and sodium phosphate to distilled water. Remel M5 collection media, lot number 846140, was purchased from Remel, Inc. Remel M5 is a liquid media designed for the collection and transport of viruses. Remel M5 contains vancomycin, amphotericin B, colistin, and protein stabilizers to support maintenance of viral agent viability. Remel M5 is packaged in 3 mL vials containing glass beads. Remel M5 was poured from the vials, while simultaneously straining the glass beads, into a glass beaker creating 50 mL lots. Fifty microliters (µL) of Y-30 emulsion antifoaming agent, manufactured by Sigma Aldridge Company, was added to the 50 mL to reduce foaming of Remel M5 while operating the XMX during sample collection, as noted in previous studies conducted by USAFSAM (Cooper, 2010). The PBS and Remel M5 solutions were transferred to 50 mL conical collection tubes. Each 50 mL collection tube received either 5 mL of PBS or Remel M5 solution. Collection tubes were prepared for experimental sample collection using this procedure.

Particle Concentration Ratio Experimental Data Collection

Three XMX samplers (referred to as: XMX1, XMX2, and XMX3) had their concentration ratios as a function of particle size determined at two secondary flow rates, 5 and 10 lpm. XMX1 was placed in the ATC. No collection tube was installed in the liquid impinger module. Instead, a special connector and a piece of Tygon tubing

approximately 0.5 m long were attached to the liquid impinger tube, as shown in Figure 9, and the other end of the tube was attached to the inlet of an APS (referred to as: APS1), as shown in Figure 10. APS1 substituted for XMX1's vacuum pump as the generation source of the secondary flow. APS1 then simultaneously drew a flow of 5 lpm of sampling air through XMX1's virtual impactor and measured the particle concentration of the secondary flow as a function of particle diameter. A test aerosol of ARD, TA1, was lofted in the ATC and maintained at a relatively constant particle concentration distribution. The chamber ARD particle concentration as a function of particle diameter was measured by a second APS, APS2. XMX1 was operated for

Figure 9: Special connector and tubing connected to liquid impinger tube

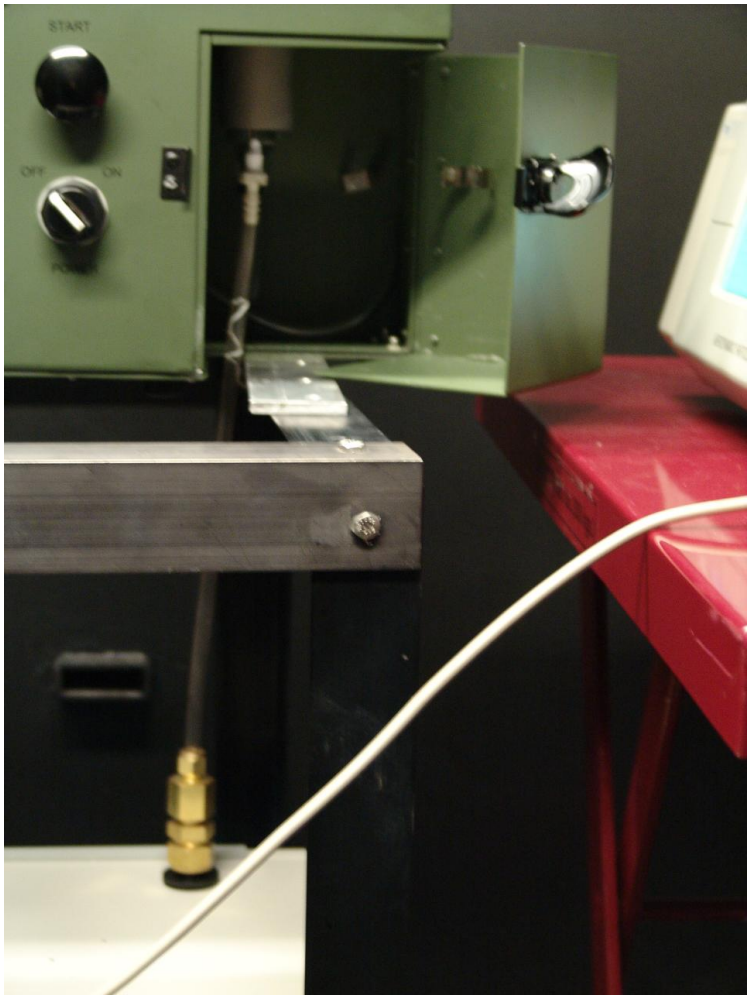

Figure 10: Tubing connecting liquid impinger tube to aerodynamic particle sizer

100 minutes and a total of 20 pairs of samples, each five minutes in duration, were simultaneously collected by APS1 and APS2. This process was then repeated with XMX2 and XMX3.

Next, the 0.5 m long tube and special connector connecting APS1 and the liquid impinger tube of XMX3 were replaced by a 0.2 m long piece of Tygon tubing with a special connector attached to a one-to-four flow splitter, as shown in Figure 11. APS1

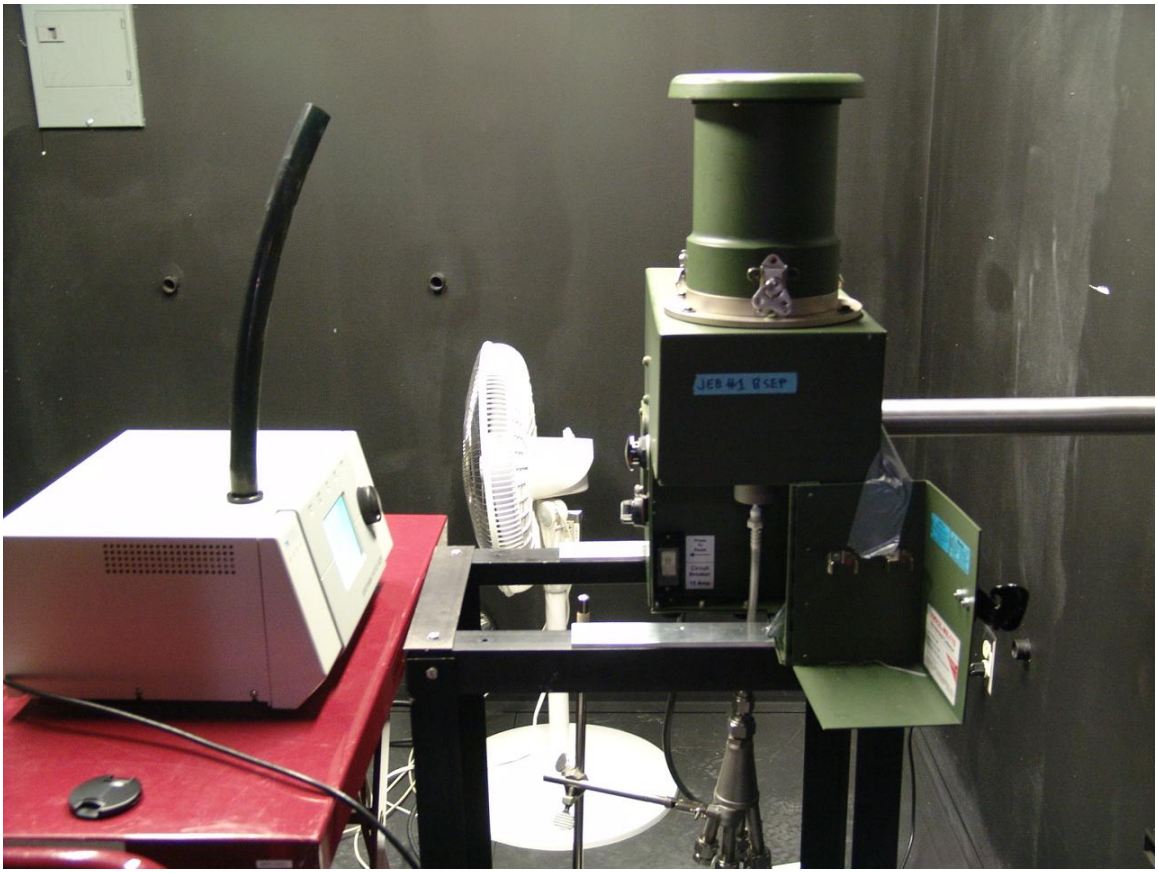

Figure 11: Tubing connecting liquid impinger tube to one-to-four flow splitter

was moved approximately 0.5 m from its original location on the ATC floor, and another APS, APS3, was brought into the ATC and positioned on the floor approximately 1.0 m from APS1. The inlets of APS1 and APS3 were then connected to opposite legs of the one-to-four splitter with conductive silicon tubing, as shown in Figure 12, and the remaining two legs of the one-to-four splitter were capped, as shown in Figure 13. APS1 and APS3 substituted for XMX3's vacuum pump as the generation source of the secondary flow. APS1 and APS3 simultaneously drew a combined flow of 10 lpm of sampling air through the virtual impactor and measured the particle concentration of the

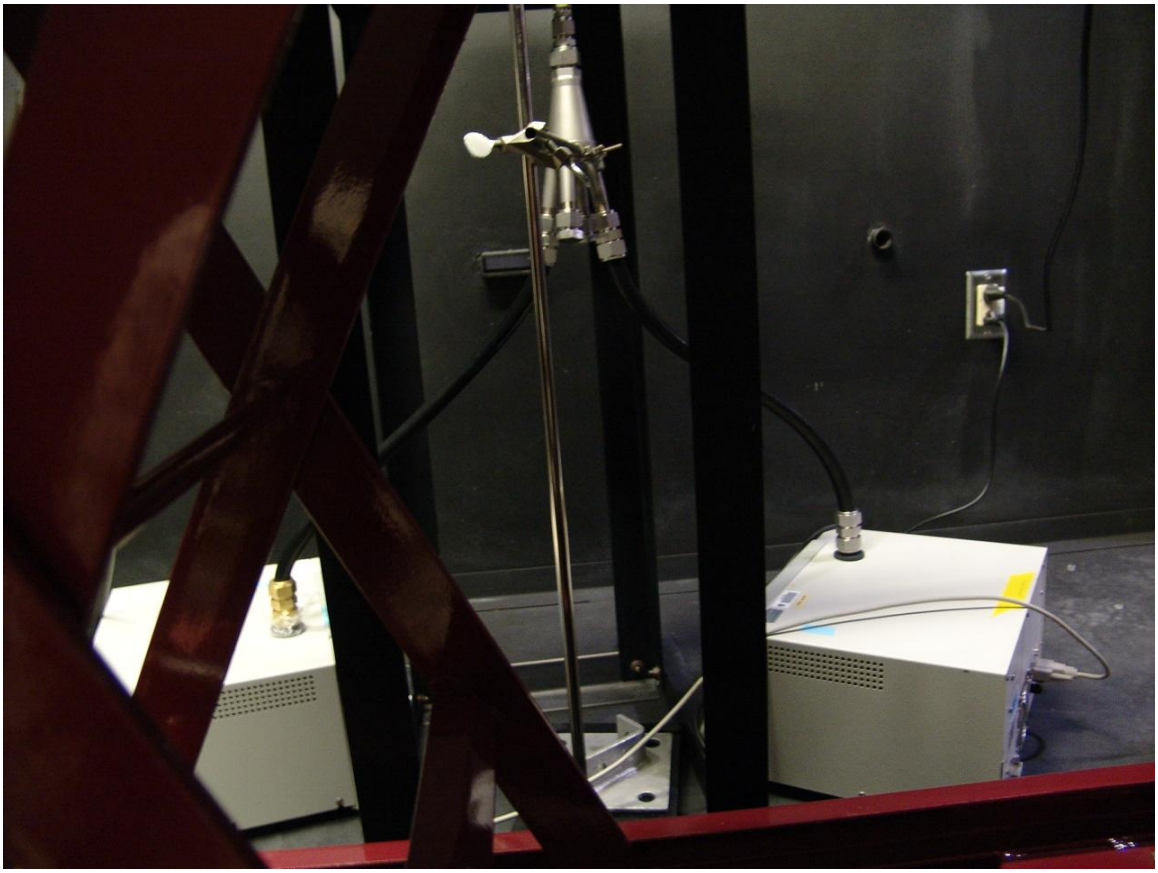

Figure 12: Tubing connecting two branches of one-to-four flow splitter to two aerodynamic particle sizers

secondary flow as a function of particle diameter. TA1 was lofted in the ATC and maintained at a relatively constant particle concentration distribution. The chamber ARD particle concentration as a function of particle diameter was measured by APS2. XMX3 was operated for 100 minutes, and a total of 20 sets of samples, each five minutes in duration, were simultaneously collected by APS1, APS3, and APS2. This process was then repeated with XMX1 and XMX2.

Figure 13: Two branches of one-to-four flow splitter capped

Collection Media Particle Capture and Retention Experimental Data Collection

Three XMX samplers, XMX1, XMX2, and XMX3, were used to evaluate the capture and retention of four sizes of FPSL spheres in two different collection media, PBS solution and Remel M5. This evaluation was made at two different secondary flow rates: 'standard', approximately 15 lpm, and 'reduced', approximately 5 lpm. XMX1 was placed in the ATC; APS1, APS2, and APS3 were removed from the ATC; and a UV-APS, APS4, was placed in the ATC, as shown in Figure 14. The UV-APS measures particle size just as an APS does; however, it also measures the intensity and color of

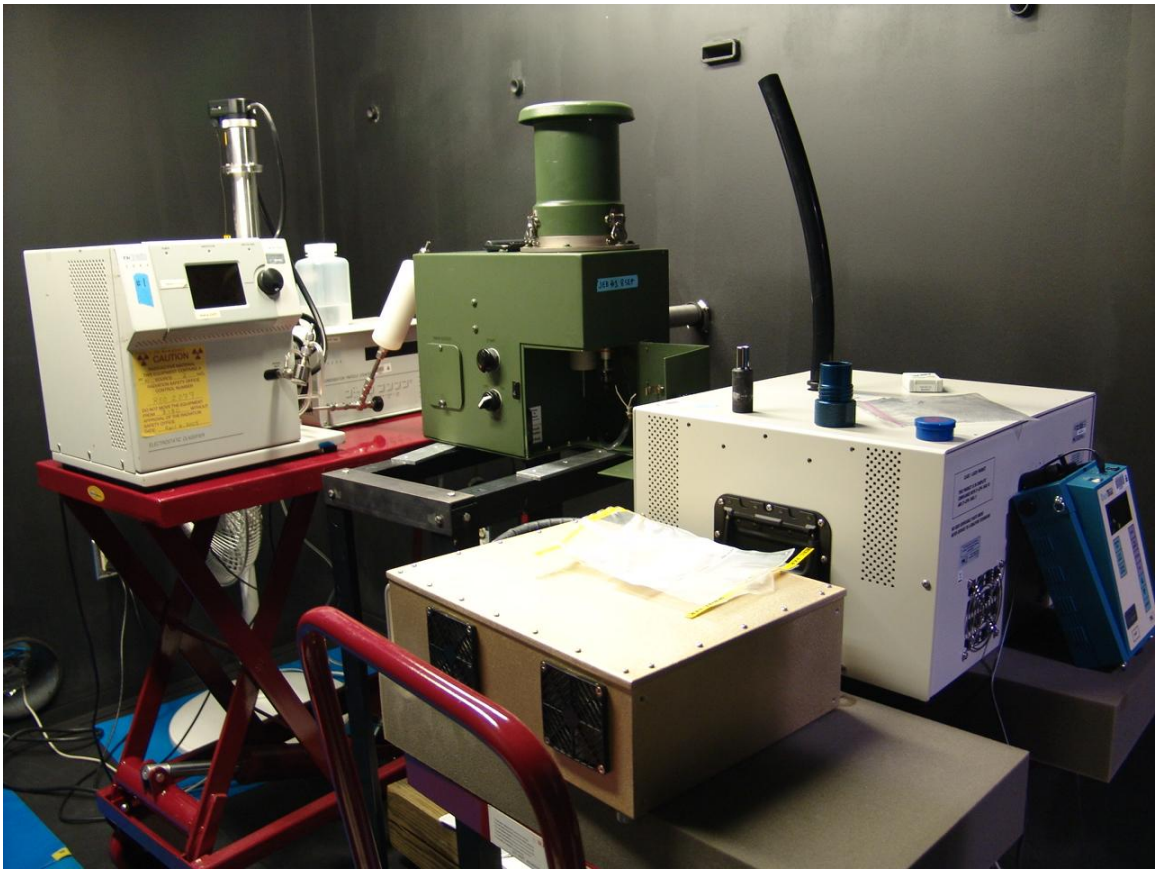

Figure 14: Ultra-violet aerodynamic particle sizer with black inlet tubing

fluorescent light emitted by the particles. Therefore, the UV-APS simultaneously can discriminate particles both by size and fluorescent light they emit. A test aerosol, TA2, of two sizes and colors of FPSL spheres was lofted in the ATC and maintained at a relatively constant particle concentration distribution. The ATC aerosol concentration as a function of particle diameter and emitted fluorescent light intensity was measured by APS4. XMX1 was operated with its flow secondary flow reducer installed. A collection tube with 5 mL of PBS solution collection media was installed in the liquid impinger module. XMX1 and APS4 were operated simultaneously for a five minute sampling

period. The collection tube was removed from the liquid impinger module and immediately capped. A second collection tube with 5 mL of PBS solution collection media was installed in the liquid impinger module and XMX1 and APS4 were again operated simultaneously for a five minute sampling period. This process was repeated eight more times so that a total of ten samples, each five minutes in duration were collected. Following the collection of ten samples using PBS solution as the collection media, this process was repeated ten times with the only change being that the collection tube was filled with 5 mL of Remel M5 collection media. Afterwards, the secondary flow reducer was removed. Ten samples were collected using 5 mL of PBS solution as collection media. This process was then repeated with XMX2 and XMX3.

After collecting 30 samples with XMX3, XMX3 was removed from the ATC and XMX1 was placed in the ATC. A test aerosol of two sizes and colors of FPSL spheres, TA3, was lofted in the ATC and maintained at a relatively constant particle concentration distribution. The ATC aerosol concentration as a function of particle diameter and emitted fluorescent light intensity was measured by APS4. XMX1 was operated with its secondary flow reducer installed. A collection tube with 5 mL of PBS solution collection media was installed in the liquid impinger module. XMX1 and APS4 were operated simultaneously for a five minute sampling period. The collection tube was removed from the liquid impinger module and immediately capped. A second collection tube with 5 mL of PBS solution collection media was installed in the liquid impinger module, and XMX1 and APS4 were again operated simultaneously for a five minute sampling period. This process was repeated eight more times so that a total of ten samples, each five

minutes in duration were collected. Following the collection of ten samples using PBS solution as the collection media, this process was repeated ten times with the only change being that the collection tube was filled with 5 mL of Remel M5 collection media. Following the collection of ten samples using Remel M5 as the collection media, the secondary flow reducer was removed. Ten samples were collected using 5 mL of PBS solution as collection media. This process was then repeated with XMX2 and XMX3. In total, 180 samples were collected using XMX1, XMX2, and XMX3 for two different FPSL aerosols at two different secondary flow rates. A summary of the sampling collection performed for the evaluation of particle capture and retention is presented in Table 4.

Table 4: Summary of the sampling collection performed for the evaluation of particle capture and retention in collection media

XMX	Secondary flow rate	Collection media	Test aerosol	# of samples
XMX1	Reduced	PBS solution	TA2	10
XMX1	Reduced	Remel M5	TA2	10
XMX1	Standard	PBS solution	TA2	10
XMX1	Reduced	PBS solution	TA3	10
XMX1	Reduced	Remel M5	TA3	10
XMX1	Standard	PBS solution	TA3	10
XMX2	Reduced	PBS solution	TA2	10
XMX2	Reduced	Remel M5	TA2	10
XMX2	Standard	PBS solution	TA2	10
XMX2	Reduced	PBS solution	TA3	10
XMX2	Reduced	Remel M5	TA3	10
XMX2	Standard	PBS solution	TA3	10
XMX3	Reduced	PBS solution	TA2	10
XMX3	Reduced	Remel M5	TA2	10
XMX3	Standard	PBS solution	TA2	10
XMX3	Reduced	PBS solution	TA3	10
XMX3	Reduced	Remel M5	TA3	10
XMX3	Standard	PBS solution	TA3	10

Fluorometric Calibration Curves

The performance of PBS solution and Remel M5 collection media to capture and retain aerosol particles during a five minute sampling period was measured. In order to evaluate the performance of collection media to capture and retain aerosol particles, a method had to be developed to measure the number of particles in liquid collection media. Fluorometry was selected as the method employed to measure the number of particles in liquid collection media. Fluorometry is a type of electro-magnetic spectroscopy in which fluorescent light emanating from a sample is analyzed. The intensity of the emanating fluorescent light is proportional to the amount of fluorescing material in the liquid media. Fluorescent PSL (FPSL) spheres were chosen as test aerosol particles because the number of FPSL spheres captured and retained in the collection media could be measured by fluorometric analysis.

Four sizes of FPSL spheres were chosen for this experimental study, ranging from 0.7 to 3.1 micrometers in diameter (Table 3). These four sizes were chosen for three primary reasons: they fall within or near the 1.0 to 10 μm range over which the XMX virtual impactor is designed to concentrate particles into the secondary flow; permit evaluation of collection media performance for submicron particles; and all may be readily aerosolized by the SJA. Since the FPSL spheres are aerosolized in pairs of different size and color, fluorometric analysis can distinguish between particles of different sizes when present together in the same collection media.

Stock samples of known concentrations were prepared for each of the four FPSL spheres. These stock samples were then added to measured amounts of each collection

media to create a volume of collection media with known concentrations of two sizes of FPSL spheres to create calibration standards. These calibration standards were analyzed using a Fluorometer, model Fluorolog-3, manufactured by HORIBA Jobin Yvon, and fluorescent intensities were recorded for each calibration standard. Linear calibration equations were determined to express the concentrations for each size FPSL sphere in PBS solution or Remel M5 collection media. The calibration concentration ranges for each FPSL sphere and collection media combination evaluated are presented in Table 5. The calibration plots are presented in Appendix B.

Table 5: Calibration concentration ranges for fluorescent PSL spheres in collection media

Test aerosol	Diameter (μm)	Color	Lowest concentration (number per mL)	Highest concentration (number per mL)
2	1.0	Blue	12,500	2,275,000
2	3.1	Green	1,250	201,500
3	0.7	Blue	1,250	500,000
3	1.9	Green	1,250	500,000

Microscopic Analysis

Fluorometric analysis of collection media was used to measure the concentration of FPSL spheres captured and retained in the collection media during a five minute sample collection period. While fluorometry is an accepted, accurate, and relatively fast method for measuring FPSL sphere concentration in collection media, it can provide no qualitative information regarding the condition of the FPSL spheres that are captured and retained in the collection media. Therefore, microscopic analysis was performed on 10% of the samples collected to assess two characteristics: the occurrence of physical alteration of FPSL spheres due to sample collection and the feasibility of determining FPSL concentration in collection media by microscopic counting technique.

Microscopic analysis of FPSL spheres was performed using an Axioskop microscope, manufactured by Carl Zeiss International. The Axioskop was equipped with a set of optical filters to enable independent viewing of individual colors, wavelengths, of light. Stock samples of the four FPSL spheres were microscopically examined to verify their morphology, fluorescent characteristic, and relative sizes. The Axioskop optical filter set did not permit independent viewing of fluorescing blue light, thereby rendering definitive microscopic analysis of blue FPSL spheres in collection media impossible. Therefore, only green FPSL spheres in collection media were microscopically assessed.

One sample was randomly selected from each of the eighteen sets of ten samples noted in Table 4 for microscopic analysis. Each randomly selected sample was processed by following the same procedure using the Axioskop, a vortexer, a micropipette, a Petroff Hausser Counting Chamber (PHCC) slide, and slide slip cover. First, the PHCC slide was prepared using a stock sample of 3.1 µm green FPSL spheres and placed in the jig of the Axioskop that holds a slide in a fixed position. The Axioskop was adjusted using the 10X magnification lens until images of the FPSL spheres were in sharp focus when viewed by the camera of the Axioskop. The Axioskop settings were then unchanged, so as to eliminate the need for adjustments during microscopic analysis of the eighteen selected samples.

The PHCC slide and slide slip cover were cleaned with methanol and dried. The sample collection tube was vortexed for 30 seconds, and a 10 µL aliquot of collection media was extracted from the collection tube using the micropipette. The aliquot was ejected onto the PHCC slide, and the slip cover was placed onto the slide. The slide slip

cover was slid slightly back and forth on the PHCC slide until no air bubbles were noted under the slide slip cover. The PHCC slide was placed onto the Axioskop so that the cell of the PHCC slide was under the lens of the Axioskop. The PHCC slide was moved slightly until several of the green FPSL spheres were seen and qualitatively evaluated for apparent physical alteration. After completing qualitative evaluation of several green FPSL spheres, the PHCC slide was then positioned in the jig of the Axioskop. A picture of the area being viewed was taken by the camera of the Axioskop. The image file of the picture was opened, a 400 µm by 400 µm area of the image was randomly selected, and the number of green FPSL spheres in this area were counted and recorded. The depth of the PHCC slide cell is 0.02 mm; therefore, the volume of collection media from which the number of green FPSL spheres was counted was 3.2×10^{-6} mL.

Data Analysis

Calculation of Virtual Impactor Concentration Ratio.

The concentration ratio (CR) of XMX virtual impactors was calculated using ARD particles over 42 size channels ranging from 0.542 to 10.37 µm at secondary flow rates of 5 and 10 lpm. The CR was calculated by dividing the particle number concentration for each of the 42 size channels measured by an APS analyzing the air flow through the liquid impinger tube by the particle number concentration for each of the 42 size channels measured by an APS analyzing the air inside the ATC. The two APSs used to analyze the air flow through the liquid impinger tube and the air in the ATC were the same model; therefore, there was no need to apply any correction factors to any of the size channel data. A two-way analysis of variance with several observations per cell was

performed on the calculated CR data for each particle size channel to evaluate the significance of secondary flow rate on the CR and inter-instrument XMX CR variability. The mean and standard deviation of the CR for each particle size channel were calculated using the data from all the XMXs, and the mean CR with upper and lower 89% confidence interval limits were plotted as a function of particle size for secondary flow rates of 5 and 10 lpm.

Calculation of Capture and Retention of Particles in Collection Media.

The concentration of FPSL spheres in collection media was measured via fluorometric analysis. The number of FPSL spheres captured and retained in collection media was calculated by multiplying the FPSL sphere concentration in collection media by the volume of collection media remaining in the collection tube after the five minute sample collection period. The number of particles that flowed through the liquid impinger tube was calculated by multiplying together the particle concentration in the ATC, secondary flow rate, the CR for the FPSL sphere at the secondary flow rate, and the sampling time. The particle capture and retention efficiency (CRE) was calculated by dividing the number of FPSL spheres captured and retained in the collection media by the number of particles that flowed through the liquid impinger tube. Single factor ANOVA evaluations were performed to the calculated CRE data for each size of FPSL spheres to evaluate the significance of secondary flow rate and collection media on the CRE. The distribution of the sample sets, which each contained 30 observations, were evaluated and normal approximation was found reasonable by application of the Central Limit Theorem (McClave, et al., 2008).

IV. Results and Analysis

XMX Volumetric Flow Rates

Three flow rates were measured for each of the five XMX units made available for this study: total flow, standard secondary flow, and reduced secondary flow. Each of these flow rates were calculated by averaging ten measurements obtained during separate periods, approximately five minutes in duration, while operating an XMX. Total flow measurements were corrected for temperature, as the exhaust flow temperature was significantly above standard normal temperature. The results for total flow rate and secondary flow rate measurements are presented in Table 6 and Table 7, respectively. All measured XMX flow data are presented in Appendix C. XMX1, XMX2, and XMX3 were used to collect experimental data in the ATC and XMX4 and XMX5 were not. The mean and standard deviation for the three flow rates were calculated for two groupings of XMXs, the three XMXs used to collect experimental data in the ATC and all five XMXs, and are presented in Table 8. Using the data in Table 6, the standard deviation of the ten

Table 6: Measured XMX total flow rates

XMX	Serial #	Final exhaust temperature (°C)	Total flow rate (slpm)	Standard deviation (slpm)
XMX1	X2064	54.7	692	8
XMX2	X2110	54.9	675	8
XMX3	X2207	54.6	683	6
XMX4	X2120	53.2	685	7
XMX5	X2206	53.4	714	10

Table 7: Measured XMX secondary flow rates

XMX	Standard secondary flow rate (slpm)	Standard deviation (slpm)	Reduced secondary flow rate (slpm)	Standard deviation (slpm)
XMX1	16.017	0.032	5.3686	0.0493
XMX2	15.940	0.048	4.8439	0.0213
XMX3	15.071	0.084	4.8052	0.0493
XMX4	14.749	0.116	6.2851	0.0368
XMX5	12.333	0.078	4.5740	0.0185

Table 8: Measured average flow rates for two groupings of XMXs

XMX group	Average total flow rate (slpm)	Standard deviation (slpm)	Average standard secondary flow rate (slpm)	Standard deviation (slpm)	Average reduced secondary flow rate (slpm)	Standard deviation (slpm)
XMX: 1-3	683	9	15.676	0.525	5.0059	0.3147
XMX: 1-5	690	15	14.822	1.495	5.1754	0.6851

measurements for each of the five XMXs total flow rate ranged from 0.9% for XMX3 to 1.4% for XMX5 of the total flow rate. Using the data presented in Table 7, the standard deviation of the ten measurements for each of the five XMXs standard secondary flow rate ranged from 0.2% for XMX1 to 0.8% for XMX4 of the standard secondary flow rate, and the standard deviation of the ten measurements for each of the five XMXs reduced

secondary flow rate ranged from 0.4% for XMX5 to 1.0% for XMX3 of the reduced secondary flow rate. Therefore, the variability of the three flow rates measured for the five XMXs, from least to greatest, are ordered: standard secondary flow rate, reduced secondary flow rate, and total flow rate. Using the data presented in Table 8, the standard deviation of the total flow rate, standard secondary flow rate, and reduced secondary flow rate for the group of XMX1, XMX2, and XMX3, were 1.3%, 3.3%, and 6.3% of their corresponding average flow rates, respectively, and the standard deviation of the total flow rate, standard secondary flow rate, and reduced secondary flow rate for the group of all five XMXs were 2.2%, 10.1%, and 13.2% of their corresponding average flow rates, respectively. Therefore, the variability of the three flow rates measured for the two groups of XMXs was lower for the group of three XMXs used to collect experimental data in the ATC than it was for the group of all five XMXs made available for the study.

Dycor reports that the XMX total flow rate, standard secondary flow rate, and reduced secondary flow rate are 800 lpm, 12 lpm, and between 4 lpm and 5 lpm, respectively. Using the data presented in Table 6, Table 7, and the three Dycor reported flow rates, small-sample hypothesis two-tailed t-tests about population means were performed at a 0.02 level of significance to evaluate hypotheses regarding the three XMX flow rates. Results of these hypotheses tests are presented in Table 9. The null hypotheses for the total flow rate and standard secondary flow rate were rejected, and the null hypothesis for the reduced secondary flow rate was not rejected, indicating significant differences in the reported and experimentally measured total and standard secondary flow rates.

Table 9: Hypotheses test results for the three XMX flow rates

Test performed	Null hypothesis	Alternate hypothesis	Rejection region: $t_{0.01}$	Test statistic: t	Result
Total flow rate	$\mu = 800$ lpm	$\mu \neq 800$ lpm	3.747	-16.625	Reject null hypothesis
Standard secondary flow rate	$\mu = 12$ lpm	$\mu \neq 12$ lpm	3.747	4.221	Reject null hypothesis
Reduced secondary flow rate	$\mu = 4.5$ lpm	$\mu \neq 4.5$ lpm	3.747	2.204	Do not reject null hypothesis

Virtual Impactor Concentration Ratio as a Function of Particle Size and Secondary Flow Rate

The concentration ratio (CR) of the virtual impactors of three XMXs was determined. The CR was determined by dividing the particle concentration distribution data for 42 size channels ranging from 0.542 µm to 10.37 µm, measured by an APS monitoring the ambient air inside the ATC, by the particle concentration data, for the same 42 size channels, simultaneously measured by another APS monitoring the air of the secondary flow exiting the XMX impinger tube. The 42 size channels were logarithmically positioned across the size range, with the size listed for each channel being at the logarithmic center of each individual size channel. CRs were determined for secondary flow rates of 5 lpm and 10 lpm. Twenty pairs of samples were collected by the two APSs for each of the six experimental combinations produced by the three XMXs and two secondary flow rates, which were then used to determine the CRs for each of the 42 size channels. Thus, a total of 5,040 CR data points were determined, due to the APSs having collected 20 samples, each having data for 42 size channels, for each of the six experimental combinations of XMX and secondary flow rate.

A two-way analysis of variance (ANOVA) with several observations per cell was performed on the data for each of the 42 size channels as the CR varies significantly as a function of particle size (Tucker, 2005). These 42 ANOVA evaluations were performed using Excel® 2007 software, produced by Microsoft Corporation. For these 42 ANOVA evaluations, the CR was the dependent variable, the XMXs were three groups, the secondary flow rates were two blocks, and an interaction between XMX and secondary flow rate was considered. The F ratios for variations between groups, XMXs, blocks, secondary flow rates, and the interaction between groups and blocks, XMXs and secondary flow rates, were calculated and compared to their respective critical F ratio values for a 0.025 level of significance, all of which are presented in Table 10. General summary tables for the 42 ANOVA evaluations are presented in Appendix D. For all 42 size channels, the variation between XMXs, secondary flow rates, and interaction of XMXs and secondary flow rates were found to be significant. Results for hypotheses tests regarding secondary flow rate and inter-XMX variability are presented in Table 11. The null hypotheses for secondary flow rate and inter-XMX variability were rejected, indicating significant inter-instrument variability and significant difference in CR for secondary flow rates of 5 and 10 lpm.

Table 10: Results of two-way ANOVA evaluations on XMX concentration ratio by XMX, secondary flow rate, and XMX/secondary flow rate interaction for 42 aerodynamic diameter size channels

Size channel (µm)	XMX		Secondary rate flow		Interaction	
	F-ratio	F-critical	F-ratio	F-critical	F-ratio	F-critical
0.542	94.01	3.83	844.2	5.18	83.49	3.83
0.583	97.79	3.83	865.8	5.18	73.79	3.83
0.626	103.4	3.83	920.7	5.18	51.82	3.83
0.673	97.01	3.83	998.7	5.18	40.66	3.83
0.723	89.88	3.83	1155	5.18	39.97	3.83
0.777	93.25	3.83	1385	5.18	38.63	3.83
0.835	93.95	3.83	1818	5.18	40.71	3.83
0.898	75.57	3.83	1808	5.18	37.25	3.83
0.965	85.22	3.83	2173	5.18	35.91	3.83
1.037	63.87	3.83	2050	5.18	30.48	3.83
1.114	91.40	3.83	2911	5.18	39.31	3.83
1.197	95.57	3.83	3617	5.18	47.77	3.83
1.286	110.5	3.83	3384	5.18	54.05	3.83
1.382	161.4	3.83	4117	5.18	76.29	3.83
1.486	115.1	3.83	4011	5.18	60.32	3.83
1.596	116.7	3.83	3329	5.18	56.23	3.83
1.715	91.82	3.83	2783	5.18	49.42	3.83
1.843	85.18	3.83	1982	5.18	33.89	3.83
1.981	87.62	3.83	2240	5.18	21.26	3.83
2.129	61.98	3.83	1829	5.18	31.03	3.83
2.288	61.41	3.83	1685	5.18	27.26	3.83
2.458	31.99	3.83	973.6	5.18	16.09	3.83
2.642	27.43	3.83	517.1	5.18	13.85	3.83
2.839	25.39	3.83	349.2	5.18	9.45	3.83
3.051	23.78	3.83	482.1	5.18	6.90	3.83
3.278	12.45	3.83	237.0	5.18	4.00	3.83
3.523	21.28	3.83	365.7	5.18	9.52	3.83
3.786	19.10	3.83	181.2	5.18	11.81	3.83
4.068	21.36	3.83	226.4	5.18	17.68	3.83
4.371	62.68	3.83	685.0	5.18	67.06	3.83
4.698	168.4	3.83	1853	5.18	190.0	3.83
5.048	72.39	3.83	729.0	5.18	76.43	3.83
5.425	49.94	3.83	471.7	5.18	54.94	3.83
5.829	67.68	3.83	899.8	5.18	106.5	3.83
6.264	27.11	3.83	237.5	5.18	30.02	3.83
6.732	51.86	3.83	472.5	5.18	71.94	3.83
7.234	26.96	3.83	251.1	5.18	30.45	3.83
7.774	21.58	3.83	195.3	5.18	18.26	3.83
8.354	18.66	3.83	241.7	5.18	16.66	3.83
8.977	9.27	3.83	96.67	5.18	7.96	3.83
9.647	4.69	3.83	29.94	5.18	4.30	3.83
10.37	6.15	3.83	128.8	5.18	7.05	3.83

Table 11: Hypotheses test results for secondary flow rate and XMX inter-instrument variability

Test performed	Null hypothesis	Alternate hypothesis	Rejection region: F critical	Test statistic: F ratio	Result
Compared CRs for different secondary flow rates	CR at 5 lpm equal to CR at 10 lpm	CR at 5 lpm not equal to CR at 10 lpm	5.18	Min: 29.94 Max: 4,117 Ave:1,322	Reject null hypothesis
Compared CRs for three XMXs	CR XMX1 equal to CR XMX2 equal to CR XMX3	CRs not equal for all three XMXs	3.83	Min: 4.69 Max: 168.4 Ave: 65.30	Reject null hypothesis

To gain a greater understanding of the nature and impact of the variability of the CR between XMXs, these data points were evaluated using JMP® statistical discovery software, version 8.0, produced by SAS Institute, Inc. The CR was the dependent variable and was coded as a continuous numeric variable. XMX was an independent variable and was coded as a nominal numeric variable and assigned a value of 1, 2, or 3, corresponding to XMX1, XMX2, and XMX3, respectively. Secondary flow rate was an independent variable and was coded as a continuous numeric dummy variable and assigned a value of 0 or 1, corresponding to 10 lpm or 5 lpm, respectively. Size channel was an independent variable and was coded as a nominal numeric variable and took on the value of the logarithmic center point of the size channel being represented. A two-way ANOVA was performed on the data, treating size channel as a fixed effect with 42 blocks, secondary flow rate as a fixed effect with two groups, and XMX as a random effect. The percentage of the model total error due to XMX and residuals for each size channel are presented in Table 12 and average 43.32% and 56.68%, respectively.

Therefore, despite there being significant inter-instrument variability for the CR across the XMXs, the majority of the total error is due to random variability.

Table 12: Percentage of total error due to XMX and residuals

Size channel (µm)	% of total error due to XMX	% of total error due to residual
0.542	48.59	51.41
0.583	51.44	48.56
0.626	57.49	42.51
0.673	58.60	41.40
0.723	56.88	43.12
0.777	58.14	41.86
0.835	57.79	42.21
0.898	53.22	46.78
0.965	56.62	43.38
1.037	50.83	49.17
1.114	57.47	42.53
1.197	56.48	43.52
1.286	58.63	41.37
1.382	63.39	36.61
1.486	58.29	41.71
1.596	59.50	40.50
1.715	55.08	44.92
1.843	57.15	42.85
1.981	61.49	38.51
2.219	49.90	50.10
2.288	50.78	49.22
2.458	37.87	62.13
2.642	34.92	65.08
2.839	34.60	65.40
3.051	33.94	66.06
3.278	21.31	78.69
3.523	30.50	69.50
3.786	27.40	72.60
4.068	28.05	71.95
4.371	41.44	58.56
4.698	49.08	50.92
5.048	43.24	56.76
5.425	38.35	61.65
5.829	36.51	63.49
6.264	29.91	70.09
6.732	35.82	64.18
7.234	29.68	70.33
7.774	28.10	71.90
8.354	25.51	74.49
8.977	15.38	84.62
9.647	8.50	91.50
10.37	11.44	88.56

The mean and standard deviation for all experimental CR data points for the three XMXs for each particle size channel at secondary flow rates of 5 lpm and 10 lpm were calculated. Due to there being significant inter-instrument variability for the CR across the XMXs, 89% confidence intervals were constructed for the CR as a function of particle diameter using the calculated means and standard deviation and employing Chebyshev's Rule (McClave, et al., 2008). The mean, upper limit for 89% confidence interval (CI), and lower limit for 89% CI of the CR for all three XMXs as a function of particle size channel are plotted for secondary flow rates of 5 lpm and 10 lpm in Figure 15 and Figure 16, respectively. The mean CRs for XMXs used in this study for sub-micrometer particles are presented in Table 13.

An analysis of the virtual impactor CR data at the two secondary flow rates tested suggest that the product of the secondary flow rate and the CR at each particle size might be a characteristic constant or predictable value. The product of the secondary flow rate and mean CR for each particle size channel combination tested were plotted and are presented in Figure 17. Single factor ANOVA evaluations were performed to compare values of this product for secondary flow rates of 5 lpm and 10 lpm over two sub-ranges of particle sizes, 0.542 μm to 1.486 μm and 5.048 μm to 10.37 μm, and the full range of particle sizes, 0.542 μm to 10.37 μm to obtain a cursory perspective on the possibility of such a relationship between secondary flow rate and CR. The results of these ANOVA evaluations are presented in Table 14 and indicate that such a relationship should not be rejected based solely on a significance level of 0.05.

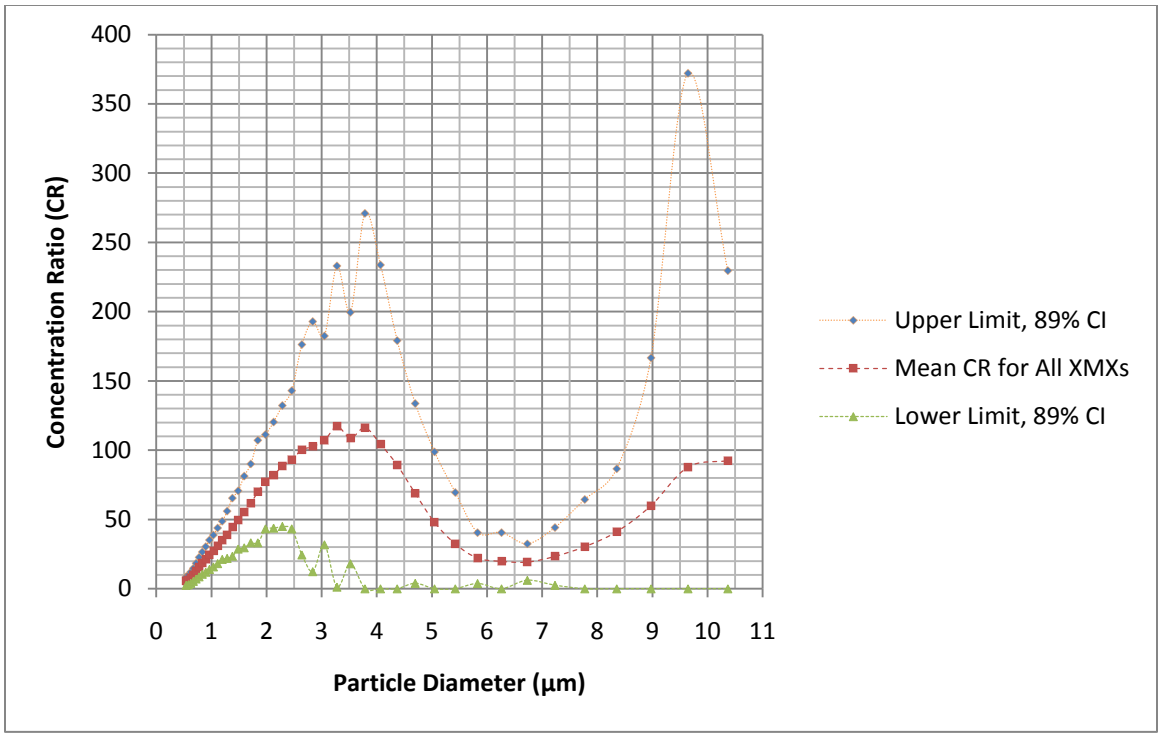

Figure 15: Mean concentration ratio as a function of particle size for all XMXs at secondary flow rate of 5 lpm

Collection Media Particle Capture and Retention as a Function of Particle Size and Secondary Flow Rate

The concentration of particles captured and retained in the collection media was measured using fluorometry for the samples collected for the secondary rates, collection media, and test aerosols listed in Table 4. The capture and retention efficiency (CRE) for each sample was calculated by dividing the number of particles captured and retained in the collection media by the theoretical number of particles, based upon secondary flow rate, CR, and the particle concentration in the ATC, that passed through the liquid impinger and into the collection tube. The average calculated CREs for the twelve combinations of sampling conditions are presented in Table 15. Single factor ANOVA

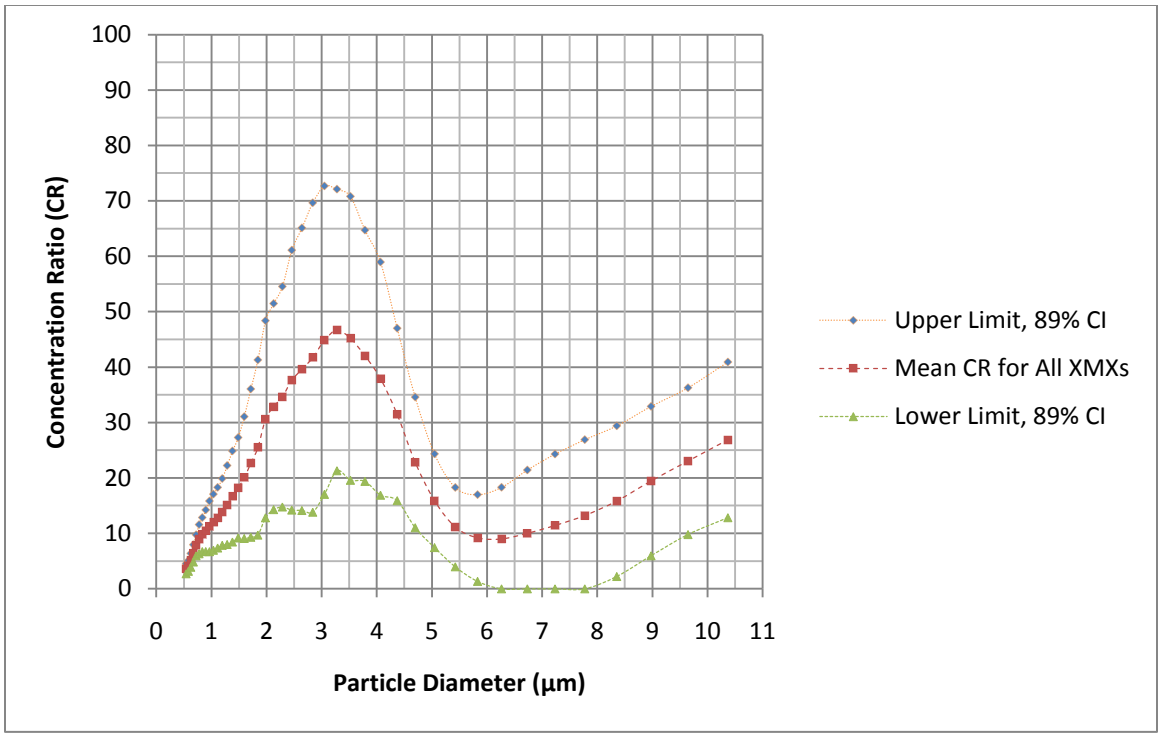

Figure 16: Mean concentration ratio as a function of particle size for all XMXs at secondary flow rate of 10 lpm

Table 13: Mean and standard deviation of CR for sub-micrometer particles

Particle size (µm)	Secondary flow rate (lpm)	Mean CR	Standard deviation
0.542	5	5.65	1.03
0.542	10	3.62	0.30
0.583	5	6.44	1.15
0.583	10	4.13	0.32
0.626	5	8.06	1.36
0.626	10	5.13	0.41
0.673	5	10.1	1.6
0.673	10	6.38	0.52
0.723	5	12.8	1.9
0.723	10	7.84	0.63
0.777	5	15.7	2.3
0.777	10	8.94	0.88
0.835	5	18.5	2.7
0.835	10	9.78	1.02
0.898	5	21.2	3.1
0.898	10	10.5	1.2
0.965	5	24.6	3.5
0.965	10	11.3	1.5

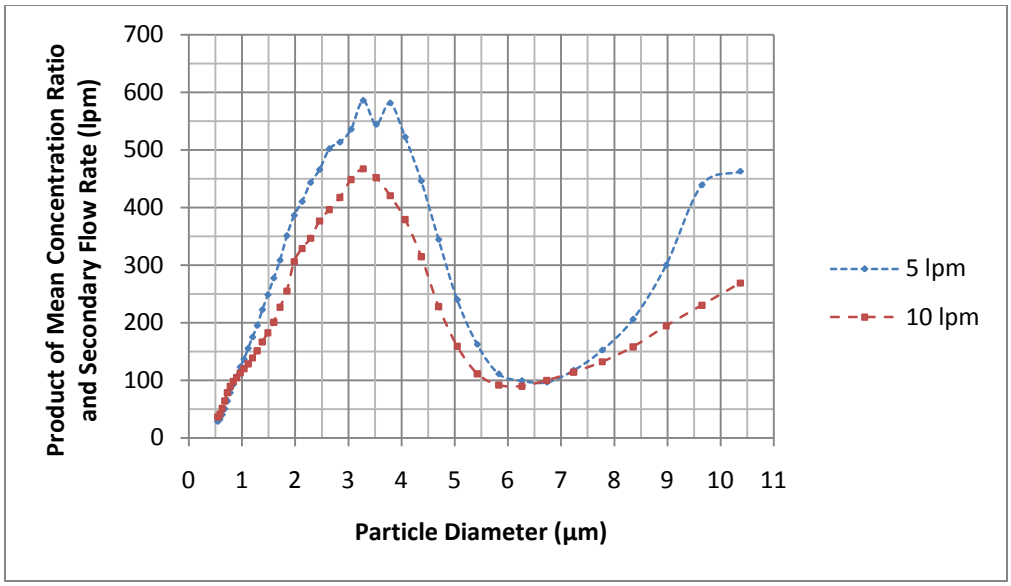

Figure 17: Product of mean concentration ratio and secondary flow rate as a function of particle size

Table 14: P-values for product of CR and secondary flow rate ANOVA comparison

Particle size range	P-value
0.542 µm to 1.486 µm	0.573
5.048 µm to 10.37 µm	0.140
0.542 µm to 10.37 µm	0.074

evaluations were performed to compare CREs and determine if there were significant differences in CRE due to collection media and secondary flow rate for each of the four sizes of particles tested. General summary tables for these ANOVA evaluations are presented in Appendix E. The results of these ANOVA evaluations are presented in Table 16. Results for hypotheses tests regarding CRE regarding collection media and secondary flow rate for each particle size with a level of significance of 0.025 are presented in Table 17 and indicate that there are significant differences in the CREs of 1.0, 1.9, and 3.1 µm FPSL spheres due to collection media, PBS solution compared to

Remel M5 collection media, and secondary flow rate, reduced compared to standard secondary flow rate.

Table 15: CRE means for sampling condition combinations

Collection media	Secondary flow rate (lpm)	Particle diameter (μm)	Average CRE
PBS solution	Reduced	0.7	0.173
PBS solution	Standard	0.7	0.246
Remel M5	Reduced	0.7	0.201
PBS solution	Reduced	1.0	0.059
PBS solution	Standard	1.0	0.108
Remel M5	Reduced	1.0	0.080
PBS solution	Reduced	1.9	0.096
PBS solution	Standard	1.9	0.213
Remel M5	Reduced	1.9	0.217
PBS solution	Reduced	3.1	0.623

Table 16: P-values for CRE ANOVA comparisons

Particle diameter (μm)	CRE comparison description	P-value	Factor associated with higher CRE
0.7	PBS solution collection media with standard and reduced secondary flow rates	0.0879	Standard secondary flow rate
1.0	PBS solution collection media with standard and reduced secondary flow rates	0.0104	Standard secondary flow rate
1.9	PBS solution collection media with standard and reduced secondary flow rates	<0.0001	Standard secondary flow rate
3.1	PBS solution collection media with standard and reduced secondary flow rates	<0.0001	Reduced secondary flow rate
0.7	Reduced secondary flow rate with PBS solution and Remel M5	0.8326	Remel M5 collection media
1.0	Reduced secondary flow rate with PBS solution and Remel M5	0.0072	Remel M5 collection media
1.9	Reduced secondary flow rate with PBS solution and Remel M5	<0.0001	Remel M5 collection media
3.1	Reduced secondary flow rate with PBS solution and Remel M5	<0.0001	PBS solution collection media

Table 17: Hypotheses test results for collection media performance at 0.025 level of significance

Test performed	Null hypothesis	Alternate hypothesis	P-value	Result
Measure CRE using 0.7 μm FPSL sphere using PBS solution for reduced and standard secondary flow rates	CREs equal	CREs not equal	0.0879	Do not reject null hypothesis
Measure CRE using 1.0 μm FPSL sphere using PBS solution for reduced and standard secondary flow rates	CREs equal	CREs not equal	0.0104	Reject null hypothesis
Measure CRE using 1.9 μm FPSL sphere using PBS solution for reduced and standard secondary flow rates	CREs equal	CREs not equal	<0.0001	Reject null hypothesis
Measure CRE using 3.1 μm FPSL sphere using PBS solution for reduced and standard secondary flow rates	CREs equal	CREs not equal	<0.0001	Reject null hypothesis
Measure CRE using 0.7 μm FPSL spheres at reduced secondary flow rate using PBS solution and Remel M5 collection media	CREs equal	CREs not equal	0.8326	Do not reject null hypothesis
Measure CRE using 1.0 μm FPSL spheres at reduced secondary flow rate using PBS solution and Remel M5 collection media	CREs equal	CREs not equal	0.0072	Reject null hypothesis
Measure CRE using 1.9 μm FPSL spheres at reduced secondary flow rate using PBS solution and Remel M5 collection media	CREs equal	CREs not equal	<0.0001	Reject null hypothesis
Measure CRE using 3.1 μm FPSL spheres at reduced secondary flow rate using PBS solution and Remel M5 collection media	CREs equal	CREs not equal	<0.0001	Reject null hypothesis

Analysis of Virtual Impactor Concentration Ratio Variability

A potential source of virtual impactor CR variability was sought. An evaluation of the XMX design and assembly instructions suggest that the orientation of the final nozzle could vary between XMXs following assembly. Due to the gaps in the circular sidewall of the final nozzle, shown in Figure 7, and the flow of a portion of the total flow passing through these gaps as the flow is drawn by the main blower to the exhaust, differences in the flow patterns in the final nozzle could contribute to virtual impactor CR variability. Overlay plots of the CR as a function of particle size channel for the 20 individual samples for each of the three XMXs at secondary flow rates of 5 lpm and 10 lpm were produced, presented in Appendix F, and evaluated to qualitatively investigate the CR variability of each XMX. This qualitative investigation indicated that XMX1 exhibited much greater CR variability at 5 lpm than either XMX2 or XMX3. Similarly, this qualitative investigation indicated that XMX2 exhibited much greater CR variability at 10 lpm than either XMX1 or XMX3. The XMXs were disassembled, cleaned, and reassembled between experimental data collection at 5 lpm and 10 lpm. The orientation of the final nozzles during reassembly was neither controlled nor noted; therefore, differences in final nozzle orientation between the experimental data collection at 5 lpm and 10 lpm may have been a source of CR variability, with the final nozzle orientation of XMX1 at 5 lpm and that of XMX2 at 10 lpm being in orientations that lead to notable CR variability.

The CRE data was quantitatively evaluated by using JMP® statistical discovery software to fit a full linear regression model with interactions to the CRE data to identify

the most important effects in CRE variability. The CRE was the dependent variable and was coded as a continuous numeric variable. XMX1 was an independent variable and was coded as a continuous numeric dummy variable and assigned a value of 1 or 0, corresponding to when the data record was for XMX1 or was not for XMX1, respectively. A variable for XMX2 was coded similarly to the variable coded for XMX1. No variable was coded for XMX3; therefore, XMX3 was included in the model baseline. The secondary flow rate was an independent variable and coded as a continuous numeric dummy variable and assigned a value of 0 or 1, corresponding to when the data record was for standard secondary flow or reduced secondary flow, respectively; therefore, standard secondary flow was included in the model baseline. The collection media was an independent variable and coded as a continuous numeric dummy variable and assigned a value of 0 or 1, corresponding to when the data record was for PBS solution or Remel M5 collection media, respectively; therefore, PBS solution was included in the model baseline. Particle size was an independent variable and was coded as a nominal numeric variable and was assigned a value of 0.7 μm, 1.0 μm, 1.9 μm, or 3.1 μm corresponding to the particle size for the data record. The particle size of the model baseline was 3.1 μm. The model was refined by removing effects, either single effects or interactions, as repeated model building revealed them as not being significant effects. Seven effects were found to be significant in predicting CRE values and are presented with their corresponding P-values in Table 18. No other model effects had P-values less than 0.05. These results are in agreement with CRE ANOVA comparisons and suggest the possibility that the final nozzle orientation of XMX1 may have been in a position leading

to notable CR variability as the XMXs were disassembled, cleaned, and reassembled between experimental data collection for FPSL sphere aerosols TA2 and TA3 (Table 3).

Table 18: Significant effects for predicting CRE

Model effect	P-value
XMX1	<0.0001
Reduced secondary flow	<0.0001
Remel M5	<0.0001
Particle size of 1.0 μm	<0.0001
Particle size of 1.9 μm	<0.0001
Interaction of reduced secondary flow and particle size	<0.0001
Interaction of Remel M5 and particle size	<0.0001

Microscopic Analyses of FPSL Spheres in Collection Media

Microscopic analysis was performed to determine the particle concentration in collection media for 10% of the samples noted in Table 4. Due to the relatively low concentration of FPSL spheres captured and retained in the collection media and the protocol used in performing the microscopic concentration analysis, only three concentrations were observed: 0, 3.125×10^5, and 6.25×10^5, corresponding to the presence of either 0, 1, or 2 FPSL spheres in the 3.2×10^{-6} mL observation volume for the PHCC slide. The average percent error and deviation between the FPSL particle concentrations determined by fluorometry and microscopy were 449% and 2.25×10^5 FPSL spheres per mL, respectively. No physical alteration of 1.9 μm or 3.1 μm green FPSL spheres was observed while performing microscopic analysis. Examples of the appearance of 1.9 μm and 3.1 μm green FPSL spheres as seen using the Axioskop microscope are shown in Figure 18 and Figure 19, respectively. Particle size appears

larger in the images due to the abundance of fluorescent light emitted. Due to the lack of the proper optical filter, observation of 0.7 μm and 1.0 μm blue FPSL spheres in collected samples was not possible.

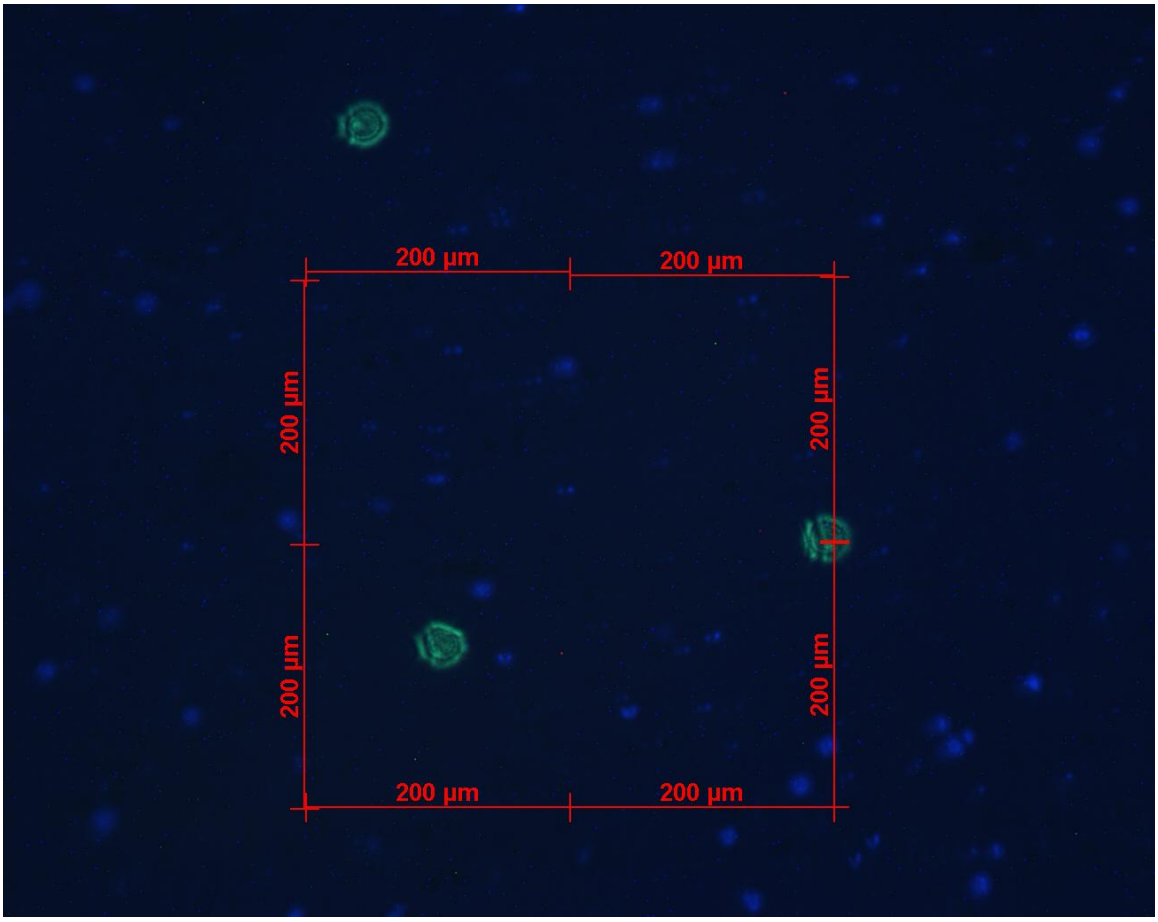

Figure 18: Appearance of 1.9 μm green FPSL spheres

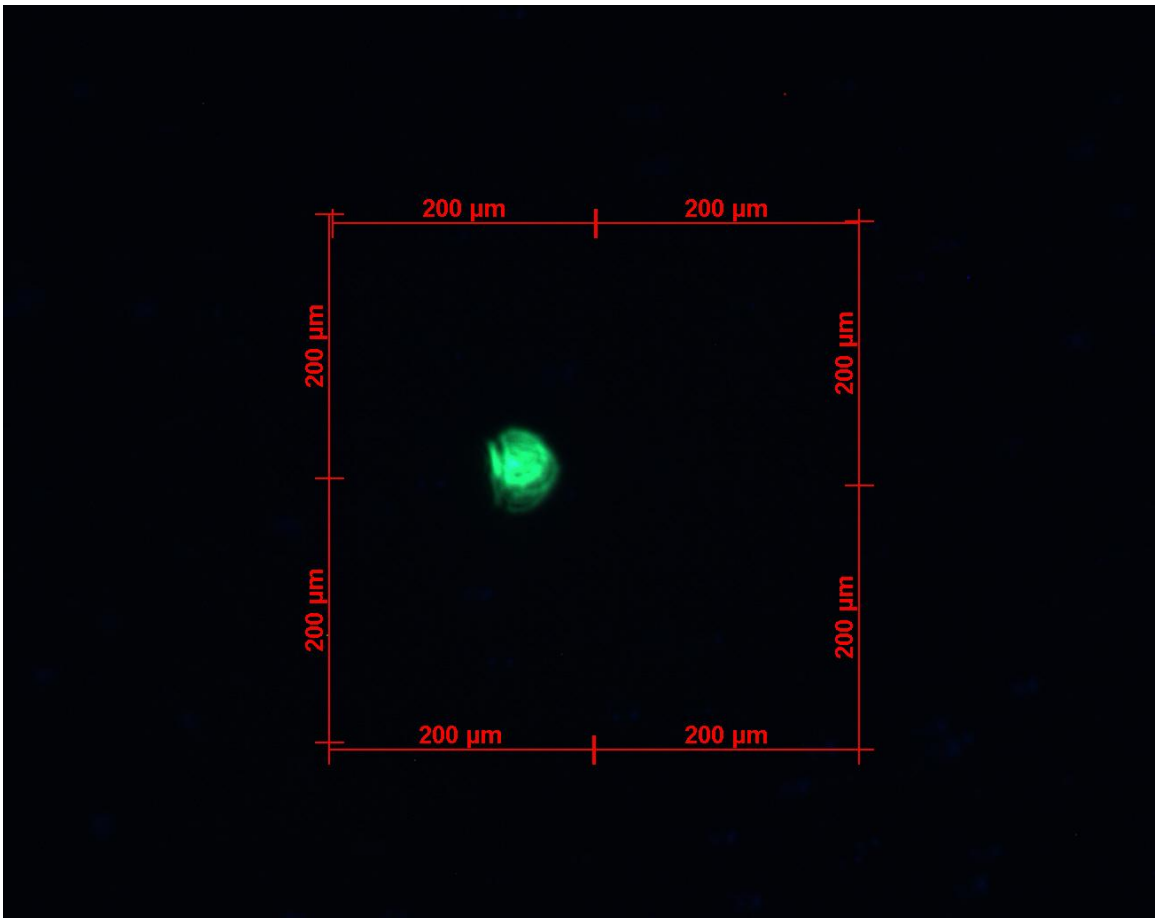

Figure 19: Appearance of 3.1 µm green FPSL spheres

V. Discussion and Conclusions

Discussion Overview

This thesis evaluated the performance of the XMX high volume air sampler. Criteria evaluated included volumetric flow rates, virtual impactor CR, and the capture and retention of particles in two different collection media. Overall limitations of this research included: the use of only ARD to determine the virtual impactor CR, the virtual impactor CR was determined for only two secondary flow rates, the size of the ATC did not permit simultaneously operating XMXs in parallel during experimental trials, the collection media were evaluated with only four sizes of FPSL spheres, and the microscopic evaluation could not be performed for the two smallest sizes of FPSL spheres that were used.

Impact of Secondary Flow Rate on Virtual Impactor Performance

This study demonstrated that virtual impactor CRs are significantly different for all 42 size channels evaluated (all p-values < 0.001) at secondary flow rates of 5 and 10 lpm. There are no known published studies regarding the effect of secondary flow rate on the XMX virtual impactor CR. The data of this study suggest that the product of the secondary flow rate and the CR at each individual particle size might be a characteristic constant, or possibly a predictable value, of the XMX virtual impactor. The CR is strongly a function of particle size and exhibits a characteristic tendency to have an intermediate minimum value for particles 6 μm in size for both secondary flow rates tested. The CRs were shown to have their overall highest value range for particles

smaller than 5μm in diameter, overlapping with the respirable particle size range (Hinds, 1999). Further, the CRs averaged no less than approximately 10 for the XMX's reported operating particle size range of 1.0 to 10 μm for both secondary flow rates tested. The average CR for the three XMXs was found to not exceed 83% of the ratio of the total flow and secondary flow rates at a secondary flow rate of 5 lpm and to not exceed 67% of the same ratio at a secondary flow rate of 10 lpm. Therefore, at least 17% and 33% of the particles ingested by the XMX would not flow through the impinger tube at secondary flow rates of 5 lpm and 10 lpm, respectively. Further, the average CR typically did not exceed 43% of the ratio of the total flow and secondary flow rates at a secondary flow rate of 5 lpm and did not exceed 36% of the same ratio at 10 lpm. Therefore, typically less than half of the particles of the polydispersed ARD aerosol ingested by the XMX flowed through the impinger tube at the secondary flow rates tested. While Dycor does not claim that the XMX concentrates particles less than 1.0 μm in diameter in the secondary flow, this research showed the XMX does concentrate sub-micrometer particles in the secondary flow. The mean CRs for XMXs used in this study for sub-micrometer particles are presented in Table 13 and suggest that extending the accepted operating range for the XMX to as small as approximately 0.5 μm should be considered.

This study found there was significant inter-instrument CR variability across the three XMXs evaluated for all 42 size channels evaluated (all p-values < 0.02). However, the percent of total error due to inter-instrument variability was found to be slightly less on average than the percent of total error due to random variability. The variability of the

CR was so significant that the ratio of the upper and lower limits of the 89% confidence intervals for secondary flow rates of 5 and 10 lpm exceeded 10 and 3, respectively, for the five minute sampling trials performed. However, there might be a simple explanation for the high CR variability identified in this study. Upon consideration of general fluid mechanics theory, aerosol particle characteristics, the design of the XMX, and the assembly instructions for the virtual impaction module, this study has formulated a hypothesis for a source of at least a notable portion of the significant inter-instrument CR variability. This study hypothesizes that inconsistent positioning of the final nozzle when inserting it into the liquid impingement module (LIM) body during assembly is a source of CR variability. The gaps in the circular sidewall of the final nozzle, shown in Figure 7, permit a portion of the total flow previously separated at the first particle separation stage, to pass through the final nozzle as it is drawn by the main blower to the exhaust. The assembly instructions do not state that the final nozzle should be positioned in any specific manner when inserted into the LIM body; therefore, the location of the gaps in the final nozzle sidewall would tend to be in varying orientation to the portion of the total flow passing through the final nozzle, which would likely lead to substantially different flow patterns in the final nozzle, thereby possibly significantly altering the CR. Qualitative analysis of overlay plots of CR as a function of particle diameter for each XMX, presented in Appedix F, and the results of a fit model process of the CRE data suggest that final nozzle orientation should be considered as a potential source of significant virtual impactor CR variability.

Effects of Secondary Flow Rate and Collection Media on Capture and Retention of Particles

This study found that there was significant difference in CRE between reduced and standard secondary flow rate when using PBS solution as collection media for 1.0, 1.9, and 3.1 μm FPSL spheres (p-values of 0.0104, <0.0001, and <0.001, respectively). However, while reduced secondary flow rate was associated with superior CRE performance for 3.1 μm FPSL spheres, standard secondary flow rate was associated with superior CRE performance for 1.0 and 1.9 μm FPSL spheres. No significant difference in CRE was detected between reduced and standard secondary flow rates for 0.7 μm FPSL spheres when using PBS solution as collection media. This CRE comparison between reduced and standard secondary flow rates could not be tested using Remel M5 collection media due to excessive foaming of Remel M5 at the standard secondary flow rate.

This study found that there was significant difference in CRE between PBS solution and Remel M5 collection media when operating at reduced secondary flow rate for 1.0, 1.9, and 3.1 μm FPSL spheres (p-values of 0.0072, <0.0001, and <0.001, respectively). However, while PBS solution was associated with superior CRE performance for 3.1 μm FPSL spheres, Remel M5 collection media was associated with superior CRE performance for 1.0 and 1.9 μm FPSL spheres. No significant difference in CRE was detected between PBS solution and Remel M5 collection media for 0.7 μm FPSL spheres when operating at reduced secondary flow rate, indicating that Remel M5 was no better than PBS solution at capturing and retaining 0.7 μm FPSL spheres, which

supports the work of Cooper that suggested that Remel M5 was superior in maintaining viral agent viability in sub-micrometer particles when operating the XMX at reduced secondary flow rate as compared to PBS solution (Cooper, 2010). The CRE results for all four sizes of FPSL spheres were consistent with those of Grinshpun, who found that maximum reaerosolization occurred for 1.0 μm particles, due to their greater likelihood of being entrained in bubbles rising through the collection liquid, and increasingly diminished for particle sizes both smaller and larger than 1.0 μm when using an AGI-4 liquid impinger (Grinshpun, et al., 1997).

Implications of Measured XMX Flow Rates, Virtual Impactor Performance, and Collection Media Particle Capture and Retention on Sampling Protocols

This study found that the measured standard secondary flow rate was significantly different from the standard secondary flow rate reported by the XMX manufacturer (p-value <0.01). As has been already noted, there is large variation in CR based on secondary flow rate, significant inter-instrument variability in CR, and a wide range between the upper and lower limits of the 89% confidence interval for the XMX CRs. Taken together, these findings strongly suggest that it is not feasible to develop an accurate or precise air concentration LOD applicable to all XMXs when using an XMX to collect a sample; however, it may be possible to estimate acceptable air concentration LODs for individual XMXs. Further, as there is such significant variability in XMX performance characteristics, basing command decisions upon the results obtained by analyzing a single sample may be unwise in cases when use or presence of a naturally

occurring biological agent is suspected, as the potential for a false negative analysis due solely to XMX performance variability could be high.

The CRE was found to be superior for FPSL spheres with sizes of 1.0 and 1.9 μm at the standard secondary flow rate, as compared to the reduced secondary flow rate, when using PBS solution as collection media, but the opposite was found for 3.1 μm FPSL spheres and no difference was detected for these sampling conditions for 0.7 μm FPSL spheres. Additionally, the CRE was found to be superior for FPSL spheres with sizes of 1.0 and 1.9 μm when using Remel M5 collection media, as compared to PBS solution collection media, but the opposite was found for 3.1 μm FPSL spheres and no difference was detected for these sampling conditions for 0.7 μm FPSL spheres. Therefore, since no clear preference was indicated for selecting a single, optimal combination of secondary flow rate and collection media to ensure maximum CRE for all four FPSL sphere sizes tested and XMX performance varied to such a degree that single sample analysis appears unwise, the results of this study suggest that sampling protocols would likely be more effective if they were to include collecting at least three samples, one each at the reduced secondary flow rate using PBS solution and Remel M5 collection media and one at the standard secondary flow rate using PBS solution as collection media when responding to incidents involving an unknown biological agent. If the characteristic constant or predictable value for the product of secondary flow rate and CR hypothesized in this study were to exist, then the number of particles at each particle size that flow through the liquid impinger tube would be the same for all secondary flow rates. Therefore, if such a characteristic constant or predictable value for the virtual impactor

were substantiated, then the secondary flow rate could be chosen to optimize the CRE for the particle size and selection media of interest.

Recommendations

Experimental Evaluation of Air Sampling Equipment.

The AF acquires, maintains, and fields a variety of air sampling equipment to provide CBRN surveillance and detection capabilities. The AF typically commissions governmental entities or contractors to write concept of operations, technical guidance reports, and field user manuals for air sampling equipment. In the case of the XMX, it appears that the AF neither commissioned nor conducted any notable experimental evaluation of XMX air sampling performance until 2010 (Cooper, 2010). The purpose of this research was to extend the work of Cooper and further explore CR and inter-instrument variability of the XMX due to secondary flow rate and particle size and the variability of CRE due to secondary flow rate and collection media. Future pre- and post-acquisition evaluations of air sampling equipment should, whenever possible, include informed experimental evaluation of not only technical aspects highlighted by the manufacturer, but also include those technical aspects that experience suggests are likely relevant that have not been highlighted by the manufacturer.

Improved Field Air Sampling Protocols for the XMX and Limit of Detection.

AF BE personnel currently operate the XMX at the standard secondary flow rate using distilled water or PBS solution and frequently base their occupational and environmental health site assessments (OEHSAs) upon the analytical results obtained from a single collected sample. This study demonstrated significant differences in XMX

total and standard secondary flow rates, virtual impactor CR performance due to secondary flow rate and inter-instrument variability, and CRE due to secondary flow rate and collection media. Field air sampling protocols for the XMX should require collecting and analyzing several air samples, ideally including repeat samples at all locations of interest, to provide superior, more conservative information from which improved OEHSAs can be based. Considering only those factors experimentally evaluated by AF personnel in this study and that by Cooper, this study recommends revising air sampling protocols for the XMX so that at least three samples are collected and analyzed as follows: one sample at the standard secondary flow rate using PBS solution as collection media, one sample at reduced secondary flow rate using PBS solution as collection media, and one sample at reduced secondary flow rate using Remel M5 collection media (Cooper, 2010).

The AF has documented air concentration limits of detection (LODs) for many chemical agent detection systems and has a keen interest in determining LODs for biological agent detection systems as well. However, considering the significant differences and variability in XMX performance characteristics, this study found that it is not realistic to pursue determining an accurate and precise limit of detection for any sampling protocol using the XMX to collect an air sample. Based upon the nature and degree of the virtual impactor CR and inter-instrument variability, particularly across particle sizes and secondary flow rates, this study suggests a reasonable approach to identifying a practical, actionable limit of detection when using the XMX to collect an air sample is to multiply an experimental determined limit of detection by a factor of 10 to

have greater confidence in making an OEHSA and better minimize the likelihood of a false negative test result. Additionally, the results of this and future CRE experiments will be important in determining air concentration LODs. This study recommends using FPSL spheres and fluorometry over microscopic methods to determine the concentration of collected aerosol particles in liquid media as microscopic methods are extremely time consuming and conducted on a far smaller portion of the sample than fluorometry. Microscopy should only be used if it is not possible to use fluorometric analysis to determine the concentration of FPSL spheres in liquid collection media or if qualitative evaluation of the particles in the collection media is desired.

Future Research Opportunities

Evaluation of Existing and Contemplated Air Sampling Equipment.

The AF has purchased and fielded the DFU-1000 and Biocapture® 650, manufactured by ICX Technologies, Inc., and will likely contemplate acquiring additional air sampling equipment in the future. The available performance literature for the DFU-1000, Biocapture® 650, and other air samplers under consideration should be reviewed by AF personnel with relevant technical knowledge and actual field experience so as to better insightfully identify gaps or potential shortcomings in manufacturer provided product information and charge those reviewers with proposing experimental work specifically designed to address perceived important knowledge gaps or evaluate those relevant performance characteristics for which experimental data and information is not yet available. In particular, future investigation of virtual impactor CR at additional secondary flow rates could be used to verify the hypothesis of the existence of an XMX

virtual impactor performance constant or predictable value defined as the product of the CR ratio and secondary flow rate, and, if such a constant exists, to investigate if analogous constants exist for other virtual impactors with variable secondary flow rates. Additionally, future investigation is warranted to evaluate if the orientation of the final nozzle in the LIM body is a significant source of inter-instrument CR variability. If final nozzle orientation is confirmed as a source of significant inter-instrument CR variability, then establishing a specific final nozzle orientation might reduce inter-instrument CR variability sufficiently such that acceptably accurate and precise air concentration LODs can be determined for air samples collected using the XMX.

Experimental Evaluation of Collection Media.

This study evaluated the CRE performance of PBS solution at only standard and the reduced secondary flow rates, Remel M5 at only the reduced secondary flow rate, and for only four particle sizes. Future experimental evaluation should be considered for PBS solution, Remel M5, other commercially available collection media, and additional novel collection media for additional particle sizes and secondary flow rates to attempt to identify optimal combinations of collection media and secondary flow rate to maximize CRE for specific particle sizes of interest.

Conclusions

This study evaluated the performance of the XMX virtual impactor and two collection media. The metrics used to evaluate the performance of the virtual impactor and collection media were CR and CRE, respectively. The virtual impactor CR was found to be significantly different for secondary flow rates of 5 lpm and 10 lpm.

Experimentally determined CRs were higher at a secondary flow rate of 5 lpm as compared to those at 10 lpm. However, the CR at 5 lpm was shown to have far larger variability than at 10 lpm, which suggests there would be increased difficulty in determining and decreased accuracy and precision of air concentration LODs at lower as compared to higher secondary flow rates. The experimental data suggest that the product of the secondary flow rate and CR might be a constant or predictable value for each particle size, which, if substantiated, could reduce the complexity of selecting an optimal secondary flow rate based upon particle sizes of interest. Notable CRs were experimentally determined for particles between approximately of 0.5 and 1.0 μm, which suggests that extending the operational range of the XMX to sub-micrometer particles should be considered. Additionally, this study hypothesized that inter-instrument CR variability is significantly affected by final nozzle orientation in the LIM body. If inter-instrument CR variability is reduced significantly, then determining accurate and precise air concentration LODs might be possible for air samples collected using the XMX. If inter-instrument CR variability is not reduced, then this study recommends that any experimentally determined air concentration LODs be multiplied for a factor of 10 to better account for CR variability and improve confidence in OEHSAs based upon samples collected by the XMX. However, the significant inter-instrument CR variability strongly indicates that when using the XMX, multiple samples should be collected and analyzed to minimize the risk of basing an OEHSA on a false negative test result.

The CRE of FPSL spheres in collection media was found to vary significantly for 1.0, 1.9, and 3.1 μm diameter FPSL spheres at reduced as compared to standard

secondary flow rate and for PBS solution as compared to Remel M5 collection media. No significant differences due to secondary flow rate or collection media were detected in CRE for 0.7 μm particles, which supports Cooper's hypothesis that superior maintenance of MS2 bacteriophage viability was attributable to Remel M5 as compared to PBS solution collection media (Cooper, 2010). For FPSL spheres 1.0 μm in diameter and larger, CREs were found to increase with particle size, with CREs being the largest for 3.1 μm FPSL spheres as compared to the other sizes, and were greater at reduced as compared to standard secondary flow rate when using PBS solution collection media. Additionally, CREs for 0.7 μm FPSL spheres were more than double those for 1.0 μm FPSL spheres for both secondary flow rates and collection media tested, in agreement with the results of Grinshpun (Grinshpun, et al., 1997). Fluorometry is recommended over microscopy to determine the concentration of FPSL spheres in liquid collection media. Lastly, the predicted number of particles captured and retained in collection media at each particle size is the product of the secondary flow rate, virtual impactor CR, and the collection media CRE for each particle size. Therefore, minimum air concentration LODs should coincide with maximum values of the product of secondary flow rate, virtual impactor CR, and collection media CRE for particle sizes of interest.

Appendix A: Experimental Data Collection Schedule

Table 19: Experimental data collection schedule

Date	Description	Air samplers evaluated
09-Sep-2010	Measure total flow rate	XMX1, XMX2, XMX3, XMX4, XMX5
10-Sep-2010	Measured standard secondary flow rate	XMX1, XMX2, XMX4
13-Sep-2010	Measured reduced secondary flow rate	XMX2, XMX4
13-Sep-2010	Performed 20 sampling runs for determining the virtual impactor CR ratio at a secondary flow rate of 5 lpm using TA1	XMX1, XMX2, XMX3
15-Sep-2010	Performed 30 sampling runs for determining the CRE using TA2	XMX1
16-Sep-2010	Measured reduced secondary flow rate	XMX1, XMX3
16-Sep-2010	Performed 30 sampling runs for determining the CRE using TA2	XMX2, XMX3
17-Sep-2010	Measured standard secondary flow rate	XMX3
17-Sep-2010	Performed 30 sampling runs for determining the CRE using TA3	XMX1
20-Sep-2010	Performed 30 sampling runs for determining the CRE using TA3	XMX2, XMX3
21-Sep-2010	Measure standard secondary flow rate	XMX5
21-Sep-2010	Measure reduced secondary flow rate	XMX5
23-Sep-2010	Performed 20 sampling runs for determining the virtual impactor CR ratio at a secondary flow rate of 10 lpm using TA1	XMX1, XMX2, XMX3

Appendix B: Fluorometric Calibration Curves

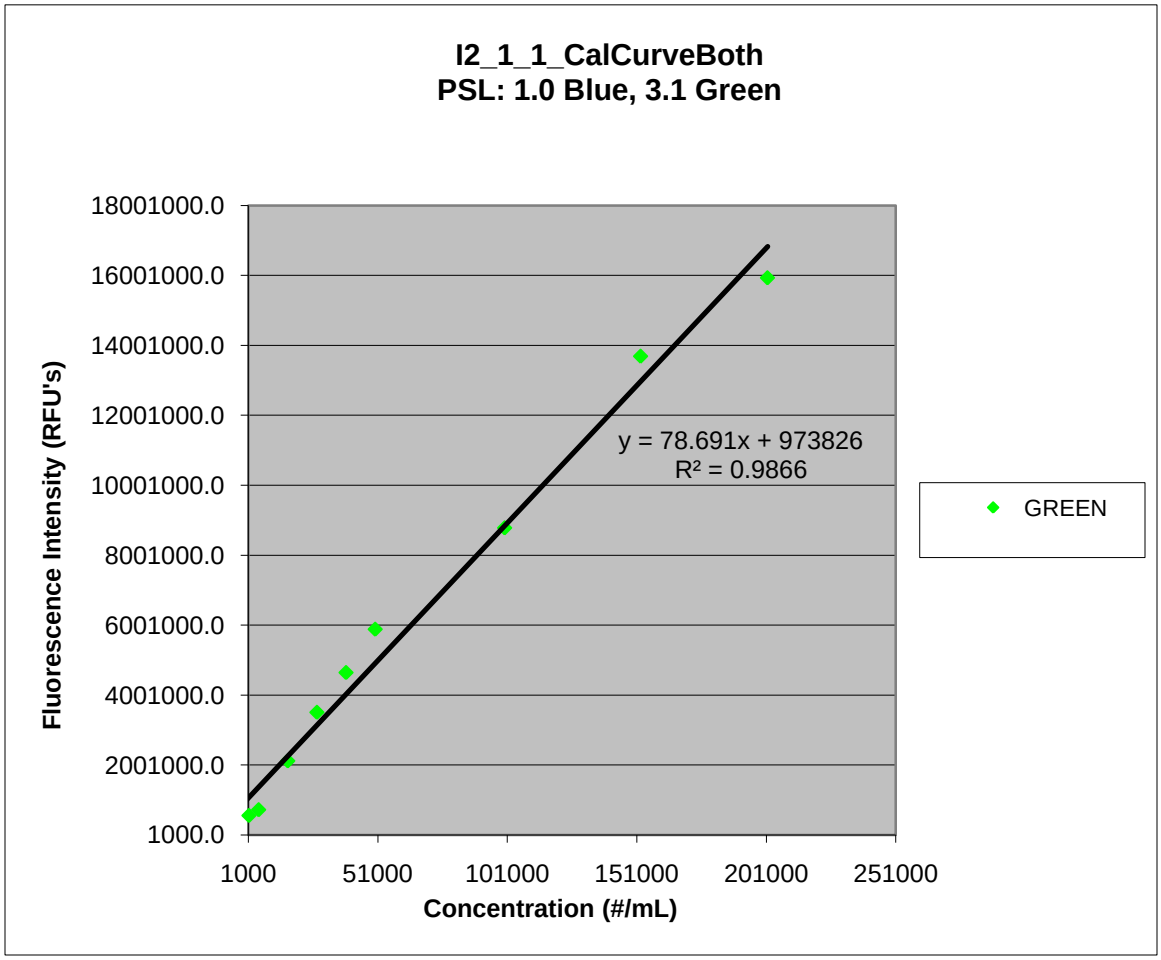

Figure 20: Fluorometric calibration curve for 3.1 µm green FPSL spheres in PBS solution

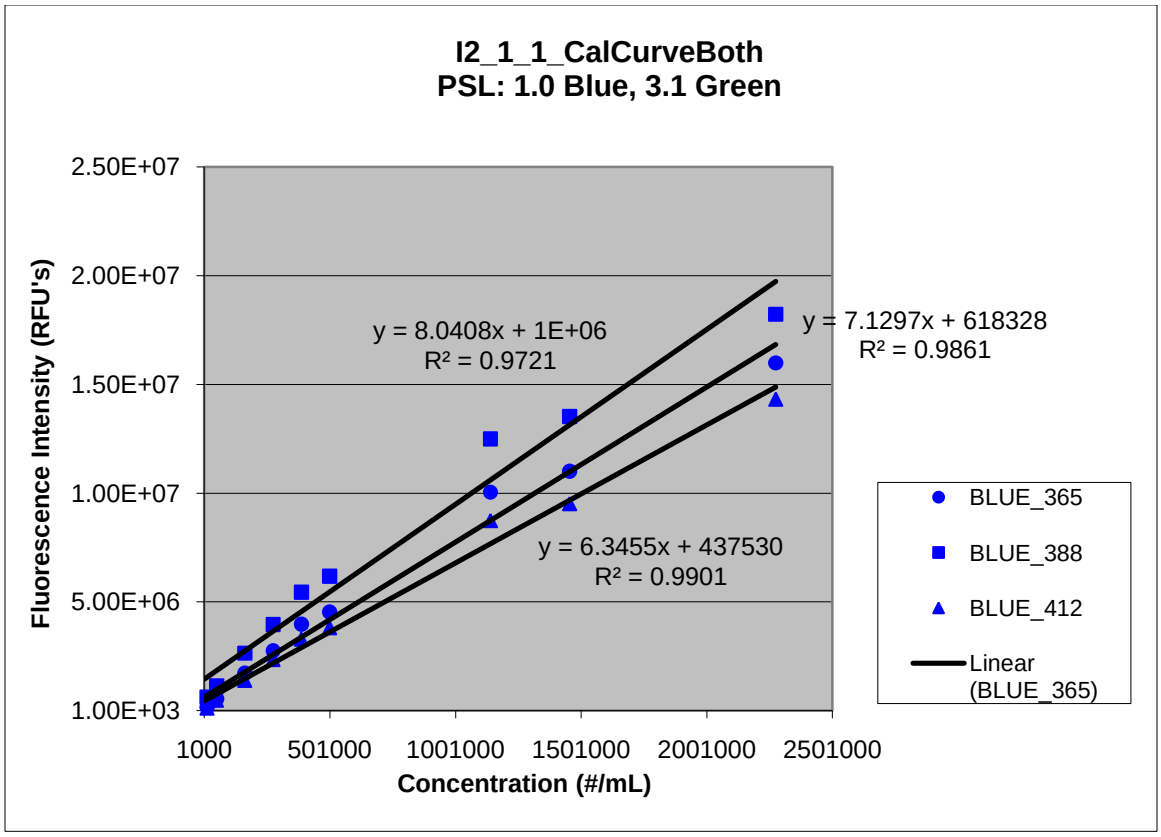

Figure 21: Fluorometric calibration curves for 1.0 µm blue FPSL spheres in PBS solution

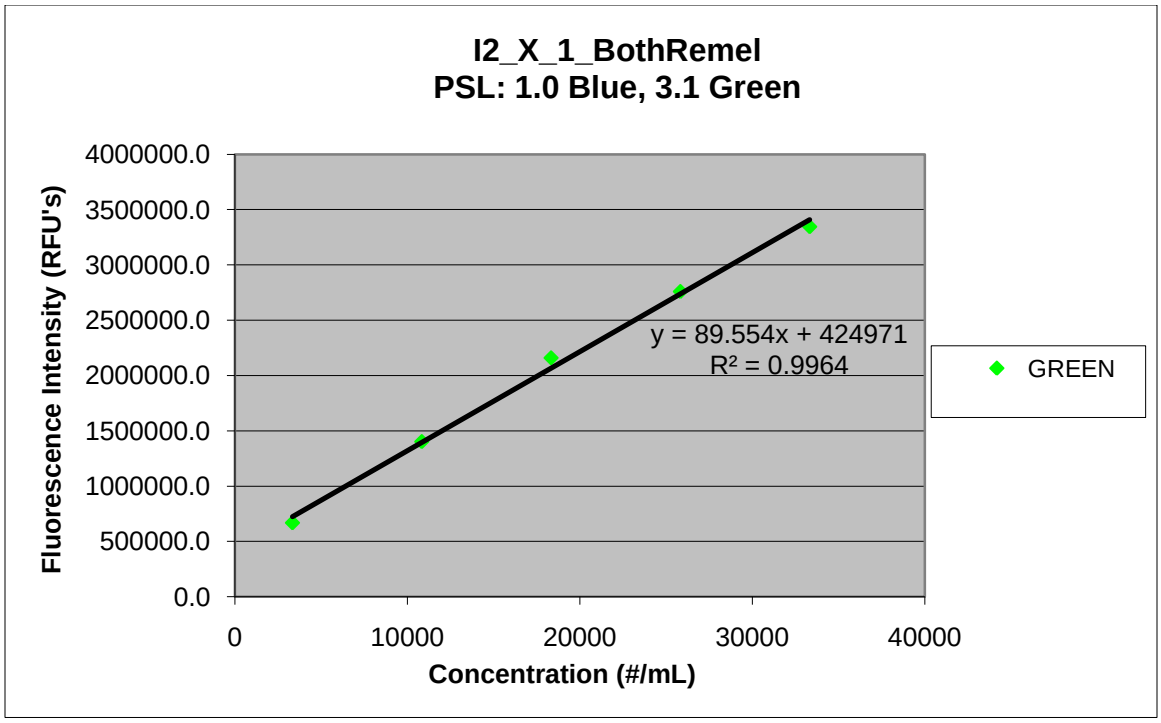

Figure 22: Fluorometric calibration curve for 3.1 µm green FPSL spheres in Remel M5

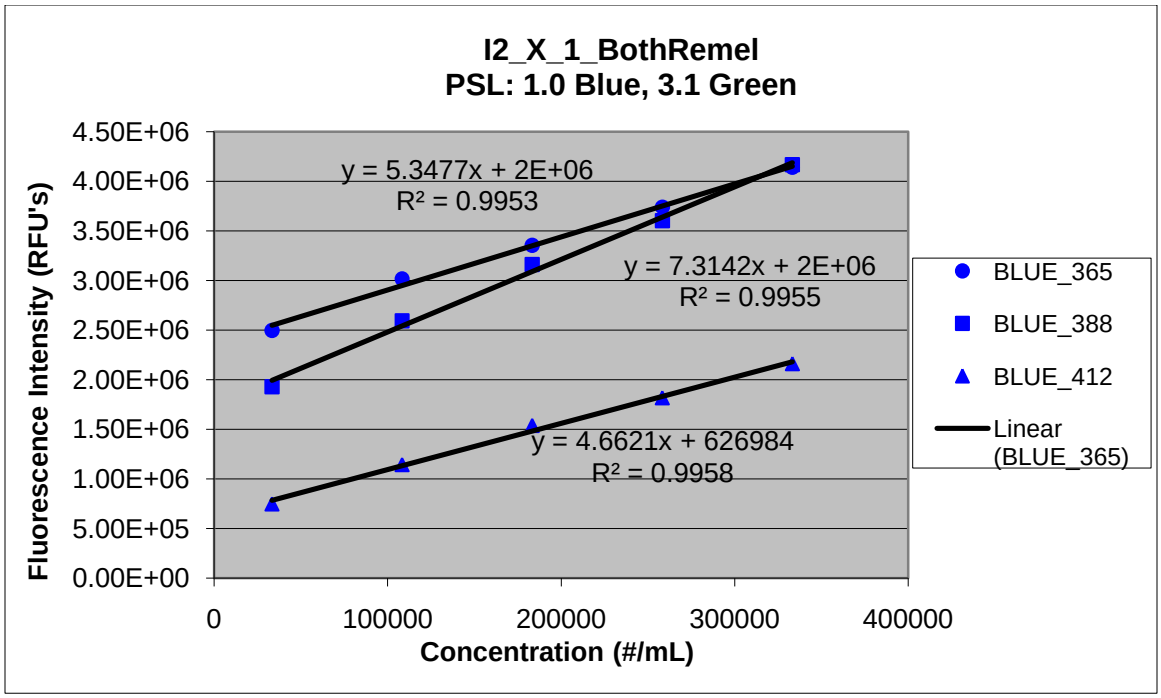

Figure 23: Fluorometric calibration curves for 1.0 µm blue FPSL spheres in Remel M5

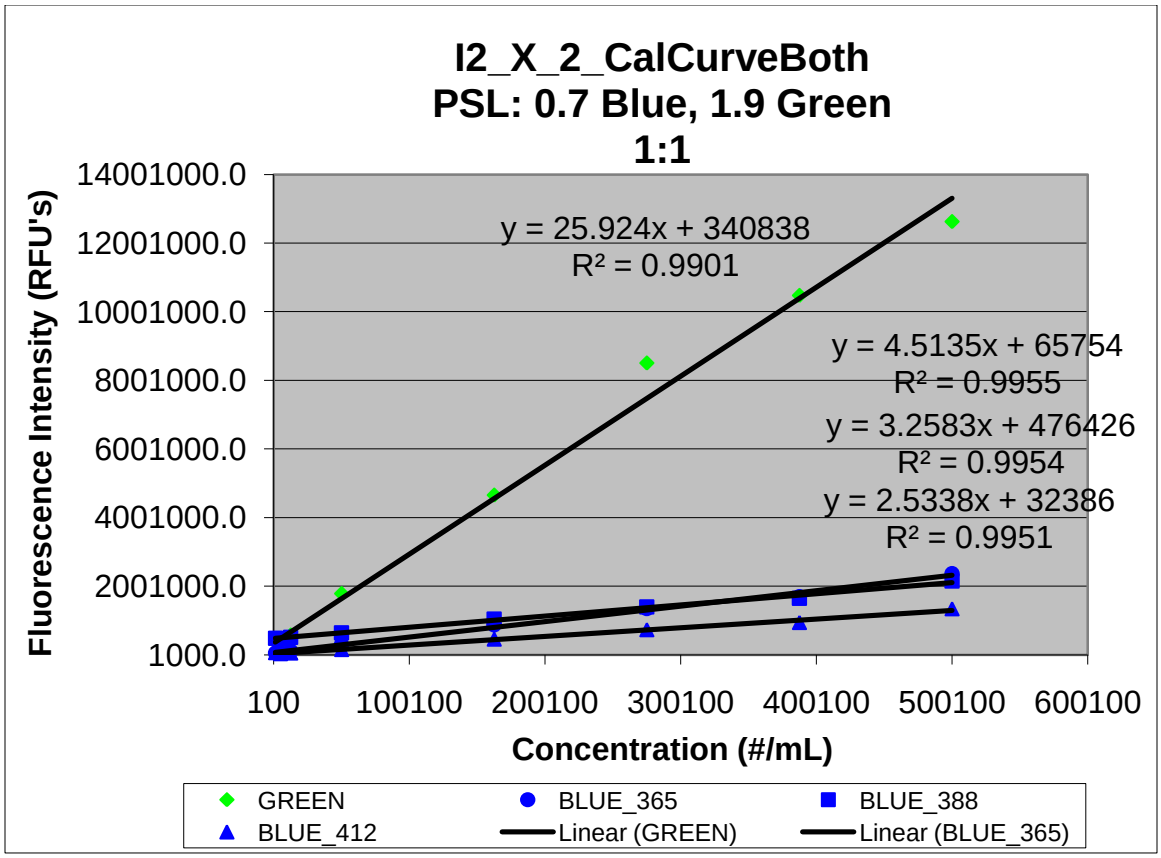

Figure 24: Fluorometric calibration curves for 1.9 µm green and 0.7 µm blue FPSL spheres in PBS solution

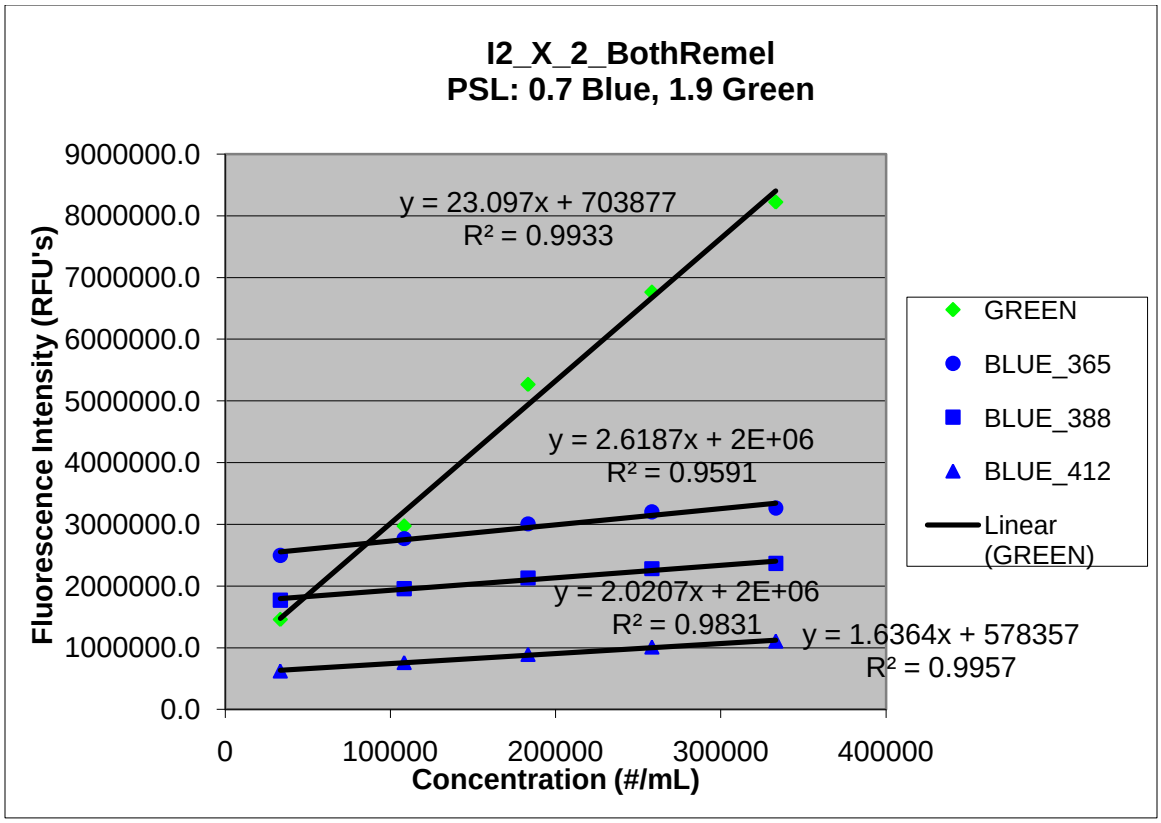

Figure 25: Fluorometric calibration curves for 1.9 µm green and 0.7 µm blue FPSL spheres in Remel M5

Appendix C: XMX Flow Rate Data

Table 20: Flow rate data for XMX1

Reduced			Standard		
5.2933	5.36863	Ave	15.992	16.0168	Ave
5.3081	0.04925	Std Dev	16.017	0.032465	Std Dev
5.3368			16.031		
5.3543			16.078		
5.3601			15.974		
5.3709			15.987		
5.3792			16.002		
5.4097			16.061		
5.4314			16.012		
5.4425			16.014		

Exhaust	deg R		STP		
749	558.1	0.949651	711.2883	692.3074	Ave
751	569.5	0.930641	698.9113	8.27754	Std Dev
755	575.2	0.921419	695.6711		
758	578.5	0.916162	694.4512		
758	581.1	0.912063	691.344		
759	583.9	0.90769	688.9365		
760	586	0.904437	687.372		
760	587.6	0.901974	685.5003		
762	589.1	0.899677	685.5542		
762	590.4	0.897696	684.0447		

Table 21: Flow rate data for XMX2

	Reduced			Standard		
	4.8125	4.8439	Ave	16.013	15.9399	Ave
	4.8231	0.021301	Std Dev	15.875	0.048414	Std Dev
	4.8254			15.861		
	4.8335			15.896		
	4.8385			15.947		
	4.8431			15.945		
	4.8586			15.946		
	4.8567			15.961		
	4.8767			15.977		
	4.8709			15.978		
	Exhaust	deg R		STP		
	749	558.1	0.949651	711.2883	692.3074	Ave
	751	569.5	0.930641	698.9113	8.27754	Std Dev
	755	575.2	0.921419	695.6711		
	758	578.5	0.916162	694.4512		
	758	581.1	0.912063	691.344		
	759	583.9	0.90769	688.9365		
	760	586	0.904437	687.372		
	760	587.6	0.901974	685.5003		
	762	589.1	0.899677	685.5542		
	762	590.4	0.897696	684.0447		

Table 22: Flow rate data for XMX3

Reduced			Standard		
4.7198	4.80516	Ave	14.908	15.0712	Ave
4.7489	0.049296	Std Dev	14.981	0.083964	Std Dev
4.8935			15.009		
4.7824			15.05		
4.7847			15.08		
4.8035			15.112		
4.8171			15.11		
4.8279			15.137		
4.8361			15.155		
4.8377			15.17		

Exhaust	deg R		STP		
743	564.4	0.93905	697.7144	682.6965	Ave
746	577	0.918544	685.234	5.795104	Std Dev
748	581.6	0.911279	681.6369		
752	584	0.907534	682.4658		
755	585.3	0.905519	683.6665		
754	586.8	0.903204	681.0157		
755	587.9	0.901514	680.643		
753	588.7	0.900289	677.9174		
755	589.6	0.898915	678.6805		
755	590.2	0.898001	677.9905		

Table 23: Flow rate data for XMX4

	Reduced			Standard		
	6.2186	6.28507	Ave	14.528	14.7485	Ave
	6.2178	0.036811	Std Dev	14.634	0.116	Std Dev
	6.3033			14.651		
	6.2804			14.763		
	6.2862			14.696		
	6.3088			14.823		
	6.3021			14.833		
	6.3112			14.819		
	6.3109			14.859		
	6.3114			14.879		
	Exhaust	deg R		STP		
	745	561.8	0.943396	702.8302	684.7139	Ave
	747	574.8	0.92206	688.7787	7.124551	Std Dev
	749	579.2	0.915055	685.3764		
	751	581.6	0.911279	684.3707		
	753	583	0.909091	684.5455		
	751	584.2	0.907224	681.3249		
	752	584.2	0.907224	682.2321		
	752	586.1	0.904283	680.0205		
	753	588.9	0.899983	677.6872		
	754	587.7	0.901821	679.9728		

Table 24: Flow rate data for XMX5

Reduced			Standard		
4.5392	4.574	Ave	12.239	12.3329	Ave
4.5579	0.018478	Std Dev	12.226	0.077765	Std Dev
4.5615			12.262		
4.5617			12.317		
4.5707			12.291		
4.5939			12.345		
4.5862			12.399		
4.5894			12.398		
4.588			12.403		
4.5915			12.449		

Exhaust	deg R		STP		
772	554.3	0.956161	738.1562	713.7926	Ave
777	569.8	0.930151	722.7273	10.327	Std Dev
779	575.5	0.920938	717.4109		
778	578.4	0.916321	712.8976		
780	580.7	0.912692	711.8994		
781	582	0.910653	711.2199		
780	583.4	0.908468	708.6047		
781	585.9	0.904591	706.4857		
781	587.4	0.902281	704.6816		
781	588.1	0.901207	703.8429		

Appendix D: General Summary Data for Concentration Ratio ANOVA Evaluations

Table 25: General summary data for concentration ratio ANOVA evaluations

Size	0.542 µm						
Source	DF	SS	MS	F	Fcond	Fcrit	P
XMX	2	27.42626	13.71313	94.00915	F2,114,0.0	3.83	<0.0001
Flow	1	123.1361	123.1361	844.1489	F1,114,0.0	5.18	<0.0001
Interaction	2	24.35679	12.1784	83.48793	F2,114,0.0	3.83	<0.0001
Error	114	16.6292	0.14587				
Total	119	191.5484					
F-XMX	F-crit	F-Flow	F-crit	F-Inter	F-crit		
94.01	3.83	844.2	5.18	83.49	3.83		
Size	0.583 µm						
Source	DF	SS	MS	F	Fcond	Fcrit	P
XMX	2	36.26261	18.1313	97.793	F2,114,0.0	3.83	<0.0001
Flow	1	160.524	160.524	865.8023	F1,114,0.0	5.18	<0.0001
Interaction	2	27.36085	13.68042	73.78672	F2,114,0.0	3.83	<0.0001
Error	114	21.13616	0.185405				
Total	119	245.2836					
F-XMX	F-crit	F-Flow	F-crit	F-Inter	F-crit		
97.79	3.83	865.8	5.18	73.79	3.83		
Size	0.626 µm						
Source	DF	SS	MS	F	Fcond	Fcrit	P
XMX	2	57.88129	28.94065	103.3694	F2,114,0.0	3.83	<0.0001
Flow	1	257.7632	257.7632	920.6713	F1,114,0.0	5.18	<0.0001
Interaction	2	29.01864	14.50932	51.82398	F2,114,0.0	3.83	<0.0001
Error	114	31.91693	0.279973				
Total	119	376.58					
F-XMX	F-crit	F-Flow	F-crit	F-Inter	F-crit		
103.4	3.83	920.7	5.18	51.82	3.83		

Size	0.673 µm						
Source	DF	SS	MS	F	Fcond	Fcrit	P
XMX	2	79.9369	39.96845	97.01128	F2,114,0.0	3.83	<0.0001
Flow	1	411.4485	411.4485	998.6663	F1,114,0.0	5.18	<0.0001
Interaction	2	33.50226	16.75113	40.65828	F2,114,0.0	3.83	<0.0001
Error	114	46.96777	0.411998				
Total	119	571.8554					
F-XMX	F-crit	F-Flow	F-crit	F-Inter	F-crit		
97.01	3.83	998.7	5.18	40.66	3.83		
Size	0.723 µm						
Source	DF	SS	MS	F	Fcond	Fcrit	P
XMX	2	113.3472	56.6736	89.87726	F2,114,0.0	3.83	<0.0001
Flow	1	728.4541	728.4541	1155.237	F1,114,0.0	5.18	<0.0001
Interaction	2	50.41342	25.20671	39.9747	F2,114,0.0	3.83	<0.0001
Error	114	71.8846	0.630567				
Total	119	964.0993					
F-XMX	F-crit	F-Flow	F-crit	F-Inter	F-crit		
89.88	3.83	1155	5.18	39.97	3.83		
Size	0.777 µm						
Source	DF	SS	MS	F	Fcond	Fcrit	P
XMX	2	182.7921	91.39606	93.24836	F2,114,0.0	3.83	<0.0001
Flow	1	1357.323	1357.323	1384.831	F1,114,0.0	5.18	<0.0001
Interaction	2	75.72103	37.86051	38.62782	F2,114,0.0	3.83	<0.0001
Error	114	111.7355	0.980136				
Total	119	1727.571					
F-XMX	F-crit	F-Flow	F-crit	F-Inter	F-crit		
93.25	3.83	1385	5.18	38.63	3.83		
Size	0.835 µm						
Source	DF	SS	MS	F	Fcond	Fcrit	P
XMX	2	237.9634	118.9817	93.94655	F2,114,0.0	3.83	<0.0001
Flow	1	2302.932	2302.932	1818.368	F1,114,0.0	5.18	<0.0001
Interaction	2	103.1124	51.55619	40.70816	F2,114,0.0	3.83	<0.0001
Error	114	144.3791	1.266483				
Total	119	2788.387					
F-XMX	F-crit	F-Flow	F-crit	F-Inter	F-crit		
93.95	3.83	1818	5.18	40.71	3.83		

Size	0.898 µm						
Source	DF	SS	MS	F	Fcond	Fcrit	P
XMX	2	289.6889	144.8445	75.57376	F2,114,0.0	3.83	<0.0001
Flow	1	3464.705	3464.705	1807.738	F1,114,0.0	5.18	<0.0001
Interaction	2	142.7792	71.3896	37.2481	F2,114,0.0	3.83	<0.0001
Error	114	218.4921	1.916597				
Total	119	4115.666					
F-XMX	F-crit	F-Flow	F-crit	F-Inter	F-crit		
75.57	3.83	1808	5.18	37.25	3.83		
Size	0.965 µm						
Source	DF	SS	MS	F	Fcond	Fcrit	P
XMX	2	418.0906	209.0453	85.22091	F2,114,0.0	3.83	<0.0001
Flow	1	5330.981	5330.981	2173.266	F1,114,0.0	5.18	<0.0001
Interaction	2	176.1905	88.09524	35.91354	F2,114,0.0	3.83	<0.0001
Error	114	279.6399	2.452981				
Total	119	6204.902					
F-XMX	F-crit	F-Flow	F-crit	F-Inter	F-crit		
85.22	3.83	2173	5.18	35.91	3.83		
Size	1.037 µm						
Source	DF	SS	MS	F	Fcond	Fcrit	P
XMX	2	436.5772	218.2886	63.87101	F2,114,0.0	3.83	<0.0001
Flow	1	7007.599	7007.599	2050.416	F1,114,0.0	5.18	<0.0001
Interaction	2	208.3541	104.1771	30.48209	F2,114,0.0	3.83	<0.0001
Error	114	389.6118	3.417648				
Total	119	8042.143					
F-XMX	F-crit	F-Flow	F-crit	F-Inter	F-crit		
63.87	3.83	2050	5.18	30.48	3.83		
Size	1.114 µm						
Source	DF	SS	MS	F	Fcond	Fcrit	P
XMX	2	624.585	312.2925	91.40102	F2,114,0.0	3.83	<0.0001
Flow	1	9945.411	9945.411	2910.799	F1,114,0.0	5.18	<0.0001
Interaction	2	268.6408	134.3204	39.31257	F2,114,0.0	3.83	<0.0001
Error	114	389.5071	3.416729				
Total	119	11228.14					
F-XMX	F-crit	F-Flow	F-crit	F-Inter	F-crit		
91.4	3.83	2911	5.18	39.31	3.83		

Size	1.197 µm						
Source	DF	SS	MS	F	Fcond	Fcrit	P
XMX	2	706.7984	353.3992	95.56916	F2,114,0.0	3.83	<0.0001
Flow	1	13373.59	13373.59	3616.598	F1,114,0.0	5.18	<0.0001
Interaction	2	353.3082	176.6541	47.77228	F2,114,0.0	3.83	<0.0001
Error	114	421.5534	3.697837				
Total	119	14855.25					
F-XMX	F-crit	F-Flow	F-crit	F-Inter	F-crit		
95.57	3.83	3617	5.18	47.77	3.83		
Size	1.286 µm						
Source	DF	SS	MS	F	Fcond	Fcrit	P
XMX	2	1117.95	558.975	110.4694	F2,114,0.0	3.83	<0.0001
Flow	1	17122.95	17122.95	3383.985	F1,114,0.0	5.18	<0.0001
Interaction	2	546.9449	273.4725	54.04598	F2,114,0.0	3.83	<0.0001
Error	114	576.8396	5.059997				
Total	119	19364.69					
F-XMX	F-crit	F-Flow	F-crit	F-Inter	F-crit		
110.5	3.83	3384	5.18	54.05	3.83		
Size	1.382 µm						
Source	DF	SS	MS	F	Fcond	Fcrit	P
XMX	2	1822.707	911.3534	161.4323	F2,114,0.0	3.83	<0.0001
Flow	1	23242.24	23242.24	4117.005	F1,114,0.0	5.18	<0.0001
Interaction	2	861.3527	430.6764	76.2877	F2,114,0.0	3.83	<0.0001
Error	114	643.5782	5.645423				
Total	119	26569.87					
F-XMX	F-crit	F-Flow	F-crit	F-Inter	F-crit		
161.4	3.83	4117	5.18	76.29	3.83		
Size	1.486 µm						
Source	DF	SS	MS	F	Fcond	Fcrit	P
XMX	2	1703.57	851.7852	115.1032	F2,114,0.0	3.83	<0.0001
Flow	1	29682.67	29682.67	4011.071	F1,114,0.0	5.18	<0.0001
Interaction	2	892.7637	446.3818	60.32036	F2,114,0.0	3.83	<0.0001
Error	114	843.6211	7.400185				
Total	119	33122.63					
F-XMX	F-crit	F-Flow	F-crit	F-Inter	F-crit		
115.1	3.83	4011	5.18	60.32	3.83		

Size	1.596 µm						
Source	DF	SS	MS	F	Fcond	Fcrit	P
XMX	2	2633.185	1316.593	116.6932	F2,114,0.0	3.83	<0.0001
Flow	1	37559.64	37559.64	3329.013	F1,114,0.0	5.18	<0.0001
Interaction	2	1268.784	634.392	56.22789	F2,114,0.0	3.83	<0.0001
Error	114	1286.207	11.28251				
Total	119	42747.81					
F-XMX	F-crit	F-Flow	F-crit	F-Inter	F-crit		
116.7	3.83	3329	5.18	56.23	3.83		
Size	1.715 µm						
XMX	2	3007.065	1503.532	91.82051	F2,114,0.0	3.83	<0.0001
Flow	1	45569.14	45569.14	2782.901	F1,114,0.0	5.18	<0.0001
Interaction	2	1618.315	809.1577	49.41515	F2,114,0.0	3.83	<0.0001
Error	114	1866.715	16.37469				
Total	119	52061.24					
F-XMX	F-crit	F-Flow	F-crit	F-Inter	F-crit		
91.82	3.83	2783	5.18	49.42	3.83		
Size	1.843 µm						
Source	DF	SS	MS	F	Fcond	Fcrit	P
XMX	2	5146.183	2573.091	85.17884	F2,114,0.0	3.83	<0.0001
Flow	1	59897.82	59897.82	1982.839	F1,114,0.0	5.18	<0.0001
Interaction	2	2047.479	1023.74	33.88957	F2,114,0.0	3.83	<0.0001
Error	114	3443.724	30.2081				
Total	119	70535.21					
F-XMX	F-crit	F-Flow	F-crit	F-Inter	F-crit		
85.18	3.83	1982	5.18	33.89	3.83		
Size	1.981 µm						
Source	DF	SS	MS	F	Fcond	Fcrit	P
XMX	2	5112.712	2556.356	87.61945	F2,114,0.0	3.83	<0.0001
Flow	1	65344.65	65344.65	2239.697	F1,114,0.0	5.18	<0.0001
Interaction	2	1246.114	623.0572	21.35537	F2,114,0.0	3.83	<0.0001
Error	114	3326.026	29.17567				
Total	119	75029.5					
F-XMX	F-crit	F-Flow	F-crit	F-Inter	F-crit		
87.62	3.83	2240	5.18	21.26	3.83		

Size	2.219 µm						
Source	DF	SS	MS	F	Fcond	Fcrit	P
XMX	2	4915.522	2457.761	61.98263	F2,114,0.0	3.83	<0.0001
Flow	1	72518.47	72518.47	1828.854	F1,114,0.0	5.18	<0.0001
Interaction	2	2461.082	1230.541	31.0332	F2,114,0.0	3.83	<0.0001
Error	114	4520.375	39.65242				
Total	119	84415.45					
F-XMX	F-crit	F-Flow	F-crit	F-Inter	F-crit		
61.98	3.83	1829	5.18	31.03	3.83		
Size	2.288 µm						
Source	DF	SS	MS	F	Fcond	Fcrit	P
XMX	2	6369.538	3184.769	61.40615	F2,114,0.0	3.83	<0.0001
Flow	1	87392.34	87392.34	1685.029	F1,114,0.0	5.18	<0.0001
Interaction	2	2827.622	1413.811	27.25997	F2,114,0.0	3.83	<0.0001
Error	114	5912.496	51.864				
Total	119	102502					
F-XMX	F-crit	F-Flow	F-crit	F-Inter	F-crit		
61.41	3.83	1685	5.18	27.26	3.83		
Size	2.458 µm						
Source	DF	SS	MS	F	Fcond	Fcrit	P
XMX	2	6070.504	3035.252	31.98711	F2,114,0.0	3.83	<0.0001
Flow	1	92382.49	92382.49	973.576	F1,114,0.0	5.18	<0.0001
Interaction	2	3052.874	1526.437	16.08641	F2,114,0.0	3.83	<0.0001
Error	114	10817.44	94.88986				
Total	119	112323.3					
F-XMX	F-crit	F-Flow	F-crit	F-Inter	F-crit		
31.99	3.83	973.6	5.18	16.09	3.83		
Size	2.642 µm						
Source	DF	SS	MS	F	Fcond	Fcrit	P
XMX	2	11749.55	5874.775	27.43358	F2,114,0.0	3.83	<0.0001
Flow	1	110727.2	110727.2	517.0656	F1,114,0.0	5.18	<0.0001
Interaction	2	5930.56	2965.28	13.84704	F2,114,0.0	3.83	<0.0001
Error	114	24412.57	214.1454				
Total	119	152819.9					
F-XMX	F-crit	F-Flow	F-crit	F-Inter	F-crit		
27.43	3.83	517.1	5.18	13.85	3.83		

Size	2.839 µm						
Source	DF	SS	MS	F	Fcond	Fcrit	P
XMX	2	16189.1	8094.551	25.38797	F2,114,0.0	3.83	<0.0001
Flow	1	111350.3	111350.3	349.2423	F1,114,0.0	5.18	<0.0001
Interaction	2	6025.35	3012.675	9.449037	F2,114,0.0	3.83	<0.0001
Error	114	36347.08	318.8341				
Total	119	169911.9					
F-XMX	F-crit	F-Flow	F-crit	F-Inter	F-crit		
25.39	3.83	349.2	5.18	9.45	3.83		
Size	3.051µm						
Source	DF	SS	MS	F	Fcond	Fcrit	P
XMX	2	11478.8	5739.401	23.77989	F2,114,0.0	3.83	<0.0001
Flow	1	116348.3	116348.3	482.0624	F1,114,0.0	5.18	<0.0001
Interaction	2	3374.076	1687.038	6.989853	F2,114,0.0	3.83	<0.0001
Error	114	27514.5	241.3553				
Total	119	158715.7					
F-XMX	F-crit	F-Flow	F-crit	F-Inter	F-crit		
23.78	3.83	482.1	5.18	6.9	3.83		
Size	3.278 µm						
Source	DF	SS	MS	F	Fcond	Fcrit	P
XMX	2	15646.88	7823.442	12.44608	F2,114,0.0	3.83	<0.0001
Flow	1	148970.5	148970.5	236.9927	F1,114,0.0	5.18	<0.0001
Interaction	2	5027.165	2513.582	3.998783	F2,114,0.0	3.83	<0.0001
Error	114	71658.89	628.5868				
Total	119	241303.4					
F-XMX	F-crit	F-Flow	F-crit	F-Inter	F-crit		
12.45	3.83	237	5.18	4	3.83		
Size	3.523 µm						
Source	DF	SS	MS	F	Fcond	Fcrit	P
XMX	2	14130.38	7065.188	21.28201	F2,114,0.0	3.83	<0.0001
Flow	1	121393.2	121393.2	365.665	F1,114,0.0	5.18	<0.0001
Interaction	2	6318.894	3159.447	9.516998	F2,114,0.0	3.83	<0.0001
Error	114	37845.65	331.9794				
Total	119	179688.1					
F-XMX	F-crit	F-Flow	F-crit	F-Inter	F-crit		
21.28	3.83	365.7	5.18	9.52	3.83		

Size	3.786 µm						
Source	DF	SS	MS	F	Fcond	Fcrit	P
XMX	2	34848.04	17424.02	19.09908	F2,114,0.0	3.83	<0.0001
Flow	1	165277.7	165277.7	181.1666	F1,114,0.0	5.18	<0.0001
Interaction	2	21556.09	10778.04	11.81419	F2,114,0.0	3.83	<0.0001
Error	114	104001.8	912.2965				
Total	119	325683.6					
F-XMX	F-crit	F-Flow	F-crit	F-Inter	F-crit		
19.1	3.83	181.2	5.18	11.81	3.83		
Size	4.068µm						
Source	DF	SS	MS	F	Fcond	Fcrit	P
XMX	2	25049.1	12524.55	21.36303	F2,114,0.0	3.83	<0.0001
Flow	1	132746.4	132746.4	226.4246	F1,114,0.0	5.18	<0.0001
Interaction	2	20730.16	10365.08	17.67964	F2,114,0.0	3.83	<0.0001
Error	114	66835.02	586.2721				
Total	119	245360.7					
F-XMX	F-crit	F-Flow	F-crit	F-Inter	F-crit		
21.36	3.83	226.4	5.18	17.68	3.83		
Size	4.371 µm						
Source	DF	SS	MS	F	Fcond	Fcrit	P
XMX	2	18332.46	9166.229	62.67892	F2,114,0.0	3.83	<0.0001
Flow	1	100177.4	100177.4	685.016	F1,114,0.0	5.18	<0.0001
Interaction	2	19614.53	9807.267	67.06236	F2,114,0.0	3.83	<0.0001
Error	114	16671.48	146.241				
Total	119	154795.9					
F-XMX	F-crit	F-Flow	F-crit	F-Inter	F-crit		
62.68	3.83	685	5.18	67.06	3.83		
Size	4.698 µm						
Source	DF	SS	MS	F	Fcond	Fcrit	P
XMX	2	11569.01	5784.504	168.4399	F2,114,0.0	3.83	<0.0001
Flow	1	63628.72	63628.72	1852.815	F1,114,0.0	5.18	<0.0001
Interaction	2	13049.29	6524.644	189.9921	F2,114,0.0	3.83	<0.0001
Error	114	3914.949	34.34165				
Total	119	92161.97					
F-XMX	F-crit	F-Flow	F-crit	F-Inter	F-crit		
168.4	3.83	1853	5.18	190	3.83		

Size	5.048 µm						
Source	DF	SS	MS	F	Fcond	Fcrit	P
XMX	2	6130.592	3065.296	72.39225	F2,114,0.0	3.83	<0.0001
Flow	1	30869.05	30869.05	729.0259	F1,114,0.0	5.18	<0.0001
Interaction	2	6472.446	3236.223	76.42899	F2,114,0.0	3.83	<0.0001
Error	114	4827.087	42.34287				
Total	119	48299.17					
F-XMX	F-crit	F-Flow	F-crit	F-Inter	F-crit		
72.39	3.83	729.02	5.18	76.43	3.83		
Size	5.425 µm						
Source	DF	SS	MS	F	Fcond	Fcrit	P
XMX	2	2886.24	1443.12	49.94302	F2,114,0.0	3.83	<0.0001
Flow	1	13629.77	13629.77	471.6945	F1,114,0.0	5.18	<0.0001
Interaction	2	3175.053	1587.526	54.94059	F2,114,0.0	3.83	<0.0001
Error	114	3294.068	28.89533				
Total	119	22985.13					
F-XMX	F-crit	F-Flow	F-crit	F-Inter	F-crit		
49.94	3.83	471.7	5.18	54.94	3.83		
Size	5.829 µm						
Source	DF	SS	MS	F	Fcond	Fcrit	P
XMX	2	763.5021	381.751	67.67701	F2,114,0.0	3.83	<0.0001
Flow	1	5075.803	5075.803	899.8408	F1,114,0.0	5.18	<0.0001
Interaction	2	1201.759	600.8793	106.5242	F2,114,0.0	3.83	<0.0001
Error	114	643.0488	5.640779				
Total	119	7684.112					
F-XMX	F-crit	F-Flow	F-crit	F-Inter	F-crit		
67.68	3.83	899.8	5.18	106.5	3.83		
Size	6.264 µm						
Source	DF	SS	MS	F	Fcond	Fcrit	P
XMX	2	805.6712	402.8356	27.10761	F2,114,0.0	3.83	<0.0001
Flow	1	3528.821	3528.821	237.4614	F1,114,0.0	5.18	<0.0001
Interaction	2	892.3606	446.1803	30.02436	F2,114,0.0	3.83	<0.0001
Error	114	1694.11	14.86061				
Total	119	6920.962					
F-XMX	F-crit	F-Flow	F-crit	F-Inter	F-crit		
27.11	3.83	237.5	5.18	30.02	3.83		

Size	6.732 µm						
Source	DF	SS	MS	F	Fcond	Fcrit	P
XMX	2	571.1091	285.5545	51.85626	F2,114,0.0	3.83	<0.0001
Flow	1	2602.061	2602.061	472.5301	F1,114,0.0	5.18	<0.0001
Interaction	2	792.2728	396.1364	71.93775	F2,114,0.0	3.83	<0.0001
Error	114	627.7587	5.506655				
Total	119	4593.201					
F-XMX	F-crit	F-Flow	F-crit	F-Inter	F-crit		
51.86	3.83	472.5	5.18	71.94	3.83		
Size	7.234 µm						
Source	DF	SS	MS	F	Fcond	Fcrit	P
XMX	2	928.0855	464.0428	26.95791	F2,114,0.0	3.83	<0.0001
Flow	1	4321.715	4321.715	251.0639	F1,114,0.0	5.18	<0.0001
Interaction	2	1048.463	524.2315	30.45449	F2,114,0.0	3.83	<0.0001
Error	114	1962.351	17.2136				
Total	119	8260.615					
F-XMX	F-crit	F-Flow	F-crit	F-Inter	F-crit		
26.96	3.83	251.1	5.18	30.45	3.83		
Size	7.774 µm						
Source	DF	SS	MS	F	Fcond	Fcrit	P
XMX	2	1967.213	983.6066	21.57953	F2,114,0.0	3.83	<0.0001
Flow	1	8900.788	8900.788	195.2761	F1,114,0.0	5.18	<0.0001
Interaction	2	1664.879	832.4393	18.26305	F2,114,0.0	3.83	<0.0001
Error	114	5196.18	45.58053				
Total	119	17729.06					
F-XMX	F-crit	F-Flow	F-crit	F-Inter	F-crit		
21.58	3.83	195.3	5.18	18.26	3.83		
Size	8.354 µm						
Source	DF	SS	MS	F	Fcond	Fcrit	P
XMX	2	2981.873	1490.937	18.66471	F2,114,0.0	3.83	<0.0001
Flow	1	19304.35	19304.35	241.6669	F1,114,0.0	5.18	<0.0001
Interaction	2	2660.984	1330.492	16.65614	F2,114,0.0	3.83	<0.0001
Error	114	9106.319	79.87999				
Total	119	34053.53					
F-XMX	F-crit	F-Flow	F-crit	F-Inter	F-crit		
18.66	3.83	241.67	5.18	16.66	3.83		

Size	8.977 µm						
Source	DF	SS	MS	F	Fcond	Fcrit	P
XMX	2	9467.699	4733.849	9.265195	F2,114,0.0	3.83	<0.0001
Flow	1	49391.81	49391.81	96.67075	F1,114,0.0	5.18	<0.0001
Interaction	2	8136.025	4068.013	7.962005	F2,114,0.0	3.83	<0.0001
Error	114	58245.81	510.9282				
Total	119	125241.3					
F-XMX	F-crit	F-Flow	F-crit	F-Inter	F-crit		
9.27	3.83	96.67	5.18	7.96	3.83		
Size	9.647 µm						
Source	DF	SS	MS	F	Fcond	Fcrit	P
XMX	2	38677.95	19338.98	4.687688	F2,108,0.0	3.83	<0.0001
Flow	1	123524	123524	29.94172	F1,108,0.0	5.18	<0.0001
Interaction	2	35507.61	17753.8	4.303449	F2,108,0.0	3.83	<0.0001
Error	108	445552.1	4125.482				
Total	113	643261.7					
F-XMX	F-crit	F-Flow	F-crit	F-Inter	F-crit		
4.69	3.83	29.94	5.18	4.3	3.83		
Size	10.37 µm						
Source	DF	SS	MS	F	Fcond	Fcrit	P
XMX	2	11396.91	5698.453	6.150918	F2,102,0.0	3.83	<0.0001
Flow	1	119358.3	119358.3	128.8355	F1,102,0.0	5.18	<0.0001
Interaction	2	13061.61	6530.805	7.04936	F2,102,0.0	3.83	<0.0001
Error	102	94496.82	926.4394				
Total	107	238313.7					
F-XMX	F-crit	F-Flow	F-crit	F-Inter	F-crit		
6.15	3.83	128.84	5.18	7.05	3.83		

Appendix E: General Summary Data for Capture and Retention Efficiency ANOVA Evaluations

Table 26: General summary data for capture and retention efficiency ANOVA evaluations

FPSL spheres	Blue 0.7 µm					
Anova: Single Factor	Secondary Flow					
SUMMARY						
Groups	Count	Sum	Average	Variance		
Reduced Secondary	25	4.335043	0.173402	0.018933		
Standard Secondary	25	6.285117	0.251405	0.031191		
ANOVA						
Source of Variation	SS	df	MS	F	P-value	F crit
Between Groups	0.076055729	1	0.076056	3.034689	0.087907	4.042652
Within Groups	1.202981436	48	0.025062			
Total	1.279037164	49				
FPSL spheres	Blue 1.0 µm					
Anova: Single Factor	Secondary Flow					
SUMMARY						
Groups	Count	Sum	Average	Variance		
Reduced Secondary	30	1.783023	0.059434	0.001218		
Standard Secondary	30	3.247173	0.108239	0.008962		
ANOVA						
Source of Variation	SS	df	MS	F	P-value	F crit
Between Groups	0.035728938	1	0.035729	7.019384	0.010373	4.006873
Within Groups	0.295222251	58	0.00509			
Total	0.330951189	59				

FPSL spheres	Green 1.9 µm					
Anova: Single Factor	Secondary Flow					
SUMMARY						
Groups	Count	Sum	Average	Variance		
Reduced Secondary	30	2.8918	0.096393	0.002072		
Standard Secondary	30	6.395672	0.213189	0.012906		
ANOVA						
Source of Variation	SS	df	MS	F	P-value	F crit
Between Groups	0.204618681	1	0.204619	27.3232	2.45E-06	4.006873
Within Groups	0.434351907	58	0.007489			
Total	0.638970589	59				
FPSL spheres	Green 3.1 µm					
Anova: Single Factor	Secondary Flow					
SUMMARY						
Groups	Count	Sum	Average	Variance		
Reduced Secondary	30	18.70022	0.623341	0.023141		
Standard Secondary	30	12.93097	0.431032	0.012185		
ANOVA						
Source of Variation	SS	df	MS	F	P-value	F crit
Between Groups	0.554736987	1	0.554737	31.40648	6.06E-07	4.006873
Within Groups	1.024461939	58	0.017663			
Total	1.579198925	59				

FPSL spheres	Blue 0.7 µm					
Anova: Single Factor	Collection media					
SUMMARY						
Groups	Count	Sum	Average	Variance		
PBS Solution	25	4.335043	0.173402	0.018933		
Remel M5	25	4.558559	0.182342	0.025288		
ANOVA						
Source of Variation	SS	df	MS	F	P-value	F crit
Between Groups	0.000999186	1	0.000999	0.04519	0.832555	4.042652
Within Groups	1.061312279	48	0.022111			
Total	1.062311465	49				
FPSL spheres	Blue 1.0 µm					
Anova: Single Factor	Collection media					
SUMMARY						
Groups	Count	Sum	Average	Variance		
PBS Solution	30	1.783023	0.059434	0.001218		
Remel M5	30	3.035707	0.10119	0.005522		
ANOVA						
Source of Variation	SS	df	MS	F	P-value	F crit
Between Groups	0.026153658	1	0.026154	7.761586	0.007199	4.006873
Within Groups	0.195438438	58	0.00337			
Total	0.221592096	59				

FPSL spheres	Green 1.9 µm					
Anova: Single Factor	Collection media					
SUMMARY						
Groups	Count	Sum	Average	Variance		
PBS Solution	30	2.8918	0.096393	0.002072		
Remel M5	30	6.519869	0.217329	0.001378		
ANOVA						
Source of Variation	SS	df	MS	F	P-value	F crit
Between Groups	0.219381392	1	0.219381	127.2086	2.98E-16	4.006873
Within Groups	0.100025622	58	0.001725			
Total	0.319407013	59				
FPSL spheres	Green 3.1 µm					
Anova: Single Factor	Collection media					
SUMMARY						
Groups	Count	Sum	Average	Variance		
PBS Solution	30	18.70022	0.623341	0.023141		
Remel M5	30	9.402288	0.31341	0.004017		
ANOVA						
Source of Variation	SS	df	MS	F	P-value	F crit
Between Groups	1.440859069	1	1.440859	106.1096	1.02E-14	4.006873
Within Groups	0.787579998	58	0.013579			
Total	2.228439066	59				

Appendix F: Overlay Plots of Concentration Ratio as a Function of Particle Diameter

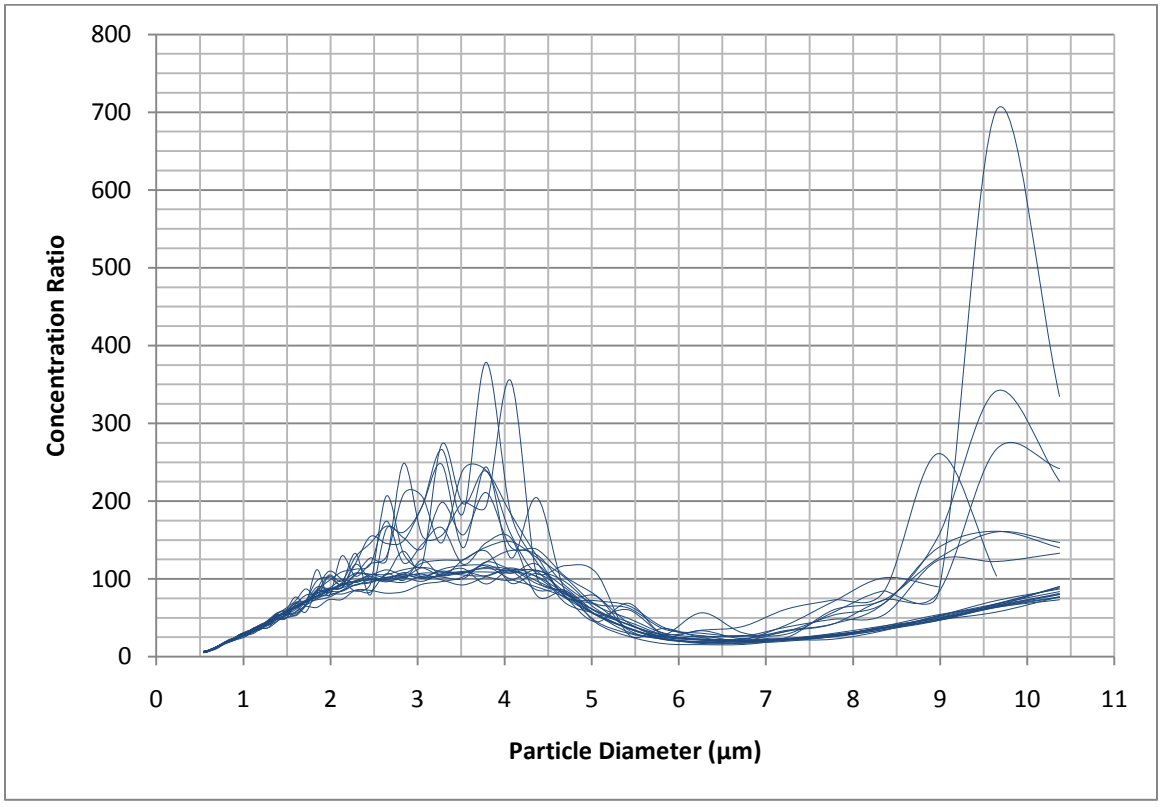

Figure 26: Overlay plots of CR as a function of particle diameter for XMX1 at a secondary flow rate of 5 lpm

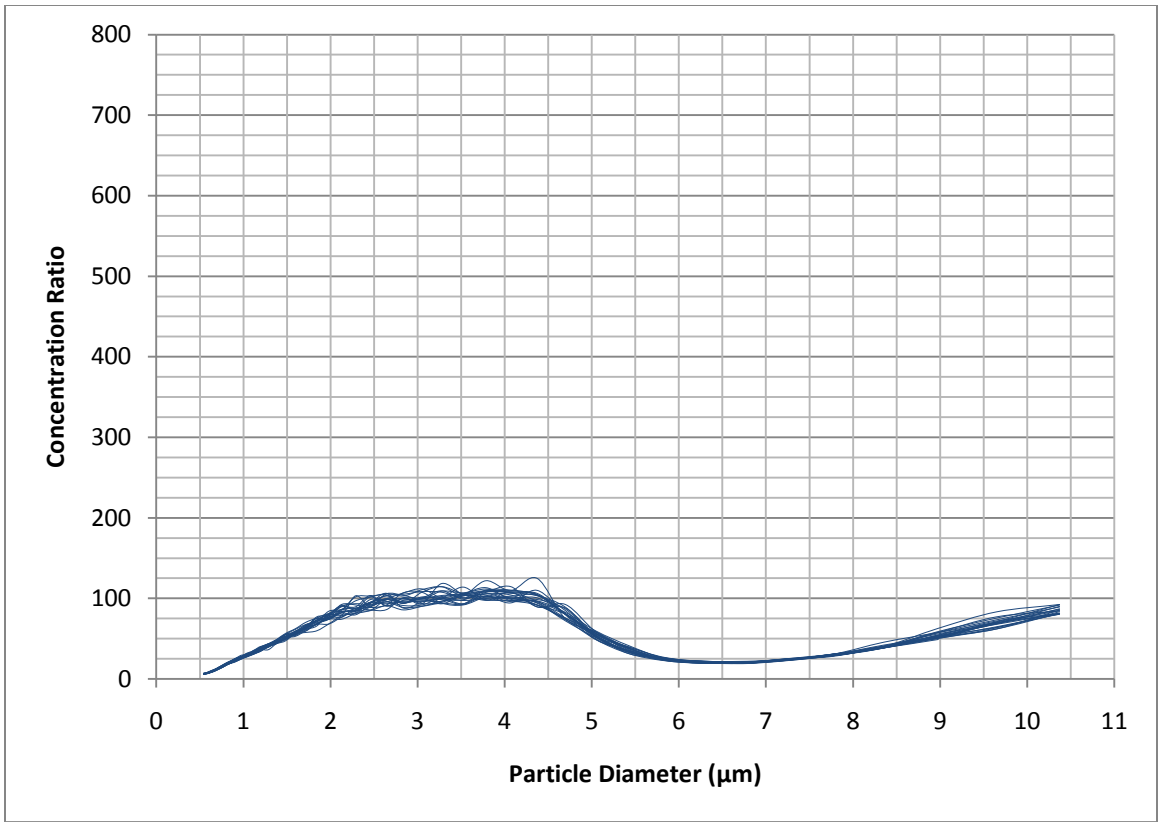

Figure 27: Overlay plots of CR as a function of particle diameter for XMX2 at a secondary flow rate of 5 lpm

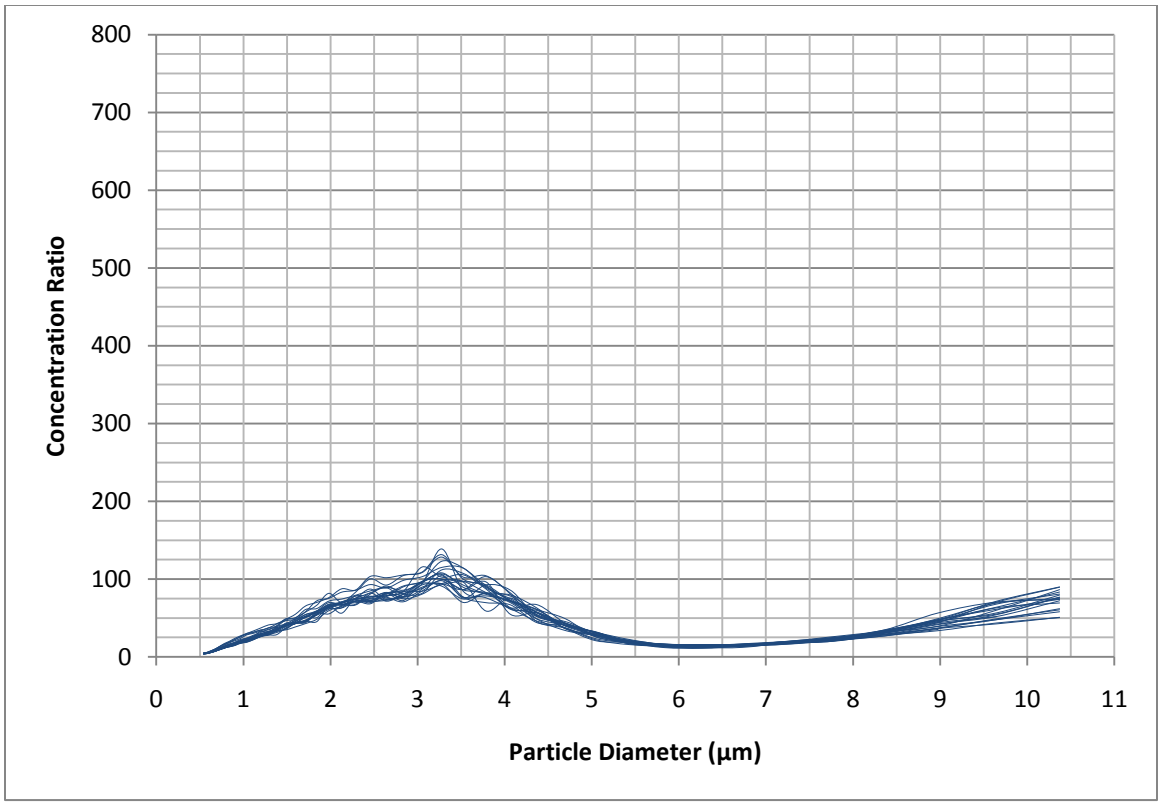

Figure 28: Overlay plots of CR as a function of particle diameter for XMX3 at a secondary flow rate of 5 lpm

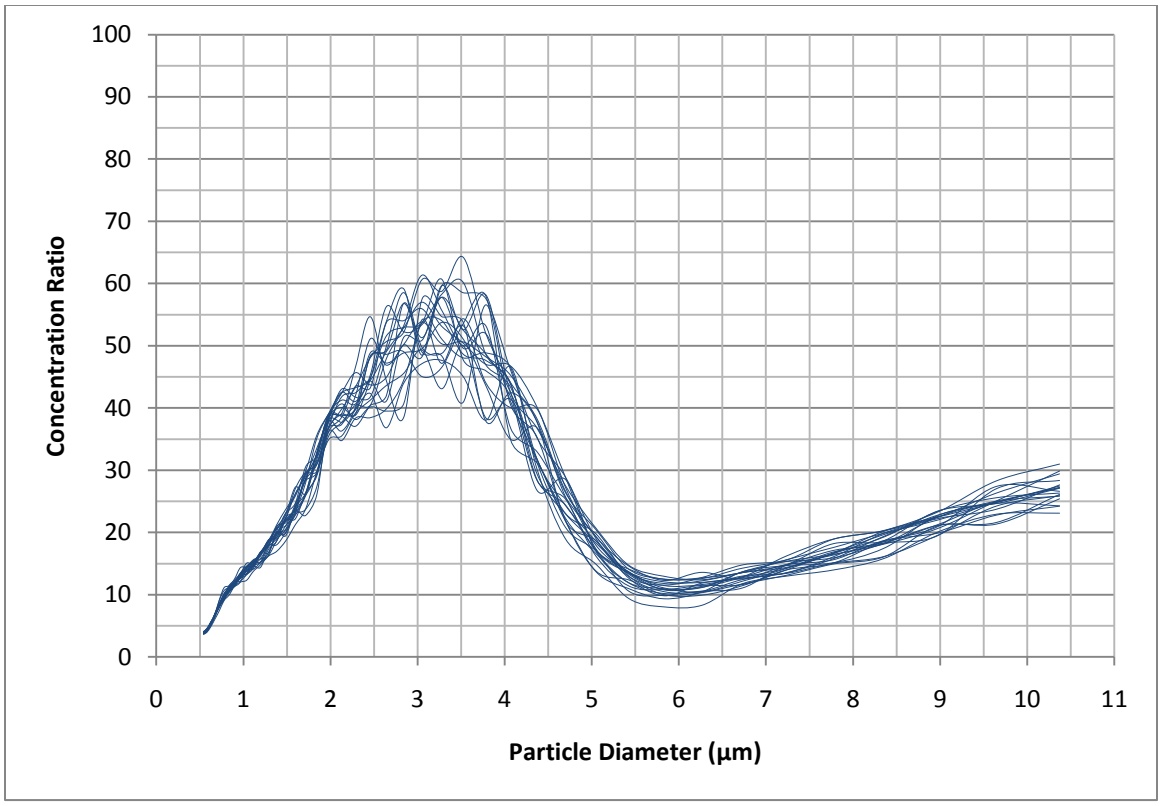

Figure 29: Overlay plots of CR as a function of particle diameter for XMX1 at a secondary flow rate of 10 lpm

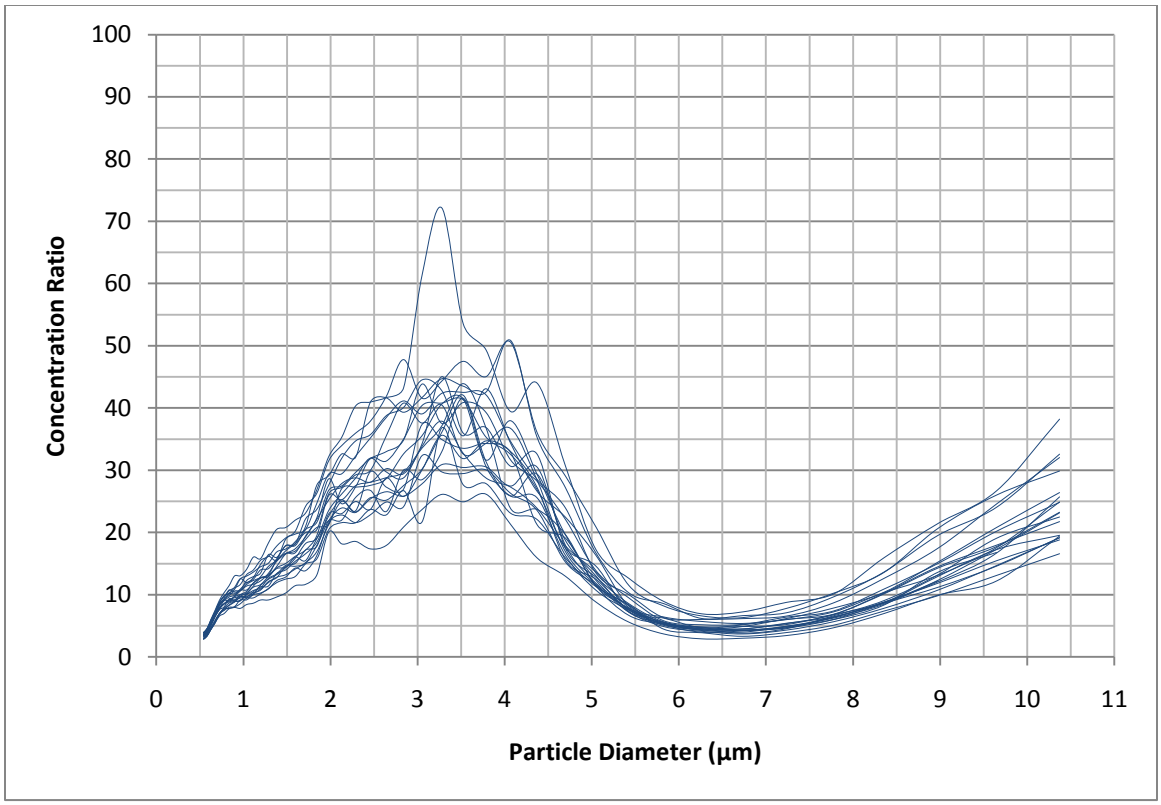

Figure 30: Overlay plots of CR as a function of particle diameter for XMX2 at a secondary flow rate of 10 lpm

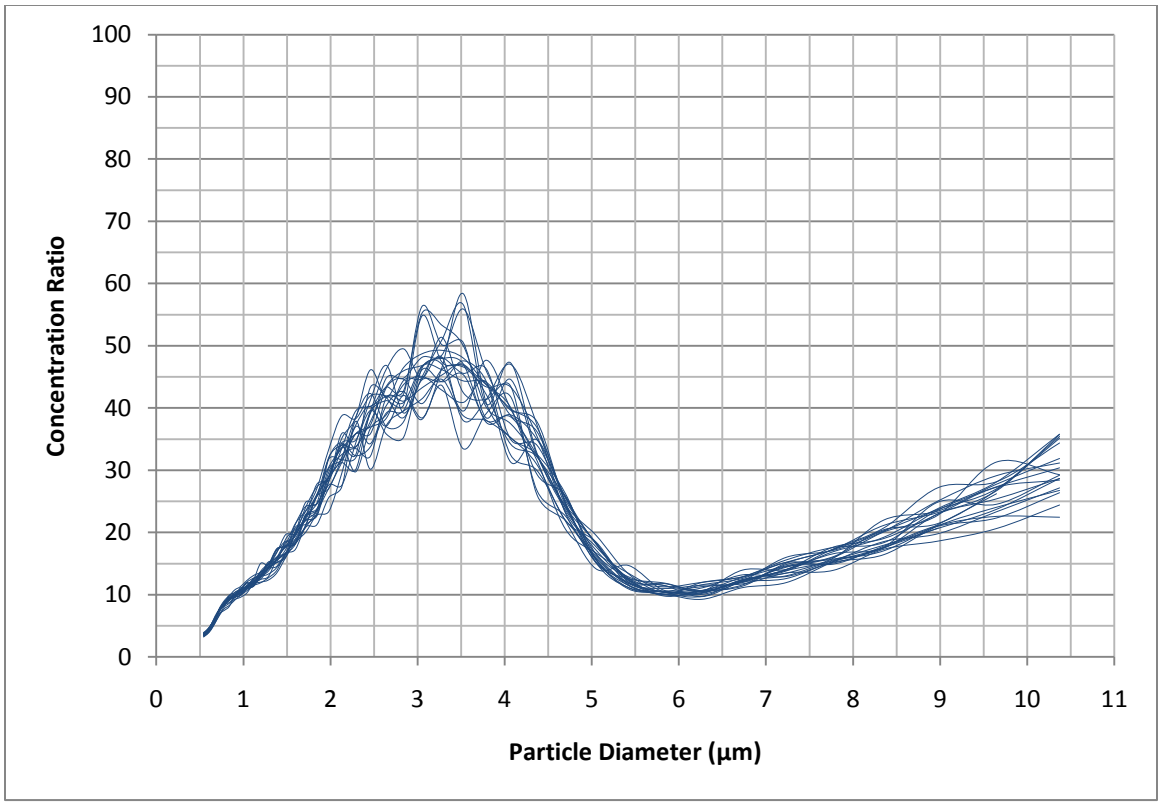

Figure 31: Overlay plots of CR as a function of particle diameter for XMX3 at a secondary flow rate of 10 lpm

Bibliography

Alibek, K. (1999). *Biohazard.* New York: Dell Publishing.

Armendariz, A. J. and D. Leith. (20002). Concentration Measurement and Counting Efficiency for the Aerodynamic Particle Sizer. *Journal of Aerosol Science*, 133-148.

Artenstein, M. S. and W. S. Miller. (1966). Air Sampling for Respiratory Disease Agents in Army Recruits. *Bacteriological Reviews*, 571-572.

Bermingham, N. and K. Luettich. (2003). Polymerase chain reaction and its applications. *Current Diagnostic Pathology,* 159-164.

Booth, T. F., B. Kournikakis, N. Bastien, J. Ho, D. Kobasa, L. Stadnyk, and others. (2005). Detection of Airborne Sever Acute Respiratory Syndrome (SARS) Coronavirus and Environmental Contamination in SARS Outbreak Units. *The Journal of Infectious Diseases,* 1472-1477.

Brasel, T. L., J. M. Martin, C. G. Carriker, S.C. Wilson, and D. C. Straus. (2005). Detection of Airborne *Stachybotrys chartarum* Macrocyclic Trichothecene Mycotoxins in the Indoor Environment. *Applied and Environmental Microbiology*, 7376-7388.

Brenner, K. P., P. V. Scarpino, and C. S. Clark. (1988). Animal Viruses, Coliphages, and Bacteria in Aerosols and Wastewater at a Spray Irrigation Site. *Applied and Environmental Microbiology*, 409-415.

Burton, N. C., S. G. Grinshpun, and T. Reponen. (2007). Physical Collection Efficiency of Filter Materials for Bacteria and Viruses. *The Annals of Occupational Hygiene,* 143–151.

Bush, G. W. (2010). *Decision Points.* New York: Crown.

Canter, D. A. (2005). Addressing Residual Risk Issues at Anthrax Cleanups: How Clean is Safe? *Journal of Toxicology and Environmental Health*, 1017-1032.

Chen, Y., E. Barber, and Y. Zhang. (1998). Sampling Efficiency of the TSI Aerodynamic Particle Sizer. *Instrumentation Science and Technology,* 363-373.

Cooper, C. W. *High Volume Air Sampling for Viral Aerosols: A Comparative Approach.* MS thesis, AFIT/GES/ENV/10M-01. Graduate School of Engineering and Management, Air Force Institute of Technology (AU), Wright-Patterson AFB OH, March 2010 (ADA519642).

Cown, W., T. Kethley, and E. Fincher. (1957). The Critical Orifice Liquid Impinger as a Sampler for Bacteria Aerosols. *Applied Microbiology,* 119-124.

Cox, C. S. and C. M. Wathes. (1995). *Bioaerosols Handbook.* Boca Raton, FL: CRC Press.

Echavarria, M., S. A. Kolavic, S. Cersovsky, F. Mitchell, J. L. Sanchez, C. Polyak, and others. (2000). Detection of Adenoviruses (AdV) in Culture-Negative Environmental Samples by PCR during an AdV-Associated Respiratory Disease Outbreak. *Journal of Clinical Microbiology,* 2982-2984.

Eisinger, J. and J. Flores. (1979). Front-face Fluorometry of Liquid Samples. *Analytical Biochemistry,* 15-21.

Griffiths, W. D., I. W. Stewart, S. J. Futter, S. L. Upton, and D. Mark. (1997). The Development of Sampling Methods for the Assessment of Indoor Aerosols. *Journal of Aerosol Science,* 437-457.

Grinshpun, S. A., K. Willeke, V. Ulevicius, A. Juozaitis, S. Terzieva, J. Donnelly, and others. (1997). Effect of Impaction, Bounce, and Reaerosolization on the Collection Efficiency of Impingers. *Aerosol Science and Technology,* 326-342.

Hermann, J. R., S. J. Hoff, K. J. Yoon, A. C. Burkhardt, R. B. Evans, and J. J. Zimmerman. (2006). Optimization of a Sampling System for Recovery and Detection of Airborne Porcine Reproductive and Respiratory Syndrome Virus and Swine Influenza Virus. *Applied and Environmental Microbiology,* 4811-4818.

Hinds, W. C. (1999). *Aerosol Technology, 2nd Edition.* New York: Wiley-Interscience.

Hodge, J. G. (2002). Bioterrorism Law and Policy: Critical Choices in Public Health. *Journal of Law, Medicine, & Ethics,* 254-261.

Hogan, C. J., E. M. Kettleson, M. H. Lee, B. Bamaswami, L. T. Angenent, and P. Biswas. (2005). Sampling Methodologies and Dosage Assessment Techniques for Submicrometre and Ultrafine Virus Aerosol Particles. *Journal of Applied Microbiology,* 1422-1434.

Hounam, R. and R. Sherwood. (1965). The Cascade Centripeter: A Device for Determining the Concentration and Size Distribution of Aerosols. *American Industrial Hygiene Association Journal*, 122-131.

Institute of Medicine. (2010). *BioWatch and Public Health Surveillance: Evaluating Systems for the Early Detection of Biological Threats.* Washington DC: National Academy of Sciences.

JPEO-CBDX. (2008). *Dry Filter Unit (DFU).* Joint Program Executive Office for Chemical and Biological Defense. 10 January 2011 http://www.jpeocbd.osd.mil/packs/Default.aspx?pg=1002.

Kesavan, J. S. and D. R. Schepers. (2006). *Characteristics and Sampling Efficiencies of Omni 3000 Aerosol Samplers.* Aberdeen Proving Grounds: Edgewood Chemical Biological Center.

Kinney, P. D. and D. Y. Pui. (1995). Inlet Efficiency Study for the TSI Aerodynamic Particle Sizer. *Particle & Particle Systems Characterization*, 188-193.

Ksiazek, T. G., D. Erdman, C. S. Goldsmith, S. R. Zaki, T. Peret, S. Emery, and others. (2003). A Novel Coronavirus Associated with Sever Acute Respiratory Syndrome. *The New England Journal of Medicine*, 1953-1966.

Kuhlmey, G. A., B. Y. Liu, and V. A. Marple. (1981). A Micro-Orifice Impactor for Sub-Micron Aerosol Size Classification. *American Industrial Hygiene Association Journal*, 790-795.

LaRoche, B. C. *Analysis of Expedient Field Decontamination Methods for the XMX/2L-MIL High-Volume Aerosol Sampler.* MS thesis, AFIT/GWM/ENP/09D-01. Graduate School of Engineering and Management, Air Force Institute of Technology (AU), Wright-Patterson AFB OH, December 2009 (ADA508193).

Lawrence, R. (2003). *Bacillus anthracis* Spores (Etiologic Agent of Anthrax) in Air. *The National Occupational Research Agenda,* 81-106. Salt Lake City, Utah: The University of Utah.

Lin, X., K. Willeke, V. Ulevicius, and S. A. Grinshpun. (1997). Effect of Sampling Time on the Collection Efficiency of All-Glass Impingers. *American Industrial Hygiene Association Journal*, 480-488.

Loo, B. W. and C. P. Cork. (1988). Development of High Efficiency Virtual Impactors. *Aerosol Science and Technology,*167-176.

Loo, B., J. Jaklevic, and F. Goulding. (1976). Dichotomous Virtual Impactors for Large-Scale Monitoring of Airborne Particulate Matter. In B. Y. Lui, *Fine Particles: Aerosol Generation, Measurement, Sampling and Analysis,* 311-350. New York: Academic Press.

Macher, J., B. Chen, and C. Rao. (2008). Field Evaluation of a Personal, Bioaerosol Cyclone Sampler. *Journal of Occupational and Environmental Hygiene,* 724-734.

Madigan, M. T., J. M. Martinko, and P. Jack. (1997). *Biology of Microorganisms.* Upper Saddle River: Prentice Hall.

Marple, V. A., K. L. Rubow, and S. M. Behm. (1991). A Microorifice Uniform Deposit Impactor (MOUDI): Description, Calibration, and Use. *Aerosol Science and Technology,* 434-446.

Marple, V., B. Liu, and R. Burton. (1990). High Volume Impactor for Sampling Fine and Coarse Particles. *Journal of Air Waste Management,* 762-767.

May, K. (1966). Multistage Liquid Impinger. *Bacteriological Reviews,* 559-570.

May, K. R. and G. J. Harper. (1957). The Efficiency of Various Liquid Impinger Samplers in Bacteria Aerosols. *British Journal of Industrial Medicine,* 287-297.

Maynard, A. D. and E. D. Kuempel. (2005). Airborne Nanostructured Particles and Occupational Health. *Journal of Nanoparticle Research,* 587-614.

McClave, J. T., P. G. Benson, and T. Sincich. (2008). *Statistics for Business and Economics.* Upper Saddle River: Pearson Prentice Hall.

Miles, A. and S. Mistra. (1938). The Estimation of Bactericidal Power of the Blood. *Journal of Hygiene,* 732-749.

National Research Council. (2007). *The Biological Threat Reduction Program of the Department of Defense: From Foreign Assistance to Sustainable Partnerships.* Washington DC: National Academy of Sciences.

Olsen, S. J., H. L. Chang, T. Y. Cheung, A. F. Tang, T. L. Fisk, S. P. Ooi, and others. (2003). Transmission of the Severe Acute Respiratory Syndrome on Aircraft. *The New England Journal of Medicine*, 2416-2422.

Peters, T. M. and D. Leith. (2003). Concentration measurement and counting efficiency of the aerodynamic particle sizer 3321. *Aerosol Science*, 627-634.

Peters, T. M., D. K. Ott, and P. T. O'Shaughnessy. (2006). Comparison of the Grimm 1.108 and 1.109 Portable Aerosol Spectrometer to the TSI 3321 Aerodynamic Particle Sizer for dry particles. *The Annals of Occupational Hygiene*, 843-850.

Remel. (2005). *Microtest M5 Multi-Microbe Media Instructions for Use.* 24 January 2011 http://www.remelinc.com/Support/MyRemelOnline/IFU.aspx.

Riemenschneider, L. M., C. Y. Wu, D. A. Lundgren, J. H. Lee, H. W. Li, J. D. Wander, and B. K. Heimbuch. (2010). Characterization of Reaerosolization from Impingers in an Effort to Improve Airborne Virus Sampling. *Journal of Applied Microbiology*, 315-324.

Romay, F. J., D. L. Roberts, V. A. Marple, B. Y. Liu, and B. A. Olson. (2002). A High-Performance Aerosol Concentrator for Biological Agent Detection. *Aerosol Science and Technology*, 217-226.

Russell, K. L., M. P. Broderick, S. E. Franklin, L. B. Blyn, N. E. Freed, E. Moradi, and others. (2006). Transmission Dynamics and Prospective Environmental Sampling of Adenovirus in a Military Recruit Setting. *Journal of Infectious Disease*, 877-885.

Schofield, L., J. Ho, B. Kournikakis, and T. Booth. (2005). *Avian Influenza Aerosol Sampling Campaign in the British Columbia Fraser Valley, 9–19 April 2004.* Defense Research and Development Canada.

Sharma, A. and S. G. Schulman. (1999). *Introduction to Fluorescence Spectroscopy.* New York: Wiley Interscience.

Simonsen, L., M. J. Dalton, R. F. Breiman, T. Hennessy, E. T. Umland, and others. (1995). Evaluation of the Magnitude of the 1993 Hantavirus Outbreak in the Southwestern United States. *The Journal of Infectious Diseases*, 729-733.

Sioutas, C., P. Koutrakis, and B. Olson. (1994). Development and Evaluation of a Low Cutpoint Virtual Impactor. *Aerosol Science and Technology*, 223-235.

Smith, G. J., D. Vijaykrishna, J. Bahl, S. J. Lycett, M. Worobey, O. G. Pybus, and others. (2009). Origins and Evolutionary Genomics of the 2009 Swine-origin H1N1 Influenza A Epidemic. *Nature,* 1122-1126.

Tucker, T. (2005). *The Preparation of Guidence Documents and Optimization of the Use of Weapons of Mass Destruction (WMD) Equipment Brooks City Base, TX.* Brooks City Base, TX: Air Force Institute of Operational Health.

Utrup, L. J. and A. H. Frey. (2004). Fate of Bioterrorism-Relevant Viruses and Bacteria, Including Spores, Aerosolized into an Indoor Air Environment. *Experimental Biology and Medicine,* 345-350.

Vaccari, D. A., P. F. Strom, and J. E. Alleman. (2006). *Environmental Biology for Engineers and Scientists.* Hoboken: John Wiley & Sons, Inc.

Verreault, D., S. Moineau, and C. Duchaine. (2008, September). Methods of Sampling for Airborne Viruses. *Microbiology and Molecular Biology Reviews,* 413-444.

Volckens, J. and T. M. Peters. (2005). Counting and Particle Transmission Efficiency of the Aerodynamic Particle Sizer. *Journal of Aerosol Science,* 1400-1408.

Willeke, K., L. Xuejun, and S. A. Grinshpun. (1998). Improved Aerosol Collection by Combined Impaction and Centrifugal Motion. *Aerosol Science and Technology,* 439-456.

REPORT DOCUMENTATION PAGE

Form Approved
OMB No. 074-0188

1. REPORT DATE *(DD-MM-YYYY)*	**2. REPORT TYPE**	**3. DATES COVERED** *(From – To)*
25-03-2011	Master's Thesis	May 2010 - Mar 2011

4. TITLE AND SUBTITLE

Evaluation of XMX/2L-MIL Virtual Impactor Performance and Capture and Retention of Aerosol Particles in Two Different Collection Media

5a. CONTRACT NUMBER

5b. GRANT NUMBER

5c. PROGRAM ELEMENT NUMBER

6. AUTHOR(S)

Black, Jon E., Major, USAF, BSC

5d. PROJECT NUMBER
None

5e. TASK NUMBER

5f. WORK UNIT NUMBER

7. PERFORMING ORGANIZATION NAMES(S) AND ADDRESS(S)
Air Force Institute of Technology
Graduate School of Engineering and Management (AFIT/EN)
2950 Hobson Way
WPAFB OH 45433-7765

8. PERFORMING ORGANIZATION REPORT NUMBER

AFIT/GIH/ENV/11-M01

9. SPONSORING/MONITORING AGENCY NAME(S) AND ADDRESS(ES)
Ott, Darrin K., Lt Col., USAF, BSC
US Air Force School of Aerospace Medicine, Department of Occupational and Environmental Health
1050 Forrer Blvd
Kettering OH 45420
Comm: (937) 656-8555; DSN: (986-8555); Email: Darrin.Ott@wpafb.af.mil

10. SPONSOR/MONITOR'S ACRONYM(S)
USAFSAM/OEHR

11. SPONSOR/MONITOR'S REPORT NUMBER(S)

12. DISTRIBUTION/AVAILABILITY STATEMENT
APPROVED FOR PUBLIC RELEASE; DISTRIBUTION UNLIMITED

13. SUPPLEMENTARY NOTES
This material is declared a work of the United States Government and is not subject to copyright protection in the United States.

14. ABSTRACT
The United States Air Force uses the XMX/2L-MIL (XMX) high volume air sampler to collect samples for biological analysis. The XMX uses a virtual impactor to concentrate particles 1.0 to 10 µm in size into a secondary flow prior to sample collection using a liquid impinger in a collection tube. There are no known published studies regarding virtual impactor inter-instrument variability, effect of reducing the secondary flow on particle concentration, or capture and retention efficiency (CRE) of particles in the collection media performance characteristics when using the XMX. These performance characteristics were evaluated by lofting test aerosols of Arizona Road Dust or fluorescent polystyrene latex (FPSL) spheres into a 14 m^3 test chamber, measuring the chamber and post-virtual impactor particle concentrations using aerodynamic particle sizers, and measuring the concentration of FPSL spheres captured and retained in the collection media using a fluorometer. Notable findings include detection of significant inter-instrument virtual impactor variability, significant difference in particle concentration at reduced secondary flow, and significant differences in CRE due to particle size and secondary flow. This research demonstrates that when using an XMX limit of detection precision is suspect and the importance of collecting and analyzing multiple samples for improved risk assessment.

15. SUBJECT TERMS
Virtual Impactor, Air Sampling, Liquid Impinger, High Volume, Concentration Ratio, Collection Media, Particle Capture, Biological Agent Detection, Health Protection, Bioterrorism, Particle Size, Occupational and Environmental Health

16. SECURITY CLASSIFICATION OF:			**17. LIMITATION OF ABSTRACT**	**18. NUMBER OF PAGES**	**19a. NAME OF RESPONSIBLE PERSON**
a. REPORT	**b. ABSTRACT**	**c. THIS PAGE**			Lieutenant Colonel Dirk P. Yamamoto (AFIT/ENV)
U	U	U	UU	144	**19b. TELEPHONE NUMBER** *(Include area code)* 937-785-3636 ext. 4511

Standard Form 298 (Rev. 8-98)
Prescribed by ANSI Std. Z39-18

Form Approved
OMB No. 074-0188